



University of  
Stavanger

Faculty of Science and Technology

## MASTER'S THESIS

Study program/ Specialization:  Master of Science in Environmental Technology/ Offshore Environmental Engineering	Spring semester, 2014  Open / Restricted access
Writer: Utsav Raj Dotel	..... (Writer's signature)
Faculty supervisor: Torfinn Havn  External supervisor(s):	
Thesis title: <b>Investigation of Corrosion Resistance Property of Cold Deformed (Bended) Duplex and Super Duplex Stainless Steel Tubes.</b>	
Credits (ECTS): 30	
Key words:  Cold Deformation, Bending, Pitting Corrosion, Pitting Potential, Duplex, Super Duplex, Hardness	Pages: 71  + enclosure: 16 (Appendix)  Stavanger, 16 June, 2014 Date/year

## **Declaration**

I, **Utsav Raj Dotel**, hereby declare that the project work entitled “**Investigation of Corrosion Resistance Property of Cold Deformed (Bended) Duplex and Super Duplex Stainless Steel Tubes**”, submitted for the partial fulfilment of the Masters of Science in Environmental Technology, to the Department of Natural Science and Mathematics, University of Stavanger during the academic year 2014 is a genuine work done originally by me under the supervision of **Prof. Torfinn Havn**. This work, in combination with the work done by Ms. Elena Bakrachevska under supervision of Prof. Havn, will be submitted for publication in a relevant journal or a conference. This report or the part of it has not been published or submitted for the academic ward of any other Institution or University. Any literature, data, or works done by others and cited within this report has been given due acknowledgement and listed in the reference section.

.....

Utsav Raj Dotel

University of Stavanger

Stavanger, Norway

## **Acknowledgement**

I would like to acknowledge and extend my heartfelt gratitude to **Prof. Torfinn Havn** for being my supervisor and providing generous and inspirational guidance, motivation and supervision throughout the project.

I would also like to warmly acknowledge the companies: **HiTech Products** and **Algheny Ludlum** for providing the Super Duplex and Duplex Specimens respectively for conducting this study.

I would like to take this opportunity to thank **Ms. Ingunn Cecilie Oddsen**, Chief Engineer at Department of Structural Engineering and Material Science, for her technical help and cooperation throughout the project.

I would like to thank **Mr. Jan Kåre Bording** and **Mr. Vegard Øien** for their cooperation and voluntary support to conduct some experimental activities for this project. I would like to appreciate instrumental support received from the laboratories of Department of Natural Science and Mathematics, University of Stavanger. Many thanks to **Mr. Anupam Bhusal** for providing me with suggestions and motivations for the completion of this work.

I am very much grateful and indebted to my parents, family members and friends for their encouragement and inspiration throughout the whole study period.

## **Abstract**

Cold deformation (bending) of stainless steel tubes is one of the efficient and cost effective methods to gain the required shapes of the tube that can be useful for different practical applications. Different mechanical properties can change after the plastic deformation of the material. The purpose of this study is to investigate the corrosion (basically pitting) resistant property of cold deformed Duplex and Super Duplex materials namely UNS S32205 and UNS S32750 respectively. The bended tubes 2.5ND and 5ND were studied and compared with the straight tubes of same materials. Accelerated coupon testing (ASTM G48) and electrochemical method (ASTM G61) were followed to accomplish the objective of this study. ASTM G48 Test method was performed to know about the pitting corrosion behaviour of material at different temperatures. Weight loss per unit area was measured after exposure at acidic environment at different temperature for different exposure duration. ASTM G61 method was adopted to determine the pitting potential for each specimens and also to find the crevice/pitting susceptibility for each specimen. The results show that the corrosion resistant property of material decreases with temperature. The pitting and crevice resistant properties of cold deformed duplex and super duplex tubes were found to be similar to that of straight tubes. No specific patterns were observed in weight loss of straight and bended parts. The specimens' weight loss per unit area was found to be under the acceptance criteria according to NORSOK Standard MDS-630. Similarly, the pitting potential of straight and bended parts for both duplex and super duplex were found to be in the similar range of about 1 V. The hardness of bended material was observed to be higher than straight one but the hardness decreased slightly after accelerated coupon testing.

## TABLE OF CONTENTS

Declaration.....	ii
Acknowledgement .....	iii
Abstract.....	iv
1. INTRODUCTION .....	1
2. LITERATURE REVIEW .....	3
2.1 Mechanism of Corrosion .....	3
2.2 Types of Corrosion .....	5
2.2.1 General Corrosion.....	5
2.2.2 Localized Corrosion .....	5
2.3 Pitting Corrosion.....	6
2.4 Crevice Corrosion.....	8
2.5 Passivation .....	8
2.6 Stainless steel.....	8
2.7 Materials of Interest.....	10
2.7.1 Duplex UNS S32205 .....	10
2.7.2 Super Duplex UNS S32705 .....	11
2.8 Polarization .....	13
2.9 Mixed potential theory.....	14
2.10 Cold Bending of Stainless Steel Tubes.....	16
2.11 Pitting Corrosion Testing and Monitoring.....	19
2.12 Hardness .....	20
3. MATERIALS AND METHODS .....	21
3.1 Specimen Preparation .....	21
3.2 ASTM G48 Test .....	23
3.2.1 Experimental Set up.....	23
3.2.2 Apparatus.....	24
3.2.3 Ferric Chloride Test Solution .....	25
3.2.4 Experimental Procedures .....	25

---

3.2.5	Examinations .....	27
3.3	ASTM G61 Test .....	29
3.3.1	Experimental Set up.....	29
3.3.2	Sodium Chloride Test Solution .....	31
3.3.3	Apparatus/Equipment .....	31
3.3.4	Experimental Procedures .....	32
3.4	Scanning Electron Microscope .....	33
3.5	Hardness Measurement.....	34
4.	RESULTS .....	35
4.1	Analysis of ASTM G48 Test on Duplex .....	35
4.2	Analysis of ASTM G48 Test on Super Duplex .....	38
4.3	Analysis of ASTM G61 on Duplex .....	52
4.4	Analysis of ASTM G61 on Super Duplex .....	57
4.5	Hardness Test.....	62
5.	DISCUSSION.....	64
6.	CONCLUSION AND RECOMMENDATIONS .....	68
	REFERENCES .....	69
	APPENDICES	

## LIST OF FIGURES

<b>Figure 1:</b> The Corrosion Puzzle (Elimination of any factor will avoid corrosion) .....	3
<b>Figure 2:</b> Electrochemical corrosion cell .....	4
<b>Figure 3:</b> Types of Pitting Corrosion .....	6
<b>Figure 4:</b> Mechanism of Pitting Corrosion .....	7
<b>Figure 5:</b> Evans Diagram for a mixed electrode state of Iron corrosion in acid .....	14
<b>Figure 6:</b> Comparison between polarization curves for AISI 420, and high temperature Nitrided AISI 410S steels tested at 25°C, tempered at 200°C.....	15
<b>Figure 7:</b> Design options for Curved Bending.....	16
<b>Figure 8:</b> Important Bending Factors.....	17
<b>Figure 9:</b> Tube Bending Equipment Parts .....	18
<b>Figure 10:</b> Effect of Bending on Cross section.....	19
<b>Figure 11:</b> Tubes cut into two parts for ASTM G61 Test .....	21
<b>Figure 12:</b> Tubes cut into two parts for ASTM G48 Test .....	22
<b>Figure 13:</b> Mechanical Saw (left) and 120-Grit Abrasive Paper (Right) .....	22
<b>Figure 14:</b> Duplex UNS S32205 Specimen ready for Testing ASTM G48 .....	23
<b>Figure 15:</b> Ferric Chloride Solution.....	25
<b>Figure 16:</b> ASTM G48 Experiment .....	26
<b>Figure 17:</b> Dimension Measurement of Straight Tubes.....	28
<b>Figure 18:</b> Dimension Measurement of Bend Tubes.....	28
<b>Figure 19:</b> Calibration of Gamry Potentiostat .....	30
<b>Figure 20:</b> Hardware setting for Open Circuit Potential.....	30
<b>Figure 21:</b> Experimental Setup for Cyclic Polarization Test.....	31
<b>Figure 22:</b> Cyclic Polarization Test .....	32
<b>Figure 23:</b> Scanning Electron Microscope .....	33
<b>Figure 24:</b> Hardness Measurement Equipment (Struers) .....	34
<b>Figure 25:</b> Comparison of weight loss on different specimens of Duplex .....	36
<b>Figure 26:</b> Crevices on Duplex Materials.....	37
<b>Figure 27:</b> Corrosion on the body of Duplex after exposure at 60 °C .....	38

<b>Figure 28:</b> SEM Image of Super Duplex Bend Tubes after G48 Test at 22°C (Left: 5ND Bend Tubes, Right: 2.5ND Bend Tubes).....	40
<b>Figure 29:</b> SEM Images of Super Duplex Straight tubes after G48 Test at 22°C .....	40
<b>Figure 30:</b> Comparison of weight loss on different specimens of Super Duplex at 30°C	41
<b>Figure 31:</b> SEM Image of Super Duplex Bend Tubes after G48 Test at 30°C (Left: 5ND Bend Tubes, Right: 2.5ND Bend Tubes).....	42
<b>Figure 32:</b> SEM Image of Super Duplex Straight Tubes after G48 Test at 30°C .....	42
<b>Figure 33:</b> Comparison of weight loss on different specimens of Super Duplex at 40°C	44
<b>Figure 34:</b> SEM Image of Super Duplex Bend Tubes after G48 Test at 40°C (Left: 5ND Bend Tubes, Right: 2.5ND Bend Tubes).....	44
<b>Figure 35:</b> SEM Image of Super Duplex Straight Tubes after G48 Test at 40°C .....	45
<b>Figure 36:</b> Comparison of weight loss on different specimens of Super Duplex at 40°C	46
<b>Figure 37:</b> SEM Image of Super Duplex Bend Tubes after G48 Test at 50°C (Left: 5ND Bend Tubes, Right: 2.5ND Bend Tubes).....	46
<b>Figure 38:</b> SEM Image of Super Duplex Straight Tubes after G48 Test at 50°C .....	47
<b>Figure 39:</b> SEM image of Super Duplex 2.5ND Bend Tube at 500X Magnification .....	47
<b>Figure 40:</b> Comparison of weight loss on different specimens of Super Duplex at 50°C	49
<b>Figure 41:</b> Comparison of weight loss on different specimens of Super Duplex at 50°C	50
<b>Figure 42:</b> Super Duplex specimens after G48 Test at 60°C.....	51
<b>Figure 43:</b> Open Circuit Potential of Straight Duplex Tube.....	52
<b>Figure 44:</b> Open Circuit Potential of 5ND Bend Duplex Tube .....	52
<b>Figure 45:</b> Open Circuit Potential of 2.5ND Bend Duplex Tube .....	53
<b>Figure 46:</b> Cyclic Polarization Curve for Straight Duplex Tube.....	54
<b>Figure 47:</b> Cyclic Polarization Curve for Straight, 5ND Bend Duplex Tube .....	55
<b>Figure 48:</b> Cyclic Polarization Curve for 2.5ND Bend Duplex Tube .....	56
<b>Figure 49:</b> Open Circuit Potential of Straight Super Duplex Tube .....	57
<b>Figure 50:</b> Open Circuit Potential of 5ND Bend Super Duplex Tube.....	57
<b>Figure 51:</b> Open Circuit Potential of 2.5ND Bend Super Duplex Tube.....	58
<b>Figure 52:</b> Cyclic Polarization Curve for Straight Super Duplex Tube .....	59

---



**Figure 53:** Cyclic Polarization Curve for 5ND Bend Super Duplex Tube ..... 60

**Figure 54:** Cyclic Polarization Curve for 2.5ND Bend Super Duplex Tube ..... 61

## LIST OF TABLES

**Table 1:** Chemical Specification of UNS S32205 ..... 11

**Table 2:** Basic Mechanical Properties of UNS S32205 ..... 11

**Table 3:** Physical Properties of UNS S32205 ..... 11

**Table 4:** Chemical composition of UNS S32750 provided by company ..... 12

**Table 5:** Chemical Specification of UNS S32750 ..... 13

**Table 6:** Basic Mechanical Properties of UNS S32750 ..... 13

**Table 7:** Physical Properties of UNS S32750 ..... 13

**Table 8:** Experimental setup for First Set of Experiment (ASTM G48) ..... 24

**Table 9:** Experimental setup for Second Set of Experiment (ASTM G48) ..... 24

**Table 10:** Experimental Setup for Third Set of Experiment (ASTM G48) ..... 24

**Table 11:** Area Calculation for Duplex Specimens ..... 35

**Table 12:** Weight Loss per Unit Area for Duplex Specimens at 22 °C ..... 35

**Table 13:** Weight Loss per Unit Area for Duplex Specimens at 30°C ..... 36

**Table 14:** Weight Loss per Unit Area for Duplex Specimens at 40°C ..... 37

**Table 15:** Area Calculation for Super Duplex Specimens ..... 39

**Table 16:** Weight Loss per Unit Area for Super Duplex Specimens at 22 °C ..... 39

**Table 17:** Weight Loss per Unit Area for Super Duplex Specimens at 30°C ..... 41

**Table 18:** Weight Loss per Unit Area for Super Duplex Specimens at 40°C ..... 43

**Table 19:** Weight Loss per Unit Area for Super Duplex Specimens at 50°C ..... 45

**Table 20:** Area Calculation for Super Duplex Specimen ..... 48

**Table 21:** Weight Loss per Unit Area for Super Duplex Specimens at 50°C ..... 48

**Table 23:** Weight loss per Unit area for Super Duplex at 60°C ..... 50

**Table 24:** Pitting Potential for different specimens ..... 62

<b>Table 25:</b> Corrosion Rate (milli inch per year) of Materials Based on Polarization Curve .....	62
<b>Table 26:</b> Hardness Values of Specimens.....	63

## **LIST OF APPENDICES**

**Appendix 1:** Images from SEM of Super Duplex

**Appendix 2:** Images from SEM of Duplex

**Appendix 3:** Cyclic Polarization Curve (Potential vs current density) for Super Duplex

**Appendix 4:** Cyclic Polarization Curve (Potential vs current density) for Duplex

## **1. INTRODUCTION**

Small stainless steel tubes are excessively used in Oil and Gas Industry, especially in Offshore Platforms. It is very important for those tube materials to be highly corrosion resistant as the offshore environment is corrosive. The use of cold bended tubes is one of the effective ways to minimize the space requirement at offshore platform and is cost effective solution for bending pipes as well. However, there remains a question if the mechanical properties of bended tubes to withstand the stress and face the corrosive environment remain similar to that of the straight tubes.

Papers published in recent times reveal that there have not been much study on the effect of cold deformation (bending) on pitting corrosion resistance properties of material; and of the few studies conducted, most of them were seen to be carried out based on only electrochemical method[1, 2]. Also, any substantial conclusion has not been made on the comparative pitting corrosion resistance properties between straight and cold bended tubes of Duplex and Super Duplex material.

### **Main Objective**

The major objective of this research work is to investigate and compare the pitting corrosion behaviour of straight and cold deformed tubes of duplex and super duplex materials, namely UNS S32205 and UNS S32750 respectively.

### **Specific Objectives**

- To observe the corrosion behaviour of specimen at different temperature following an accelerated coupon testing method (ASTM G48).
- To measure the pitting potential of different specimens using Electrochemical Method (ASTM G61).
- To compare the corrosion behaviour of straight and bended tubes from results obtained from aforesaid method.
- To measure the hardness of material and also compare the hardness between the straight and bended part before and after accelerated coupon testing (ASTM G48).

### **Rationale**

- This project is aimed at the analysis of corrosion resistance properties of Duplex and Super Duplex material using ASTM G48 and ASTM G61.
- This research will contribute researcher and corrosion engineers by giving insight about corrosive behaviour of these materials at different temperature.
- This project will act as basis for conducting further research on corrosion properties of cold deformed duplex and super duplex materials.
- This project will also help in understanding the acceptance/non-acceptance criteria for cold deformed duplex and super duplex material.

### **Limitations**

- The major limitation in this project is the performance of limited number of experiments due to restricted number of specimen and time constraints.
- Some strange behaviour for some experimental activities (G48 Test for Super Duplex Test at 40°C) was observed during the experiment, which is elaborated in the Discussion section.

## **2. LITERATURE REVIEW**

Corrosion is simply defined as the degradation of a metal by an electrochemical reaction with its environment[3]. It is one of the biggest reasons for the renewing of the plumbing. Due to corrosion the clogging processes start and accelerate leading to the increment of maintenance cost and decrement of life cycle[4]. Proper understanding of corrosion mechanism is important to address and solve the existing and future corrosion problem[5]. It is a natural process and is the result of the tendency of the natural processes to reach to the lowest energy state[6]. Corrosion is restricted mostly to Metals and Non-metals are generally not subjected to corrosion[7]. It is one of the major factors to cause high cost to the society. The study conducted by CC Technologies Laboratories, Inc. in 1999-2001, entitled “Corrosion Costs and Preventive Strategies” showed that the approximate annual direct cost of corrosion in the US was estimated to be staggering \$276 billion, 3.1 % of the GNP[8].

### **2.1 Mechanism of Corrosion**

Mostly, corrosion in metal is a redox reaction. For corrosion to occur, several factors are essential. Primary Factors include anode, cathode, medium for metal dissolution (electrolyte) and electrical connection between anode and cathode[9]. The absence of any factor among these avoids corrosion.

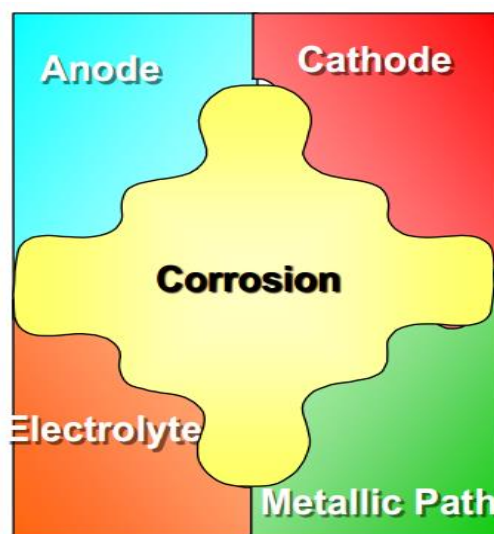


**Figure 1:** The Corrosion Puzzle (Elimination of any factor will avoid corrosion)[10]

Electrons generated at anode move towards cathode through an electronic path that reduces the positively charged ion. Similarly, positively charged ions travel from anode to cathode through ionic current path. The electrical circuit is thus completed with the flow of current from anode to cathode by ionic current path, and cathode to anode by electronic path. These anode and cathode reactions occur at the same rate. American Society For Testing and Material defines it as material loss per unit area and unit time which is corrosion rate[6, 9].

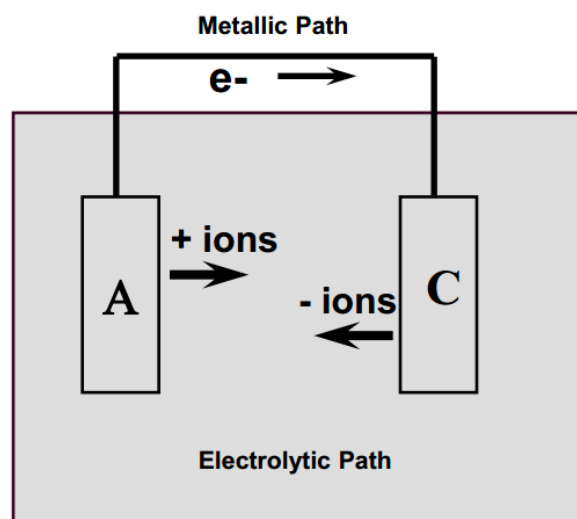
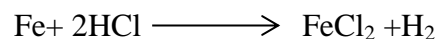
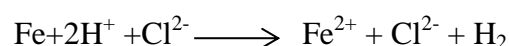


**Figure 2:** Electrochemical corrosion cell[10]

The process has been illustrated below with a suitable example of Iron placed in hydrochloric acid[11]:



The process proceeds with gradual decrement of solid iron and formation of hydrogen bubbles rising to surface. Also electrons are being exchanged.



The iron donates two electrons which are captured by hydrogen ion and reduced to hydrogen gas. Anode is the part where electrons are donated and cathode is where the electrons are absorbed. The difference in electrical potential leads to the development of electrical circuit. Electrons flow from anode to cathode and hydrogen ions move towards

cathode, and the circuit is completed. Corrosion begins with the dissolution of metal, where the rate of current flow is proportional to the corrosion rate[11].

## **2.2 Types of Corrosion**

There are different types of corrosion. In the 13<sup>th</sup> volume of “Corrosion” book published by ASM in 1989, types of corrosion are divided into General and Localized, whose definition and sub categories are presented below.

### **2.2.1 General Corrosion**

General corrosion affects the entire metal surface exposed to an environment (liquid electrolyte, gas electrolyte, hybrid electrolyte) without any localized effect. This causes the thinning of sheet or plate; or thinning of one or both sides of pipes. It is marked mostly by the roughening of the surface or by the development of corrosion product[12]. Some types of General Corrosion are mentioned below[13]:

- Atmospheric Corrosion
- Galvanic Corrosion
- High Temperature Corrosion
- Liquid Metal Corrosion
- Molten Salt Corrosion
- Biological Corrosion

### **2.2.2 Localized Corrosion**

Localized corrosion refers to the corrosion of the discrete part of the exposed surface and is often visible due to presence of pit or mark. Some types of Localized Corrosion are mentioned below[14]:

- Pitting Corrosion
- Crevice Corrosion
- Filiform Corrosion
- Oral Corrosion
- Selective Leaching Corrosion

### 2.3 Pitting Corrosion

Among different types of corrosion mentioned above, pitting corrosion is of special interest for this project as the investigation is mostly focused on pitting corrosion on duplex and super duplex straight and bended tubes. It is a form of localized corrosion where the specific fixed area on the metal surface is attacked. The reason for this corrosion is the breakdown of passive film, usually by chloride ions[15]. Pitting Corrosion selectively attacks the specific part of metal that has surface scratch or mechanically induced break, an emerging dislocation or slip step, or heterogeneous structure in terms of composition[3]. It is usually associated with active-passive-type and occurs under condition specific to each alloy and environment[16]. Pitting corrosion is the most dominant type of localized corrosion and can have various shapes. It can produce pits having semi-permeable membrane of corrosion products[17].

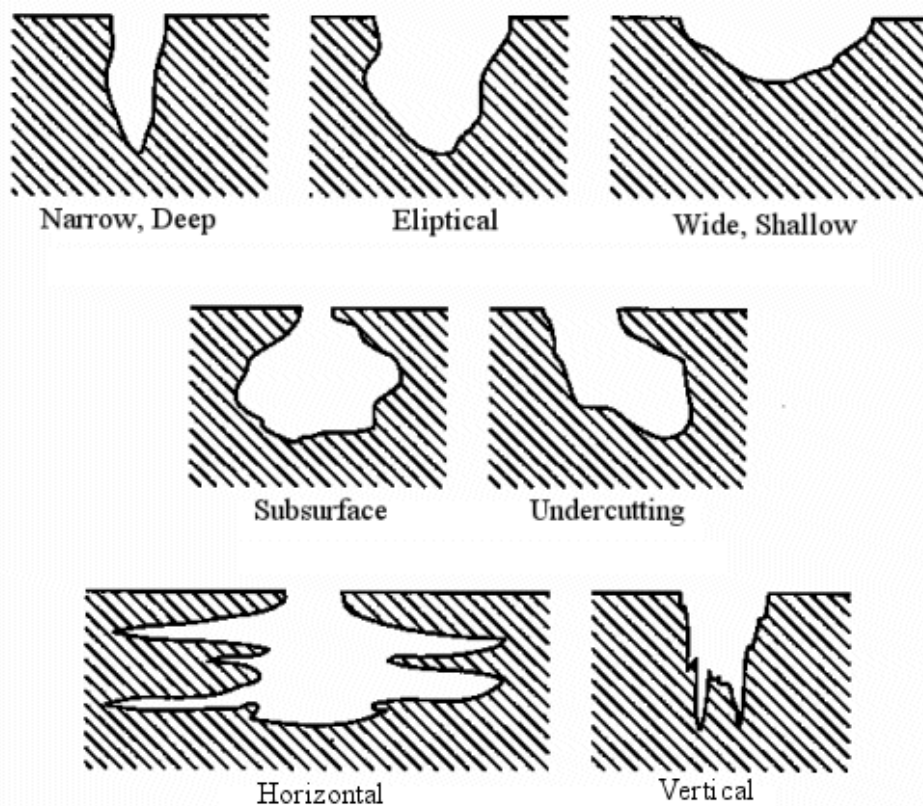


**Figure 3:** Types of Pitting Corrosion[17]



### Mechanism of Pitting Corrosion

The pitting corrosion is initiated as the consequence of breakdown of passive layer. This results in the formation of electrochemical cell and anodic and cathodic reaction starts at several localized sites[11]. Pits start to develop on those localized sites. The process is illustrated in the Figure 4.

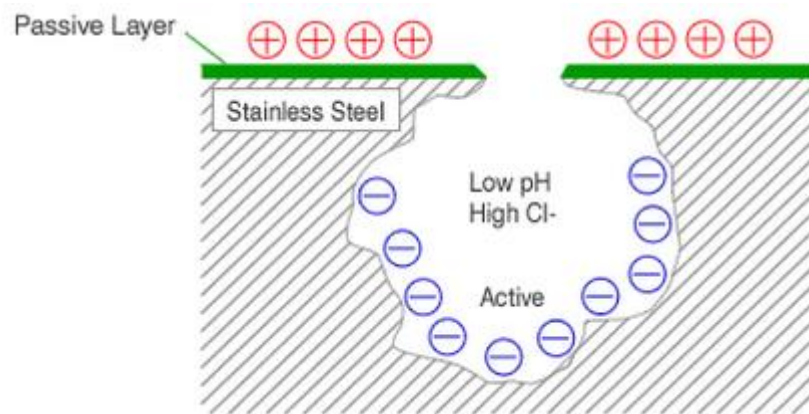


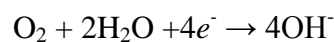
**Figure 4:** Mechanism of Pitting Corrosion[18]

The following reaction takes place when metal is in an environment (electrolyte) containing chloride ions  $\text{Cl}^-$  and molecules of oxygen ( $\text{O}_2$ ) [11]:

Anodic Reaction at the bottom of the pits on Metal:

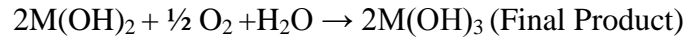
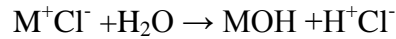


It is balanced by reaction on the adjacent surface:



The concentration of  $\text{M}^{n+}$  increases in the pits and chloride ions  $\text{Cl}^-$  migrate towards it to neutralize forming Metal Chloride  $\text{M}^+\text{Cl}^-$ . The Metal Chloride is hydrolyzed by water.

As the result of these reactions there is increase of concentration of  $\text{M}^{n+}$  inside the pits, and for neutrality to be maintained, chloride ions  $\text{Cl}^-$  migrate into the pit. That is how metal chloride ( $\text{M}^+\text{Cl}^-$ ) is formed. Further, metal chloride is hydrolyzed by water. There is formation of free acid resulting in the decrement of pH at pitting sites. The Metal hydroxide is not stable and reacts with oxygen and water to form metal hydroxide[11].



## 2.4 Crevice Corrosion

Crevice corrosion takes place at the crevices on the metal surface where the gaps are wide enough for passing the liquid into it but very narrow for them to flow[9]. The mechanism of propagation for crevice corrosion is similar to that of pitting corrosion, though the process of initiation for these two are different[15]. Design and/or accident could be the reason for the initiation of crevice corrosion. The sites for crevice corrosion due to design are flanges, rubber O-ring, washers, bolts, etc. Similarly, accident could cause cracks, seams where ultimately crevice corrosion initiates[6].

## 2.5 Passivation

Passivation can be defined as a formation of a protective layer on the surface of a metal as the result of reaction of metal surface with the environment that leads to the reduction of electrochemical activity of the metal[15]. Metals upon exposure to the atmosphere form a protective oxide film, which is called passive film, and the process of its formation is passivation. Passive film is actually diffusion barrier layer which, if stable and undamaged, protect metal from further corrosion. Different parameters govern the stability of this film, for instance, physical and chemical nature properties of passive film and environmental conditions like temperature, pH, etc. which metal experiences[19].

Philip Monnartz, on his published work in 1908 entitled “The Study of Iron Chromium Alloys with special consideration of their resistance to Acids” concluded that the stainlessness of stainless steel is the result of passivation. He gave the conclusion that the phenomenon of passivation is the responsible factor for the decrement of corrosion of metal[20].

## 2.6 Stainless steel

Steel is an alloy of carbon and iron where an addition of 10.5% chromium gives high corrosion resistant property to the alloy for it to be called stainless steel. As stated earlier, high corrosion resistant property is due to the formation of passive chromium oxide layer[21]. Steel could also be the alloy of carbon and other element. Different

combinations of elements give different properties to steel[22]. Besides carbon, all modern steel contains other elements such as manganese (Mn), some impurity atoms as sulfur (S) and phosphorus (P). That is why steel can be presented as  $Fe+C+X$ , where Fe and C are symbols for iron and carbon, and X is third element addition or impurities [23]. The stainless steel is one of the biggest achievements in the field of metallurgy and has been described as “the miracle metal” and “crowning achievement of metallurgy” by Carl Zapffe, the prominent metallurgist of 20th century[20]. Basically, stainless steel is a broad group of alloys, each of which demonstrates its individual physical, mechanical and corrosion resistant properties[24].

### **Classification of stainless steel**

There are three classification systems for the identification of stainless steels. The first one is based on the metallurgical structure and each species of stainless steel is placed into a stainless steel family. The others were developed by ASTM and SAE, namely, AISI numbering system and Unified Numbering System (UNS), which are applied to all commercial metals and alloys and define specific alloy compositions[24].

### **Austenitic Stainless Steel**

These are generally non-magnetic stainless steel that are mostly used and are most common. They have high temperature range for their usage from cryogenic to red hot temperature of furnaces[25].

### **Duplex Stainless Steel**

This is the newest family of stainless steel. Its structure consists of a mixture of ferrite and austenite and it has higher strength than both of these individual[25]. They ensure high corrosion resistance and have more uptime than carbon steels and conventional stainless steel[21]. Duplex Stainless Steel is the material of interest for this project. They are described in detail in next section namely “Materials of Interest” in this report.

### **Ferritic Stainless Steel**

Composed of iron chromium alloys, Ferritic stainless steels are the lowest cost stainless steel. It has a body centered cubic structure, and is good in ductility and formability. Compared to austenitic, the high temperature strength is quite low [26].

## **Martensitic Stainless Steel**

Martensitic stainless steels like 403, 410, 410NiMo and 420 have similar composition as ferrite group. However, they contain a balance of C and Ni vs. Cr and Mo. So austenite transforms to martensite when high temperature is reduced to low. they have a body-centered cubic crystal structure in the hardened condition[26].

## **2.7 Materials of Interest**

### **2.7.1 Duplex UNS S32205**

Duplex stainless steel is duplex alloy made up of two phases where both the phases are stainless steel. These both phases of stainless steel contain at least 11 % Cr. Duplex stainless steel mostly consists of phases: ferrite ( $\alpha$ ) and austenite ( $\gamma$ ); but there are other combinations as well, for instance, ferritic-austenitic, martensitic-ferritic and ferritic-martensitic. There also exists triplex stainless steel and it consists of three phases, ferritic-austenitic-martensitic. Typically, the chemical constitution of the duplex stainless steel is 17 -30 % Cr and 3 -13 % Ni by weight. Mn and Si are added from 0.5 to 2.0 % as a guard against oxidation. The addition of more N and Mo ensure the production of better quality steel (highly resistant to general and pitting corrosion). Carbon is kept normally in low level, but some stainless steel can have up to 0.3 % C by weight [27].

Compared with other common austenitic stainless steel, duplex stainless steel has several advantages, such as high resistance to chloride stress-corrosion cracking and excellent resistance to pitting and crevice corrosion. Also it is twice as strong as austenitic stainless steel[28].

Duplex UNS S32205 is two-phase steel: ferritic and austenitic steel that comprises 22% chromium, 3% molybdenum, 5 to 6% nickel. It has been characterized by High Yield Strength (two times that of standard austenitic stainless steel). It has been used extensively. It possesses high resistance to stress corrosion cracking, Pitting and Crevice Corrosion and Erosion[29].

The detail properties of Duplex UNS S32205 are provided below[30]:

**Table 1:** Chemical Specification of UNS S32205

Elements	Cr	Fe	Mo	N	Ni	P	S	Si
<b>Minimum</b>	<b>22.00</b>	<b>REMAINDER</b>	<b>3.00</b>	<b>0.14</b>	<b>4.50</b>			<b>0.20</b>
<b>Maximum</b>	<b>23.00</b>		<b>3.50</b>	<b>0.20</b>	<b>5.50</b>	<b>0.030</b>	<b>0.020</b>	<b>0.70</b>

**Table 2:** Basic Mechanical Properties of UNS S32205

<b>0.2% Proof Stress (N/mm<sup>2</sup>) [ksi] minimum</b>	<b>450 [65.2]</b>
<b>Ultimate Tensile Strength (N/mm<sup>2</sup>) [ksi] minimum</b>	<b>760 [94.2]</b>
<b>Elongation (%) minimum</b>	<b>25</b>
<b>Hardness (HBN)</b>	<b>270max</b>
<b>Charpy V-notch Impact at ambient Temp (J) [ft.lb]</b>	<b>80min [59min]</b>
<b>Charpy V-notch Impact at -46°C (J) [ft.lb]</b>	<b>45av, 35min [33av, 25.8min]</b>

**Table 3:** Physical Properties of UNS S32205

<b>Density (Kg.m<sup>-1</sup>)</b>	<b>7810</b>
<b>Magnetic Permeability</b>	<b>&lt;50</b>
<b>Young's Modulus (N/mm<sup>2</sup>)</b>	<b>190 x 10<sup>3</sup></b>
<b>Specific Heat, 20°C (J.Kg<sup>-1</sup>.°K<sup>-1</sup>)</b>	<b>400</b>
<b>Specific Electrical Resistance, 20°C (μO.m)</b>	<b>0.85</b>
<b>Thermal conductivity, 20°C (W.m<sup>-1</sup>.°K<sup>-1</sup>)</b>	<b>15</b>
<b>Mean coefficient of thermal expansion, 20-100°C (°K<sup>-1</sup>)</b>	<b>11 x 10<sup>-6</sup></b>

### 2.7.2 Super Duplex UNS S32705

According to UNS (Unified Numbering System) there are three basic categories of duplex stainless steel:

- Low alloy
- Intermediate alloy
- High alloyed (or super duplex)

This classification is according to their PREN number (Pitting Resistance Equivalent Number with Nitrogen).

$$\text{PREN} = \% \text{Cr} + 3.3 \% \text{Mo} + 16\text{N}$$

PREN <32 is typically for low alloy duplex grades

PREN between 32-39 is for intermediate alloys, and

PREN > 40 super duplex grade [31].

Large number of grades of super duplex exists but a common defining factor for all of them is that they all have values of pitting resistance index  $\text{PREN} = \text{Cr} + 3.3 \text{Mo} + 16\text{N} > 40$ [32].

Duplex stainless steel of UNS S32750 is called as Super Duplex stainless steel. Chemical composition provided by company in weight percentage is given in a Table 4.

**Table 4:** Chemical composition of UNS S32750 provided by company

UNS	C	N	Cr	Ni	Mo	Mn	Si	Cu	P	S
S32750	0.015	0.26	24.85	7.00	3.79	0.40	0.30	0.31	0.015	0.0005

This chemical composition gives to UNS S32750 excellent corrosion resistance and strength properties. Compared with other stainless steel or even compared with other duplex stainless steel, UNS S32750 has superior localized corrosion resistance. This opens door to various application, predominantly in harsh environment, and also in other industries , like chemical plant, desalination plant , etc.[33].

Super Duplex UNS S32750 has the most qualitative characteristics of both ferritic and austenitic steels. Due to its high content of chromium, molybdenum and nitrogen level, it has excellent corrosion resistance property (pitting and crevice) and is very suitable for high chloride containing environment. The critical pitting temperature for UNS S32750 exceeds 50 °C[30].

The detailed properties of Super Duplex S32750 have been provided below[30]:

**Table 5:** Chemical Specification of UNS S32750

Elements	C	Cr	Cu	Fe	Mo	Mn	N	Ni	P	S	Si	W
Minimum		24.0		REMAINDER	3.00		0.24	6.00			0.20	0.50
Maximum	0.030	26	0.50		5.00	1.20	0.32	8.00	0.035	0.020	0.80	1.00

**Table 6:** Basic Mechanical Properties of UNS S32750

<b>0.2% Proof Stress (N/mm<sup>2</sup>) [ksi] minimum</b>	<b>550[79.8]</b>
<b>Ultimate Tensile Strength (N/mm<sup>2</sup>) [ksi] minimum</b>	<b>800 [116]</b>
<b>Elongation (%) minimum</b>	<b>25</b>
<b>Hardness (HBN)</b>	<b>270 max</b>
<b>Reduction of Cross Section Area (%)</b>	<b>45</b>
<b>Charpy V-notch Impact at ambient Temp (J) [ft.lb]</b>	<b>80min [59min]</b>
<b>Charpy V-notch Impact at -46°C (J) [ft.lb]</b>	<b>45av, 35min [33av, 25.8min]</b>

**Table 7:** Physical Properties of UNS S32750

<b>Density (Kg.m<sup>-1</sup>)</b>	<b>7810</b>
<b>Magnetic Permeability</b>	<b>33</b>
<b>Young's Modulus (N/mm<sup>2</sup>)</b>	<b>199 x 10<sup>3</sup></b>
<b>Specific Heat, 20°C (J.Kg<sup>-1</sup>.°K<sup>-1</sup>)</b>	<b>475</b>
<b>Fracture Toughness, Kq (MPa.m)</b>	<b>475</b>
<b>Specific Electrical Resistance, 20°C (µO.m)</b>	<b>0.80</b>
<b>Thermal conductivity, 20°C (W.m<sup>-1</sup>.°K<sup>-1</sup>)</b>	<b>14.2</b>
<b>Mean coefficient of thermal expansion, 20-100°C (°K<sup>-1</sup>)</b>	<b>11.1 x 10<sup>-6</sup></b>

## 2.8 Polarization

The potential for each reaction shown above are deviated from their equilibrium potential due to occurrence of net electrode reaction i.e. net electric current flowing through the interface between metal and liquid. This deviation from equilibrium is referred to as

Polarization[34]. It can simply be stated as the difference between the real potential and the equilibrium potential.

Different techniques are used for the measurement and assessment of corrosion rate. Most of the techniques are electrochemical, for instance, corrosion potential measurement, linear polarization resistance, electrochemical impedance spectroscopy, electrochemical noise analysis, etc.[16].

## 2.9 Mixed potential theory

Principle of mixed potential is one of the important tools to analyse the phenomena of complex aqueous corrosion[35]. Evans diagram was developed for the proper understanding of several electrochemical reactions going on during the corrosion process on metal surfaces. In the following diagram, corrosion potential is the mixed potential and it is between the anodic reaction on one side and hydrogen evolution on other. Electrode potential is plotted against corrosion current in an Evan's diagram[36].

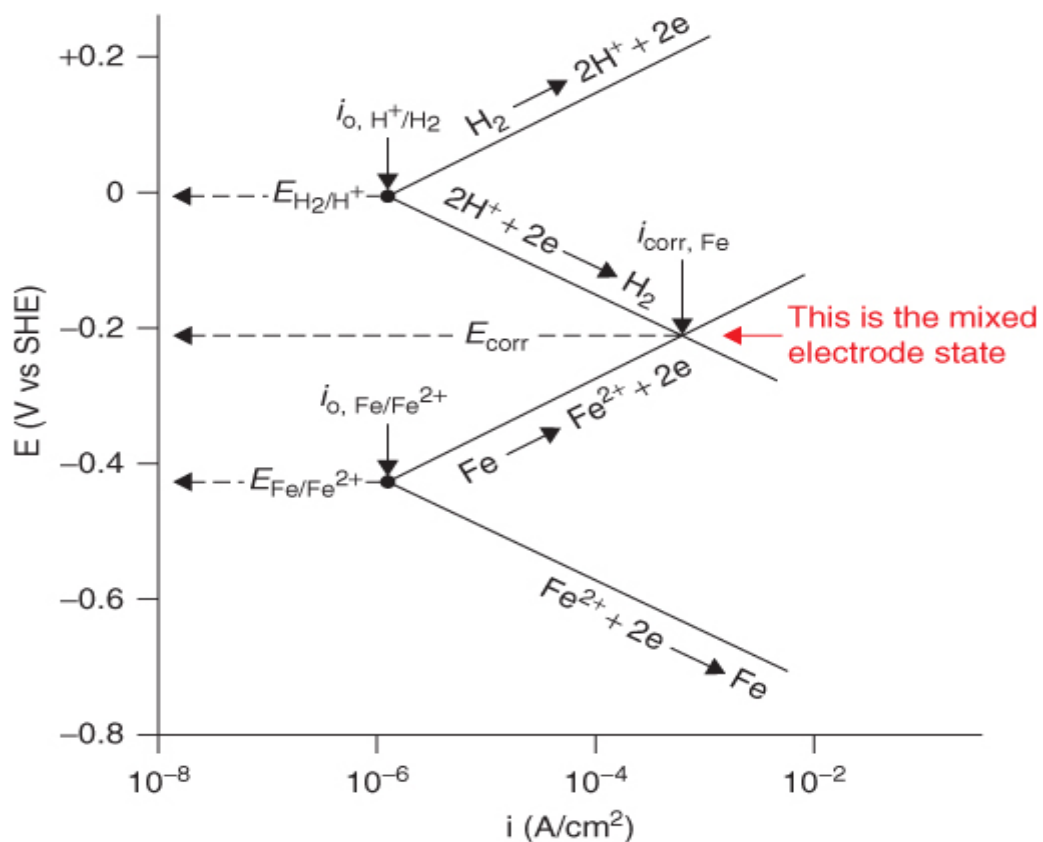


**Figure 5:** Evans Diagram for a mixed electrode state of Iron corrosion in acid[37]



“If the  $E_{corr}$  potential is changed by the value of  $+\Delta E = E - E_{corr}$ , a straight line is obtained:

$$\Delta A = \beta A \log \left( \frac{i_{app}}{i_{corr}} \right)$$

*Where  $\Delta A = E - E_{corr}$*

If the  $E_{corr}$  potential is changed by the value of  $-\Delta E$  following equation is obtained:

$$\Delta c = \beta c \log \left( \frac{i_{cnp}}{i_{corr}} \right)$$

*$\Delta$  is designated as a polarization or overpotential.*

This method is the common method used for determination of corrosion rates in metal, where by polarizing the sample, we can measure change in corrosion current”[36].

By plotting the measurement we can obtain curve known as polarization curve[38]

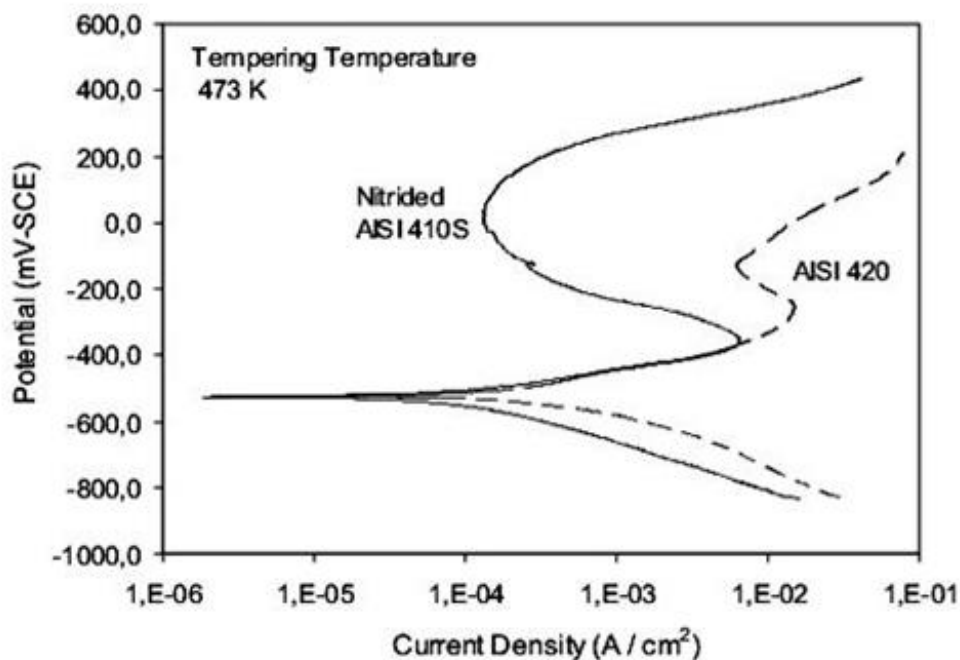


**Figure 6:** Comparison between polarization curves for AISI 420, and high temperature Nitrided AISI 410S steels tested at 25°C, tempered at 200°C[39]

## 2.10 Cold Bending of Stainless Steel Tubes

Bent tube is one of the most efficient and easiest solutions to the design task that require tubes of different shape and bending of stainless steel tubes is a very common practice. There are some benefits of bent tubes over mechanical joints and welded joints. The advantage of tube bending over mechanical joint is that crevices are avoided. Mechanical joints can trap the undesirable corrosive substances leading to crevice corrosion. In the case of welded joints, it is essential to avoid or remove the heat tint. The chemical removal of heat tint involves acidic product whereas the mechanical removal is applicable only for the outside surface of the tube. Tube bending avoids these problems yielding a continuous, even surface[40].

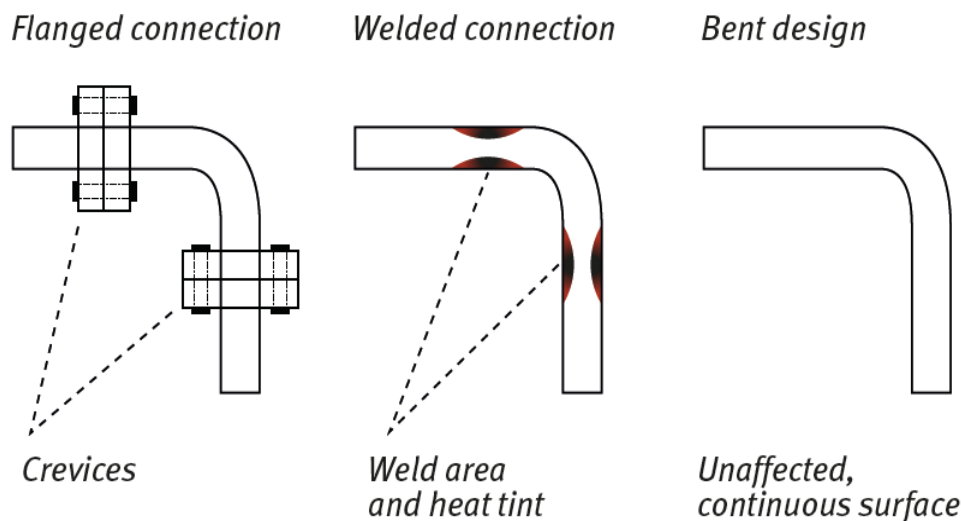


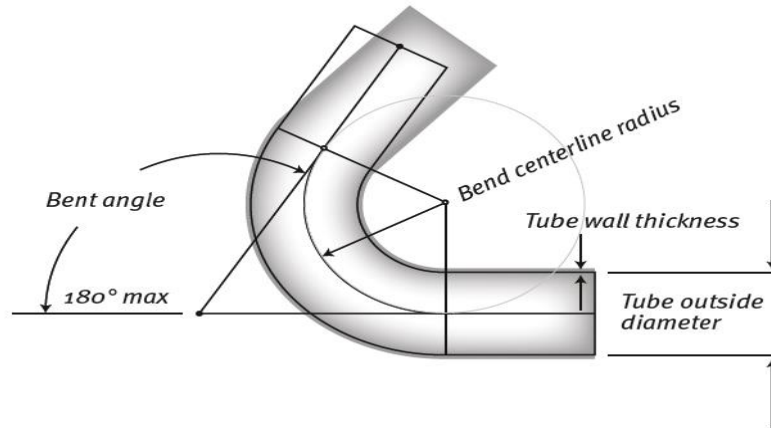
**Figure 7:** Design options for Curved Bending[40]

Wall Factor is one of the important factors to be considered for bending the tube. It determines if the tube has a thin or heavy wall. It can be defined as the ratio of outside diameter of tube to the wall thickness of the tube[40].

Wall Factor = Outside Diameter of Tube/Wall Thickness of Tube

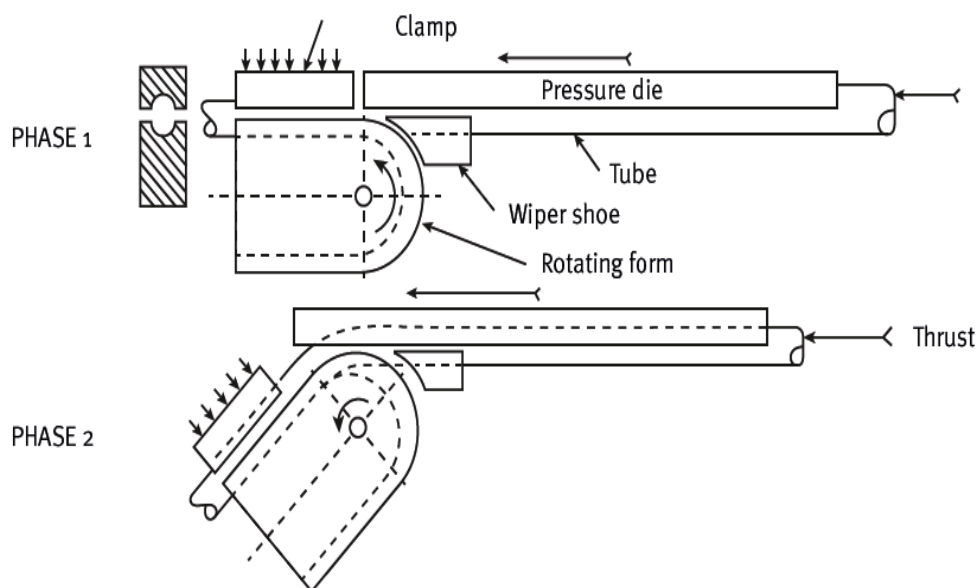
If the wall factor is larger than 30, it is considered as thin walled tube. Similarly, another factor for considering the bend of tube is degree of bend. It can be defined as ratio of bend centreline radius to the outside diameter of tube[40].

Degree of Bend= Bend Centreline Radius/Outside Diameter of Tube



**Figure 8:** Important Bending Factors[41]

These two factors are crucial while considering a tube for bending. Minimal support or probably no support is needed if the wall thickness of tube is large and the diameter is small. With the increment of tube diameter, the strength of tube decreases. Similar is the case when the wall thickness of tube decreases. The smaller the bend centreline radius, larger is the force acted upon tube[40, 42]. A common tube bending equipment is shown in Figure 9.



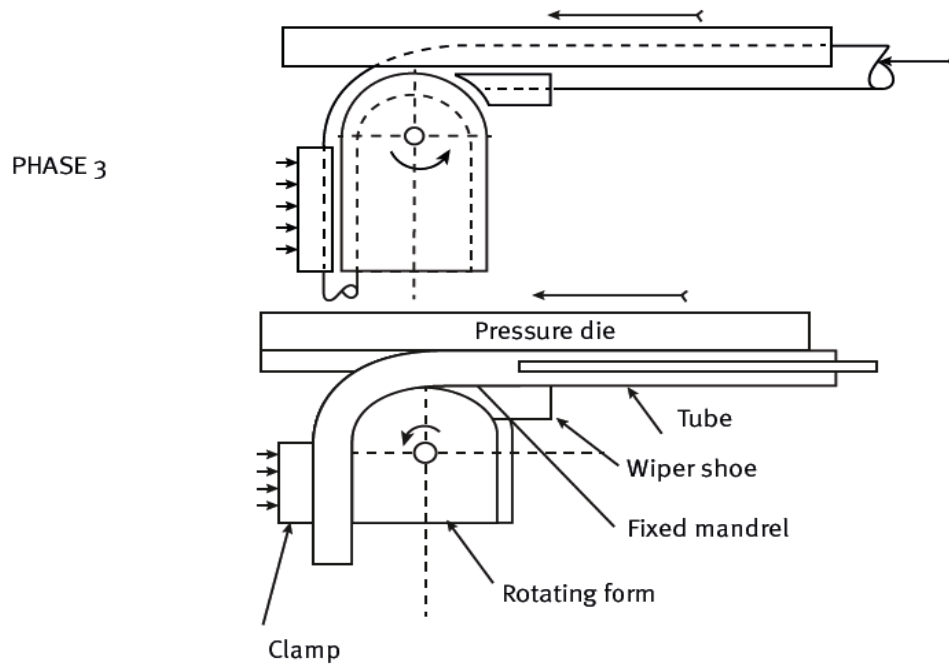


**Figure 9:** Tube Bending Equipment Parts

### **Forming Behaviour**

Duplex is mostly used in process equipment. Having high corrosion resistance their high strength is stated in the values of tensile strength and yield strength [40]. Tensile strength, also called ultimate strength, is defined as the ratio of maximum load to the original cross section area of the tube. Yield strength is the ability of material to stand gradual, progressive force without permanent deformation[43]. These qualities make the requirement of more power for bending for duplex. In general, duplex requires the two times power needed to bend the austenitic of same size[40]. The thinning and thickening of the wall thickness on outer and inner side respectively is the major effect of bending[42].

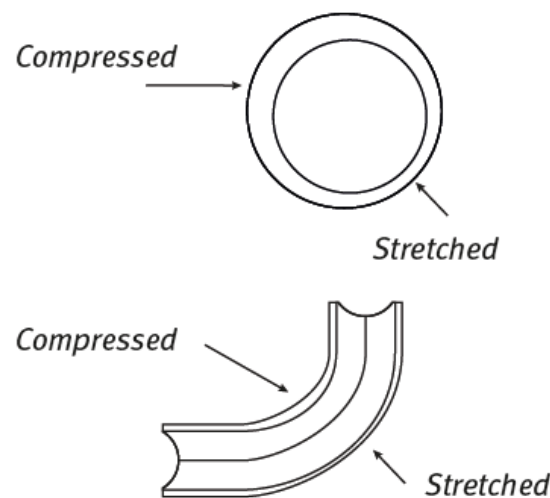


**Figure 10:** Effect of Bending on Cross section

## 2.11 Pitting Corrosion Testing and Monitoring

The aim of corrosion testing is to envisage the corrosion rate quantitatively, either it be for localized or for uniform corrosion[44]. There are different pitting corrosion testing methods. The relevant testing methods for this project are:

- Accelerated Coupon Testing
- Electrochemical Testing

Highly aggressive environment and high temperatures are used in accelerated coupon testing. Most of the ASTM standards fall in this category. Ferric Chloride Test for pitting and crevice corrosion is one of the accelerated coupon tests. This method has been described in ASTM standard G48[44]. In this test, a material is exposed in ferric chloride solution for short duration (24-72 hours) at either room temperature 22°C or elevated temperature 50°C. Ferric salt that form  $Fe^{+3}/Fe^{+2}$  is the chemical potentiostat with a potential of about +0.45 V (SCE). This test is the evaluation of resistance of an alloy to propagation of localized corrosion for most alloys, as their pitting potential is lower than +0.45 V (SCE). High ferric ion concentration (0.4 M) provides large current to the couple without much change in potential. This results in exceeding the pitting potential on the given material, especially on a concentrated  $Cl^-$  ion[44].

Cyclic Potentiodynamic Polarization is one of the most common electrochemical test for localized corrosion susceptibility. The breakdown potential ( $E_{bd}$ ) and repassivation potential ( $E_{rp}$ ) are analysed from the cyclic polarization curve. Metastable pits are quite often seen by transient burst of anodic current[44]. The procedure for this test is described in ASTM standard G61. The electrodes used in this test are:

- Working electrode -specimen to be tested
- Axillary electrode -supplies the current to the working electrode
- Reference electrode -electrode with stable and known potential

The current and voltage setting parameters for this test are shown in the Material and Method section.

## **2.12 Hardness**

“Hardness can be defined as the ability of one material to counter the penetration by another material by resistance”[45]. The hardness of a metal alloy is higher than the individual metal component due to the stronger bonding between the molecules of different materials. Thus, an addition of foreign element is likely to increase the hardness of material. The grain size is also responsible for the hardness of material. Cold deformation causes the reduction of grain size leading to the increment of hardness of material[45]. The objective of testing hardness in this study is to know about the hardness difference of bend and straight part of the material. There was also a comparison of hardness of specimens before and after the G48 Test.

### **3. MATERIALS AND METHODS**

The major objective of this work was to study and compare the pitting corrosion resistance properties of cold deformed (bend) Duplex and Super Duplex materials with the original straight tubes. The Duplex material (UNS S32205) was provided by Allegheny Ludlum, and Super Duplex (UNS S32750) was given by HiTec Products. The tubes were cold bended 2.5ND and 5 ND, and two specimens for each bend were provided. ASTM G48 and ASTM G61 Tests were performed in order to study pitting corrosion resistance.

#### **3.1 Specimen Preparation**

The specimens were long tubes, bended 2.5ND and 5ND at the middle section. 2.5ND bended tube and 5ND bended tubes are named as Smaller Bend Tube (smaller curve) and Bigger Bend Tube (Bigger curve) for convenience in this report. The tubes were required to be cut and the bended and straight sections needed to be separated. After literature review for ASTM G61 Test of materials, the tubes were decided to be cut in two parts: one with a straight section and another having a bend section along with a straight unbent part as shown in Figure 11.

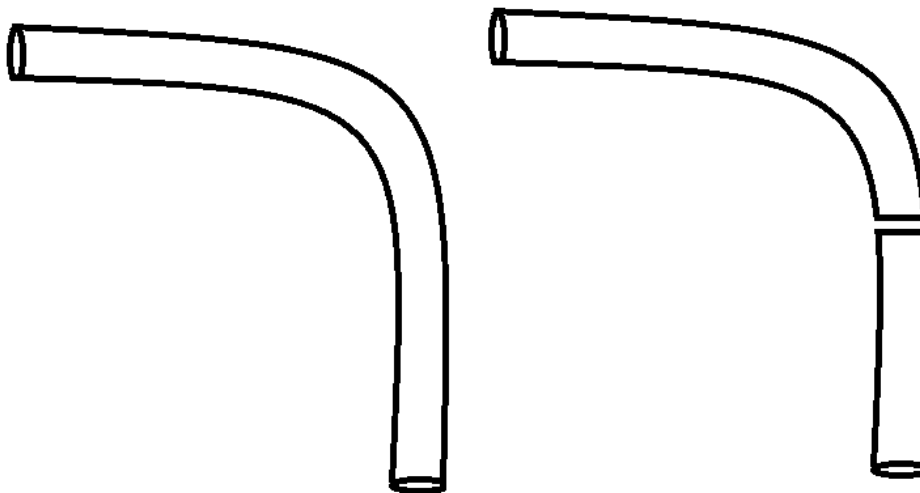


**Figure 11:** Tubes cut into two parts for ASTM G61 Test

Similarly, for ASTM G48 Test, it was necessary to separate the straight and bend parts. For this, the tubes were cut into three pieces: two straight and one bend as shown in Figure 12. Among two straight, the longer one is named as large straight and smaller one is considered as Small straight for convenience in this report.

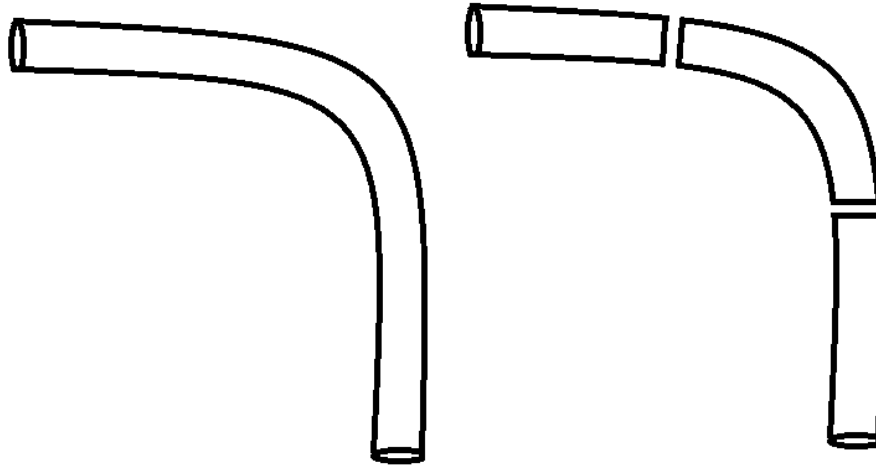


**Figure 12:** Tubes cut into two parts for ASTM G48 Test

The specimens were cut into two pieces with a Mechanical Saw. 120-grit abrasive paper was used after cutting to make the surface smooth and to avoid the rough surface at a cut edge. Afterwards, the water jet and air jet were used to clean the tubes and to avoid the remains to stick on the wall of tubes.



**Figure 13:** Mechanical Saw (left) and 120-Grit Abrasive Paper (Right)



After making the specimen ready for experiments, they were dipped in Acetone so as to remove the impurities due to touching and atmospheric dust contact. Prior to experiments, they were dried and experimental procedures were followed as designed. The specimen ready to use for experiments after cutting are shown in Figure 14.



**Figure 14:** Duplex UNS S32205 Specimen ready for Testing ASTM G48

### **3.2 ASTM G48 Test**

Standard ASTM G48 Test states Standard Test Methods for Pitting and Crevice Corrosion Resistance of Stainless Steels and Related Alloys by Use of Ferric Chloride Solution. There are six procedures mentioned in ASTM G48 viz. Method A, Method B, and likewise up to Method F. Every method describes different test procedures for pitting and crevice test for different materials. Method A- Ferric chloride pitting test is followed in this project and is responsible for determining the pitting resistance of stainless steels and nickel base, chromium bearing alloys[46].

#### **3.2.1 Experimental Set up**

Different experimental set up were designed. For Duplex and Super Duplex, the first set of experiment was performed for straight tube, 2.5ND and 5ND bend tubes at 20°C for 24 hours. The specimens were examined after test.

**Table 8:** Experimental setup for First Set of Experiment (ASTM G48)

SN	Materials	Temperature (°C)	Duration of Exposure (Hours)
1	Duplex	20	24
2	Super Duplex	20	24

Then the temperature was increased to 30°C and 40 °C with 24 hours test period for each temperature. Only super duplex was furthermore tested at 50°C. It can be seen that that test was performed with the gradual increase of temperature.

**Table 9:** Experimental setup for Second Set of Experiment (ASTM G48)

SN	Materials	Exposure time for each temperature (hours)	Temperature (°C)	Temperature (°C)	Temperature (°C)
1	Duplex	24	30	40	-
2	Super Duplex	24	30	40	50

Final set of ASTM G48 was done for Super Duplex with the initial testing temperature of 50°C. After 24 hours, the specimens were examined and temperature was further increased to 60°C.

**Table 10:** Experimental Setup for Third Set of Experiment (ASTM G48)

SN	Materials	Exposure time for each temperature (hours)	Temperature (°C)	Temperature (°C)
1	Duplex	24	-	60
2	Super Duplex	24	50	60

### 3.2.2 Apparatus

- Beakers
- Plastic Rod for Supporting Specimen
- Thermometer

- pH meter
- Water Bath
- Nylon Wire
- Vernier Calliper
- Measuring Tape
- Plastic Covers

### 3.2.3 Ferric Chloride Test Solution



**Figure 15:** Ferric Chloride Solution

More than 3 kg of reagent grade ferric chloride  $\text{FeCl}_3 \cdot 6\text{H}_2\text{O}$  was required for completing the ASTM G48 Test for all specimens. 100 g of ferric chloride was dissolved in 900 ml of distilled water resulting 6 %  $\text{FeCl}_3$  by mass. The solution was filtered to remove any insoluble particles.

### 3.2.4 Experimental Procedures

600 ml of  $\text{FeCl}_3$  Test solution was poured in 1000 ml test beaker. It was made sure that solution volume was maintained at least  $5 \text{ ml/cm}^2$  of specimen surface area. The nylon wire was used to hang the specimen in the ferric chloride solution (refer to modification section below for detail). The water bath was filled with water of desired temperature, beginning with  $20^\circ\text{C}$  being maintained. The specimens were cleaned with Acetone and dried. Prior to experiment their weights were measured. The Beakers with ferric chloride

solution were transferred in a water bath and after it reached the desired temperature, specimens were inserted in the beaker. The beakers were covered by a plastic cover and a small space was made for venting to avoid air pressure inside the beaker.

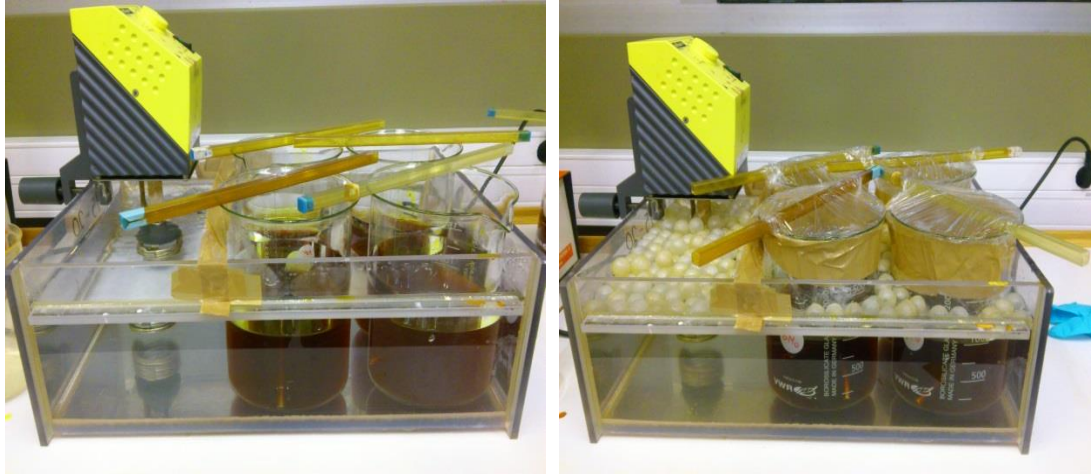


**Figure 16: ASTM G48 Experiment**

The test period at each temperature was made 24 hours. It was made sure that the volume of  $\text{FeCl}_3$  was stable and it didn't decrease due to evaporation. After 24 hours, the specimens were taken out from the solution. They were rinsed with water, cleaned with nylon brush, air jet and water jet to remove corrosion products. After cleaning, they were dipped in acetone and dried. Finally, their weights were measured and were further examined with scanning electron microscope.

### **Modifications**

Several challenges were faced while doing G48 Test. Before the experiment was started on specimen, several trials were made on 316 stainless steel tubes. It was done to assure the credibility and reproducibility of an experiment. Standard ASTM G48 was followed and after several tests, it was decided that some measures would be modified. According to G48, the specimen was supposed to be placed on a glass cradle. The 316SS was placed on glass cradle and immersed in  $\text{FeCl}_3$  test solution at  $15^\circ\text{C}$  for 24 hours. The specimen was examined after test and there was significant crevice corrosion seen on a site of connection between material and cradle. Several different options were considered to avoid huge weight loss due to crevice. One option found was to use a very thin nylon wire for hanging a specimen. The same test was performed by using nylon wire and glass

cradle for two identical 316 SS tubes at the same acidic environment. Examination of those tested materials showed that the crevice corrosion was comparatively less when nylon wire was used. The weight loss was also found insignificant. Hence, nylon wire was proposed to be used as a supporting material for specimen in test solution.

According to G48 test, the recommended temperatures for evaluation are  $22\pm 2$  °C and  $50\pm 2$  °C. In addition of testing at  $22\pm 2$  °C and  $50\pm 2$  °C, the materials were also tested at 30 °C and 40 °C to know about their pitting corrosion behaviour.

### **3.2.5 Examinations**

The specimens were examined and evaluated after ASTM G48 Test using different methods. The visual inspection and the photographic comparison were sufficient to characterize the pitting corrosion resistance of the material[46]. The weight of the specimens was measured before and after the experiments, through which the weight loss per unit area ( $m^2$ ) was calculated. The measurement of pit depth and crevice depth was performed using needles and scanning electron microscope (SEM). SEM was used to ensure the development of pits that were not visible by naked eyes, especially for Super Duplex material.

According to NORSOK Standard M-630, for Ferritic/Austenitic Stainless Steel, Type 25Cr duplex, “Corrosion test according to ASTM G 48 Method A is required. Test temperature shall be 50°C and the exposure time 24 hours. The corrosion test specimen shall be at the same location as those for mechanical testing. Cut edges shall be prepared according to ASTM G 48. The whole specimen shall be pickled before being weighed and tested. Pickling may be performed for 5 minutes at 60 °C in a solution of 20 % HNO<sub>3</sub> + 5 % HF”[47]. The pickling was performed by a company prior of providing specimen for testing.

The acceptance criteria of the material after test are[47]:

- No pitting at 20 X magnification.
- The weight loss shall be less than  $4.0 \text{ g/m}^2$

The area of each specimen was measured using a measuring tape and a Vernier calliper. The length of the tube, inner and outer diameter of the tube was measured and area was calculated using the following formula.

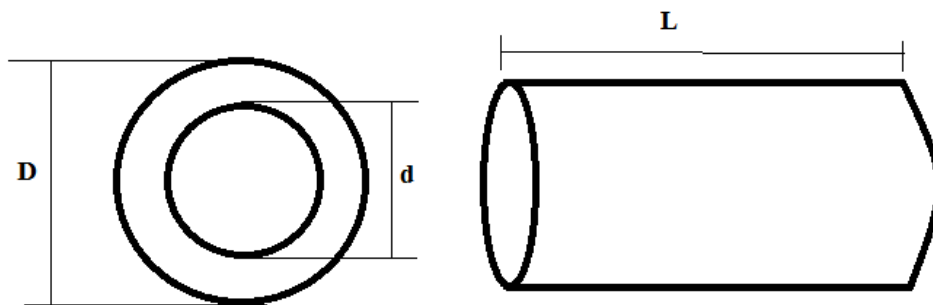


**Figure 17:** Dimension Measurement of Straight Tubes

For Straight Tubes:

$$Area = 2\left(\frac{\pi D^2}{4} - \frac{\pi d^2}{4}\right) + \pi L(D + d)$$

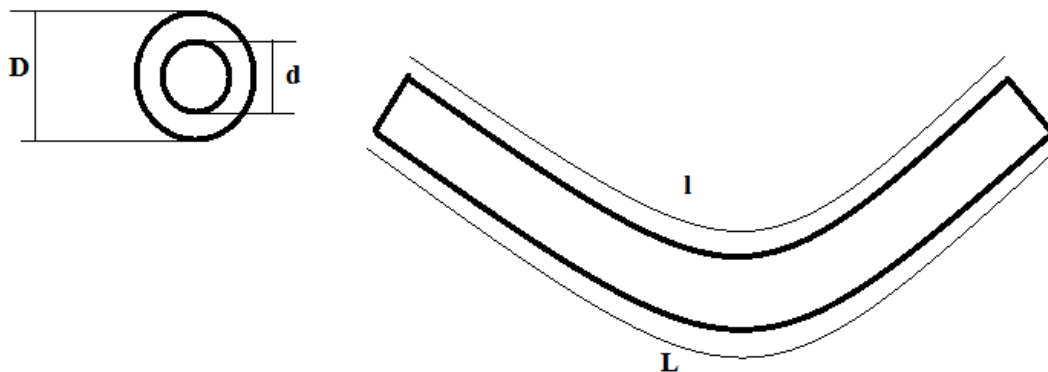


**Figure 18:** Dimension Measurement of Bend Tubes

For Bend Tubes:

$$Area = 2\left(\frac{\pi D^2}{4} - \frac{\pi d^2}{4}\right) + \pi J(D + d) \quad ; \text{Where } J = \frac{L+l}{2}$$

### 3.3 ASTM G61 Test

ASTM G61 Test states, “Standard Test Method for Conducting Cyclic Potentiodynamic Polarization Measurements for Localized Corrosion Susceptibility of Iron-, Nickel-, or Cobalt Based Alloys”. This standard also describe about the measures for experiment which can be used to check one’s experimental procedures and experimentation[48]. The ASTM G61 Test was performed in this project to determine the pitting corrosion potential of straight and cold deformed tubes of Duplex and Super Duplex tubes and to support the results obtained from ASTM G48. Gamry Potentiostat was used for conducting the potentiodynamic polarization test. Anodic Potentiostatic scan was continued in cyclic polarization (ASTM G61) until the pitting is initiated. The anodic and cathodic scans’ relative position illustrated the pitting tendency of specimen[49].

#### 3.3.1 Experimental Set up

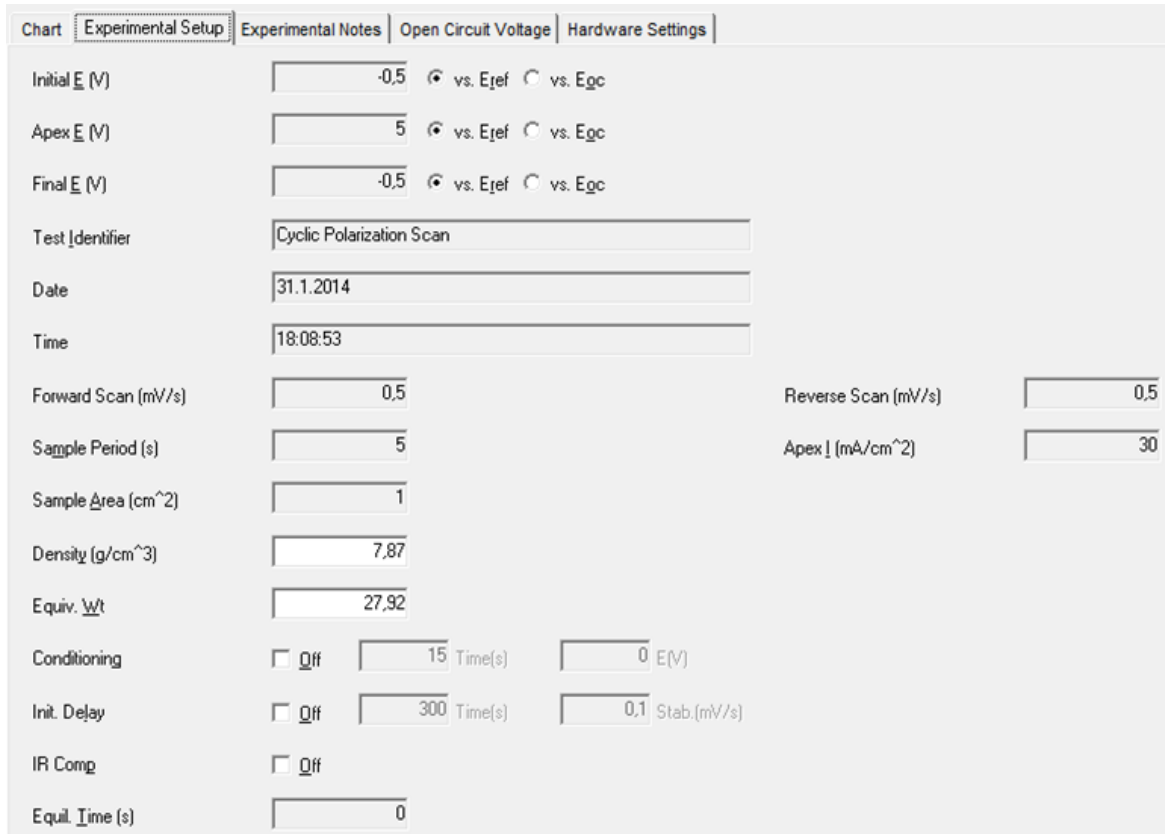
The reference electrode, counter electrode and working electrode are the major components for conducting potentiodynamic polarization test. Prior to the start of the experiment on specimen, the cyclic polarization was tested on 316SS tubes to ensure proper working of all electrodes and connecting wires. There were some unusual graph plotted initially, but this problem was overcome with the calibration of instrument and proper connection of all electrodes with their corresponding connectors.







For the cyclic polarization test, several values for Initial Potential, Peak Potential and Final Potential were assigned. The values assigned are shown in Figure 21.



Parameter	Value	Reference
Initial E (V)	-0.5	vs. E <sub>ref</sub>
Apex E (V)	5	vs. E <sub>ref</sub>
Final E (V)	-0.5	vs. E <sub>ref</sub>
Test Identifier	Cyclic Polarization Scan	
Date	31.1.2014	
Time	18:08:53	
Forward Scan (mV/s)	0.5	Reverse Scan (mV/s): 0.5
Sample Period (s)	5	Apex I (mA/cm <sup>2</sup> ): 30
Sample Area (cm <sup>2</sup> )	1	
Density (g/cm <sup>3</sup> )	7.87	
Equiv. Wt	27.92	
Conditioning	<input type="checkbox"/> Off, 15 Time(s), 0 E(V)	
Init. Delay	<input type="checkbox"/> Off, 300 Time(s), 0.1 Stab.(mV/s)	
IR Comp	<input type="checkbox"/> Off	
Equil. Time (s)	0	

**Figure 21:** Experimental Setup for Cyclic Polarization Test

### 3.3.2 Sodium Chloride Test Solution

34 g of reagent grade NaCl was dissolved in 920 ml of distilled water making 3.56 % (by weight) Sodium Chloride solution. 900 ml of the solution was transferred into the polarization cell. It was ensured that the part of specimen remained above the solution. The temperature of the solution was brought to almost  $25 \pm 1$  °C.

### 3.3.3 Apparatus/Equipment

- Beaker
- Gamry Potentiostat
- Working Electrode (Specimen)
- Reference Electrode
- Counter Electrode

- Electrode Holder
- Thermometer

### 3.3.4 Experimental Procedures

The specimen ready for testing were cleaned in acetone and dried. It was made sure that there was no any presence of visible rough surface on the specimen. The specimen was connected to two wires (for working electrode and working sense electrode). Platinum auxiliary electrode, Reference Electrode and working electrode were placed in the Sodium Chloride solution in a test cell.

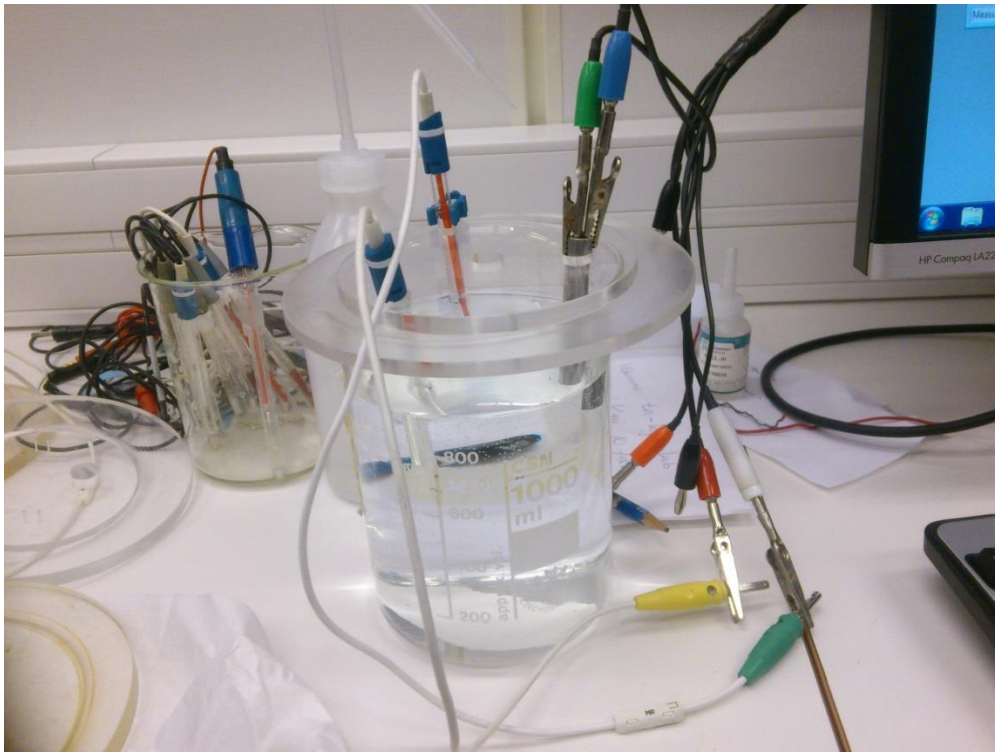


**Figure 22: Cyclic Polarization Test**

The Gamry software was started and the open circuit potential (OCP) was run for an hour. After getting OCP graph, the cyclic polarization was initiated by inserting different values for initial, peak and reverse potential. After few hours, the cyclic polarization curves were obtained. The pitting potential and critical pitting potential, repassivation potential, etc. are studied from the graph obtained.

### 3.4 Scanning Electron Microscope

Scanning Electron Microscope provides high resolution surface information and grander materials contrast. SUPRA FE-SEM was used in this project for the detection of pitting and crevice corrosion on the surface of specimen. SUPRA FE-SEM has an ultra-high resolution and is based on unique Gemini Technology. This SEM has been found to be useful for wider application in the field of materials, natural sciences, and semiconductor technology[50].

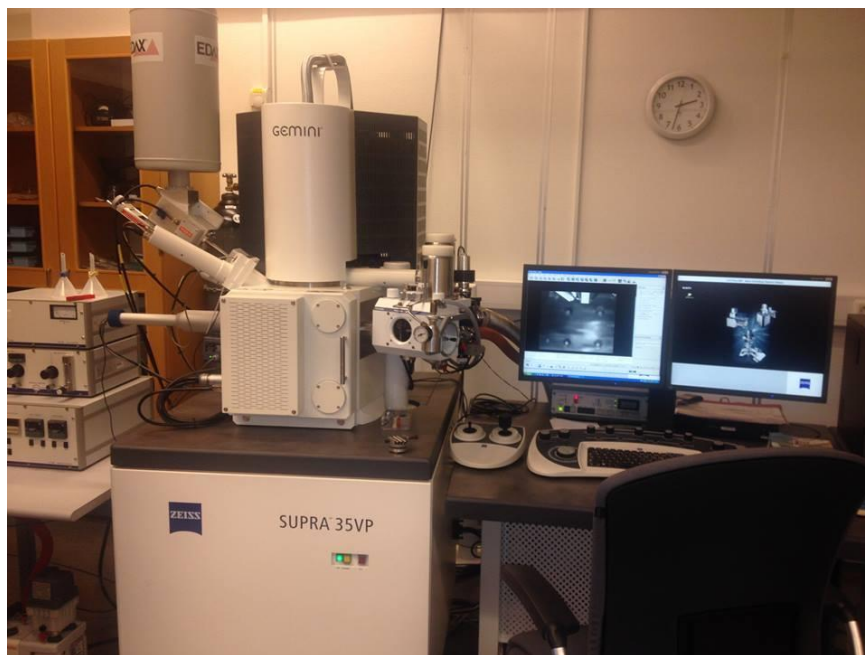


**Figure 23:** Scanning Electron Microscope

The straight and bend parts of super duplex specimens were observed on SEM. The photographs were recorded at different resolutions and observed results are shown and discussed in Results and Discussion section. The compositions of materials were also studied through this SEM. The results obtained from the observation are shown in results and discussion, and Appendix section of this report. However, the results observed are discussed in following section.

### 3.5 Hardness Measurement

The Vickers hardness method was used in this study to measure the hardness of materials. The hardness was measured before and after G48 Test. It was measured on HV10 or HV5 units based on the hardness of material. The results obtained are presented in result and discussion section.



**Figure 24:** Hardness Measurement Equipment (Struers)

## 4. RESULTS

### 4.1 Analysis of ASTM G48 Test on Duplex

The results of ASTM G48 Test performed on the Duplex UNS S32205 are presented in this section. The areas calculated for each specimen are presented in Table 11.

**Table 11:** Area Calculation for Duplex Specimens

Duplex UNS S32205	Inner Diameter (cm)	Outer Diameter (cm)	Length (cm)	Area (cm <sup>2</sup> )
Bigger Bend	0.66	0.96	12.35	63.6173
Smaller Curve	0.66	0.96	11.55	59.5458
Straight large	0.66	0.96	5.6	29.2639
Straight small	0.66	0.96	5	26.2103

The test was performed at 22°C for 24 hours under NORSOK Standard MDS-630. The weight loss per unit area for every specimen after exposure in acidic fluoride chloride solutions was calculated. Table 12 shows the weight loss per unit area for each Duplex specimen.

**Table 12:** Weight Loss per Unit Area for Duplex Specimens at 22 °C

Duplex UNS S32205	Initial Weight	Final Weight	Weight loss per unit area (g/m <sup>2</sup> )
Bigger Curve	30.9243	30.9243	0
Smaller Curve	28.67166	28.67166	0
Straight large	14.1956	14.1956	0
Straight small	12.653	12.653	0

There was no sign of corrosion on any specimen at this temperature. As it can be seen on Table 12, there was no weight loss on any of the specimen. The materials were found to be very resistant to corrosion at 22°C under acidic environment.

The second set of G48 Test was done at 30°C for 24 hours. The weight loss measured per unit area is shown in Table 13.

**Table 13:** Weight Loss per Unit Area for Duplex Specimens at 30°C

Duplex UNS S32205	Initial Weight	Final Weight	Weight loss per unit area (g/m <sup>2</sup> )
Bigger Curve	30.9243	30.919	0.833107265
Smaller Curve	28.67166	28.6706	0.178014373
Straight large	14.1956	14.1949	0.23920225
Straight small	12.653	12.65	1.144587742

There was no any visible sign of pitting corrosion on specimen after exposure at 30 °C; however, there was some weight loss. There was no any pattern found on weight loss pertaining to the size and shape of the specimen. The small straight part was found to loss more weight than other species. The bend tube with small curve (2.5ND) was seen losing the least weight. The weight losses were under the criteria of Norsok Standard MDS-630 for material acceptance which limits the acceptable weight loss to less than 4 g/m<sup>2</sup>.

The comparison of weight loss on straight and bend part of Duplex UNS S32205 after G48 Test at 30 °C are presented in Figure 25.

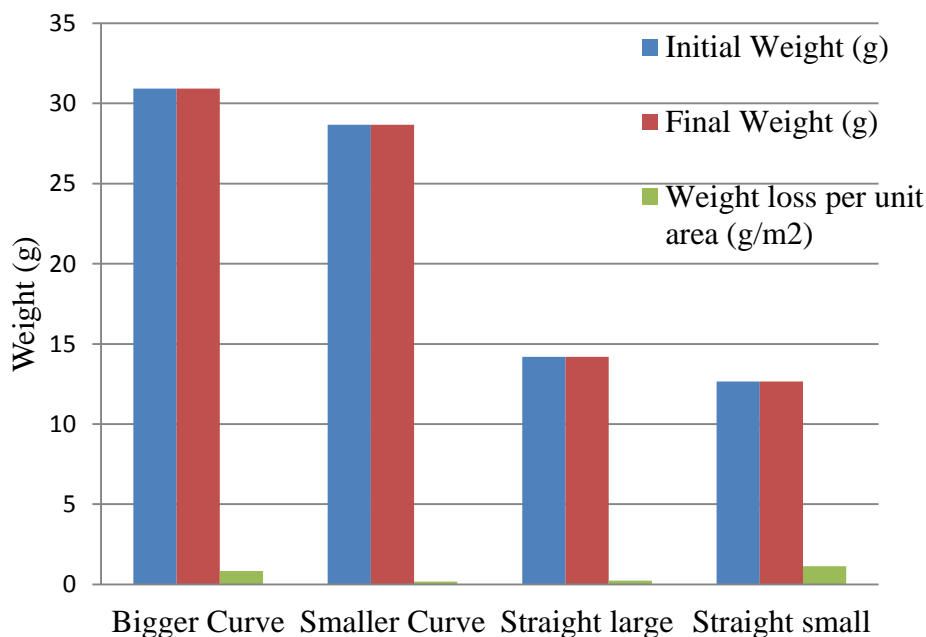


**Figure 25:** Comparison of weight loss on different specimens of Duplex



The weight was found to be lost at this temperature due to the initiation of crevice corrosion at the site of attachment of nylon wire and the metal. A very thin line of crevice was seen at that spot. But it was similar for every specimen. No any specific conclusions were drawn on relationship between shape (cold bend and straight) and pitting corrosion resistant property of the specimen. The images from SEM for Duplex are presented in Appendix.

Duplex was furthermore tested on 40 °C for 24 hours. The material heavily corroded at this temperature. There was observation of crevice corrosion on the upper side and at the spot of connection between support and materials. The result obtained at this temperature is shown in Table 14. Figure 26 illustrates the crevices formed at this temperature.

**Table 14:** Weight Loss per Unit Area for Duplex Specimens at 40°C

Duplex UNS S32205	Initial Weight	Final Weight	Weight loss per unit area (g/m <sup>2</sup> )
Bigger Curve	30.9243	30.623	47.36136204
Smaller Curve	28.67166	28.468	34.2022709
Straight large	14.1956	14.01	63.42276797
Straight small	12.653	12.523	49.59880216



**Figure 26:** Crevices on Duplex Materials

The weight loss observed from the analysis was significant (more than  $4 \text{ g/m}^2$ ). Prior to the observation, it was anticipated that the crevice corrosion formation was the reason for the initiation of very minor pits like structures. However, this condition was observed on bend and straight parts. Nylon wire played a vital role for causing crevice corrosion. Under visual inspection and while checking the strength of material by pressurizing it with a small nail, the impact was found similar on both straight and bend part. The marks made were almost identical in straight and bend parts. Also, there was no significant difference on the pattern of corrosion on straight and bend part.

After observing the corrosion on duplex at  $40 \text{ }^\circ\text{C}$ , it was decided to test a new duplex specimen at  $60 \text{ }^\circ\text{C}$ . Ferric Chloride solution was prepared and G48 test was done at  $60 \text{ }^\circ\text{C}$  for 24 hours. Figure 27 shows the corrosion on the body of straight and bend duplex tubes at  $60 \text{ }^\circ\text{C}$ .



**Figure 27:** Corrosion on the body of Duplex after exposure at  $60 \text{ }^\circ\text{C}$

#### **4.2 Analysis of ASTM G48 Test on Super Duplex**

Super Duplex UNS S32750 was tested on several temperatures with initiation from  $22 \text{ }^\circ\text{C}$ . The measured area and weight of Super Duplex specimen are shown in Table 15.



**Table 15:** Area Calculation for Super Duplex Specimens

Super Duplex UNS S32750	Inner Diameter	Outer Diameter	Length	Area
<b>Bigger Curve</b>	<b>0.5</b>	<b>0.935</b>	<b>14.794</b>	<b>67.6746</b>
<b>Smaller Curve</b>	<b>0.5</b>	<b>0.935</b>	<b>14.05</b>	<b>64.3205</b>
<b>Straight large</b>	<b>0.5</b>	<b>0.935</b>	<b>4.728</b>	<b>22.2952</b>
<b>Straight small</b>	<b>0.5</b>	<b>0.935</b>	<b>3.365</b>	<b>16.1506</b>

The result of ASTM G48 Test on Super Duplex UNS S32750 at 22°C is shown in Table 16.

**Table 16:** Weight Loss per Unit Area for Super Duplex Specimens at 22 °C

Super Duplex UNS S32750	Initial Weight (g)	Final Weight (g)	Weight loss per unit area (g/m <sup>2</sup> )
<b>Bigger Curve</b>	<b>55.5896</b>	<b>55.5896</b>	<b>0</b>
<b>Smaller Curve</b>	<b>52.8779</b>	<b>52.8779</b>	<b>0</b>
<b>Straight large</b>	<b>17.8129</b>	<b>17.8129</b>	<b>0</b>
<b>Straight small</b>	<b>12.6324</b>	<b>12.6324</b>	<b>0</b>

The material was found to be unaffected at 22 °C in acidic ferric chloride solution. There was no weight loss. The ASTM G48 and Norsok MDS-630 criteria are fulfilled by both straight and bend part of super duplex for its use in oil and gas industry. Figure 28 and Figure 29 shows the photos taken by SEM of bend and straight parts respectively of super duplex after G48 test.

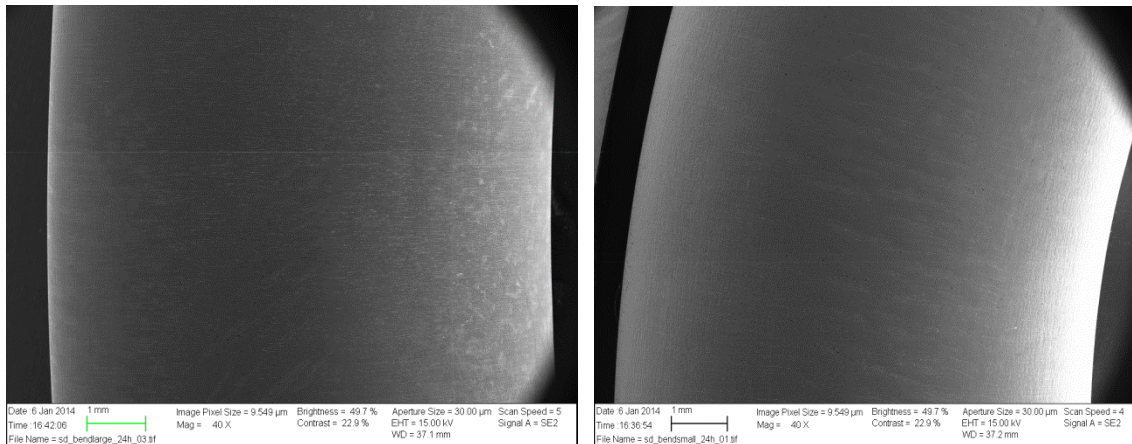


**Figure 28:** SEM Image of Super Duplex Bend Tubes after G48 Test at 22°C (Left: 5ND Bend Tubes, Right: 2.5ND Bend Tubes)

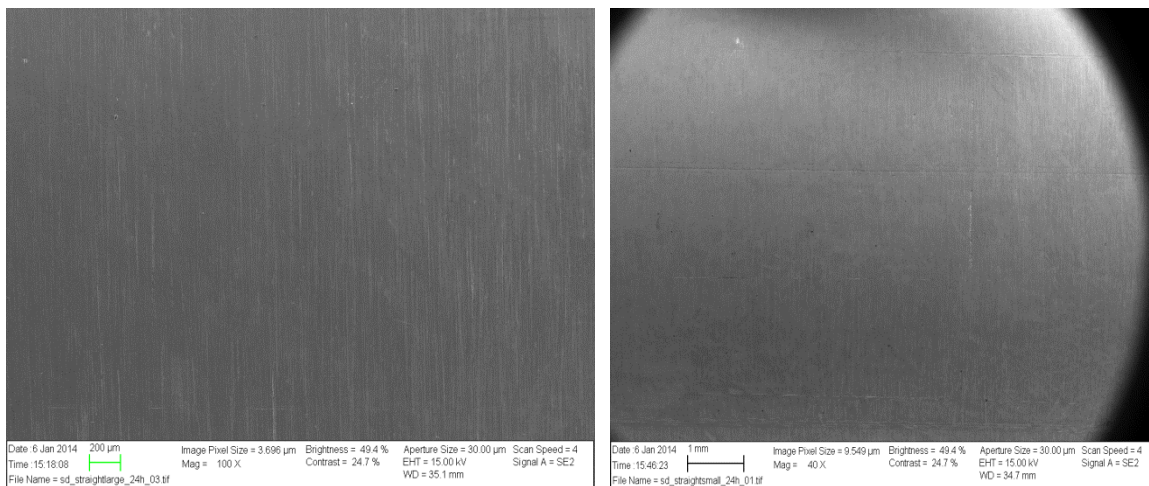


**Figure 29:** SEM Images of Super Duplex Straight tubes after G48 Test at 22°C

The images demonstrate the smooth surfaces and no any sign of corrosion on bend and straight parts of super duplex materials.

Furthermore, the results obtained after temperature was increased to 30°C are presented in Table 17.

**Table 17:** Weight Loss per Unit Area for Super Duplex Specimens at 30°C

Super Duplex UNS S32750	Initial Weight (g)	Final Weight (g)	Weight loss per unit area (g/m <sup>2</sup> )
Bigger Curve	55.5896	55.5858	0.561510245
Smaller Curve	52.8779	52.8739	0.621885296
Straight large	17.8129	17.8124	0.22426318
Straight small	12.6324	12.6316	0.495338365

There was minor weight loss in the specimens after test at 30°C. The weight loss per unit area was found to be similar for all specimens. There was no any sign of crevice corrosion. The maximum weight loss per unit area was found to be 0.62188 g for small bend and the least value was for straight with 0.49534 g. No pattern was found on the weight loss based on shape and size of materials. Figure 30 shows the comparison of weight loss on bend and straight parts of super duplex.

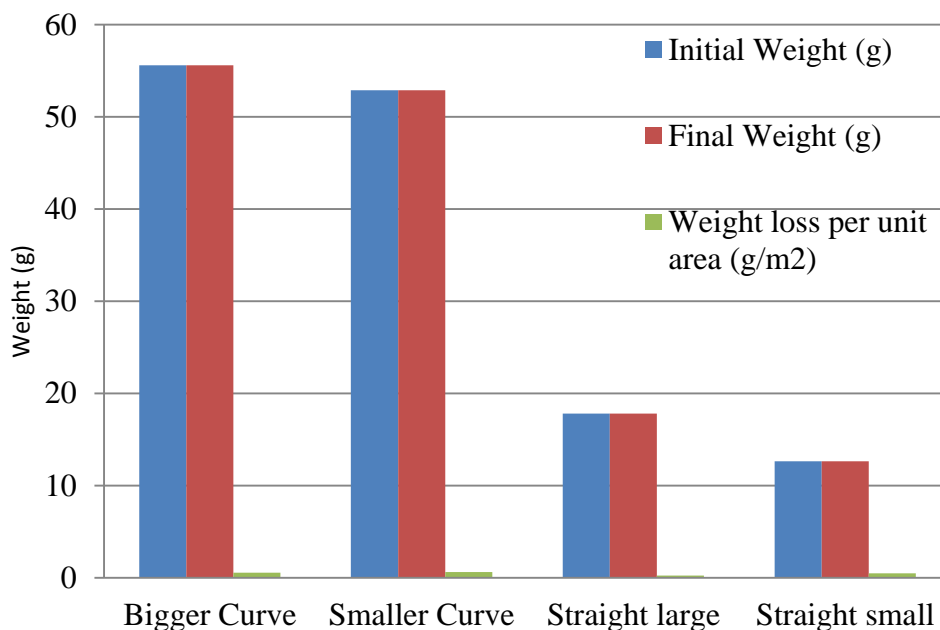


**Figure 30:** Comparison of weight loss on different specimens of Super Duplex at 30°C

Scanning Electron Microscope was used for the examination of corrosion on the material. Any sign of corrosion was not visible as illustrated in Figure 31 and Figure 32. The magnifications of 40X and/or 100X was used for visual examination. Some corrosion on the bend part was anticipated but it was not observed.

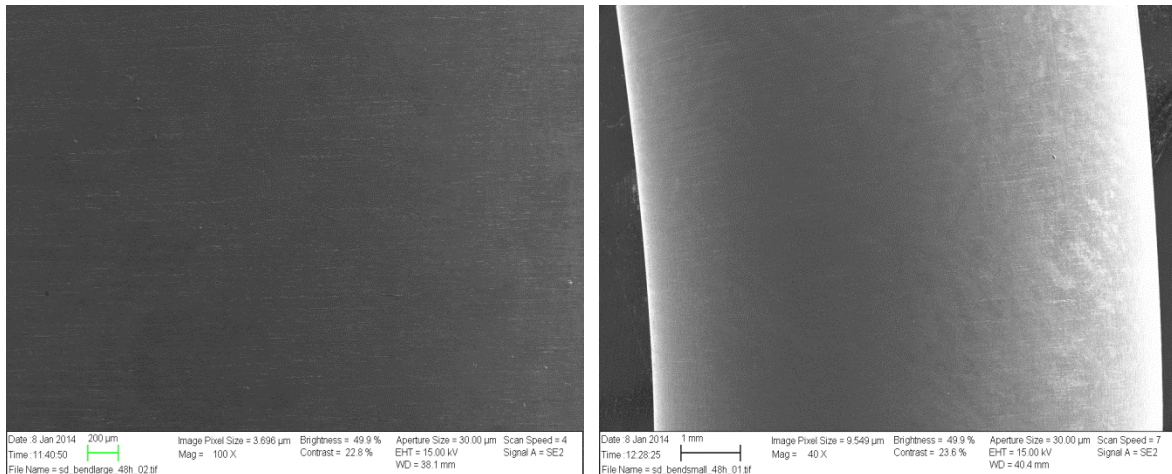


**Figure 31:** SEM Image of Super Duplex Bend Tubes after G48 Test at 30°C (Left: 5ND Bend Tubes, Right: 2.5ND Bend Tubes)

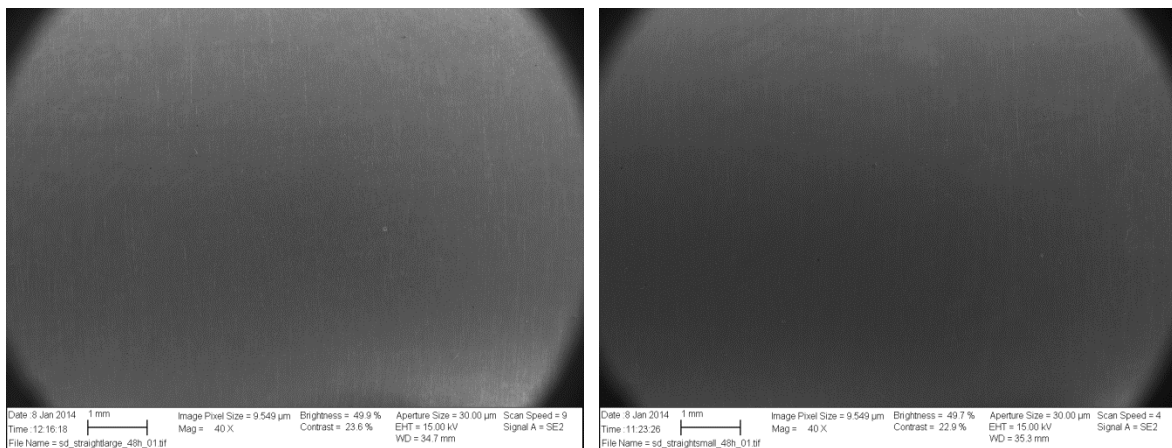


**Figure 32:** SEM Image of Super Duplex Straight Tubes after G48 Test at 30°C

The temperature was further increased to 40°C, and the results obtained are presented in Table 18.

**Table 18:** Weight Loss per Unit Area for Super Duplex Specimens at 40°C

<b>Super Duplex UNS S32750</b>	<b>Initial Weight (g)</b>	<b>Final Weight (g)</b>	<b>Weight loss per unit area (g/m<sup>2</sup>)</b>
<b>Bigger Curve</b>	<b>55.5896</b>	<b>55.503</b>	<b>12.79652295</b>
<b>Smaller Curve</b>	<b>52.8779</b>	<b>52.7586</b>	<b>18.54772896</b>
<b>Straight large</b>	<b>17.8129</b>	<b>17.7506</b>	<b>27.94319226</b>
<b>Straight small</b>	<b>12.6324</b>	<b>12.6145</b>	<b>11.08319592</b>

There was no observation of any pitting corrosion, but weight loss was calculated to be more than 4 g/m<sup>2</sup>. The large straight specimen was found to be losing maximum weight (18.54 g per square meter) and small straight was observed to have lost the least weight (11.08 g/m<sup>2</sup>). After the experiment it was noticed that there was decrement in the level of ferric chloride solution. The water evaporated from the solution through the vent. It was not expected to happen. Though, no any pitting was seen, there was a presence of thin wire like crevice structure, observed as a thin line on the surface of the tube. It was observed on the spot of hanging on Super Duplex. Nylon wire used for supporting super duplex material on ferric chloride solution was a reason for crevice corrosion on the surface. Figure 33 compares the weight loss of Super Duplex specimen at 40°C.



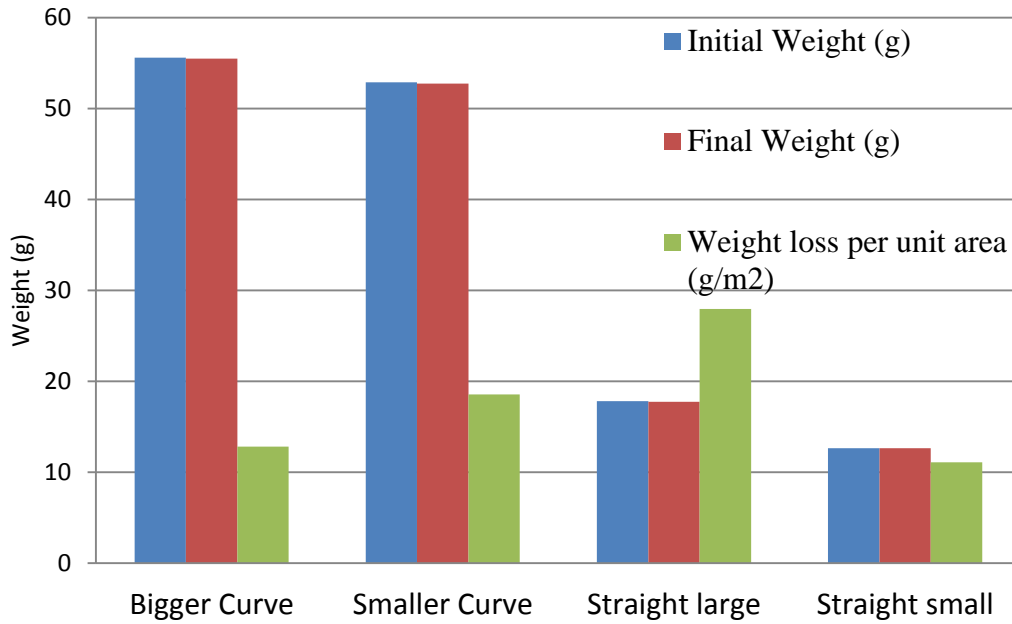


**Figure 33:** Comparison of weight loss on different specimens of Super Duplex at 40°C

The material was further taken for observation under scanning electron microscope.

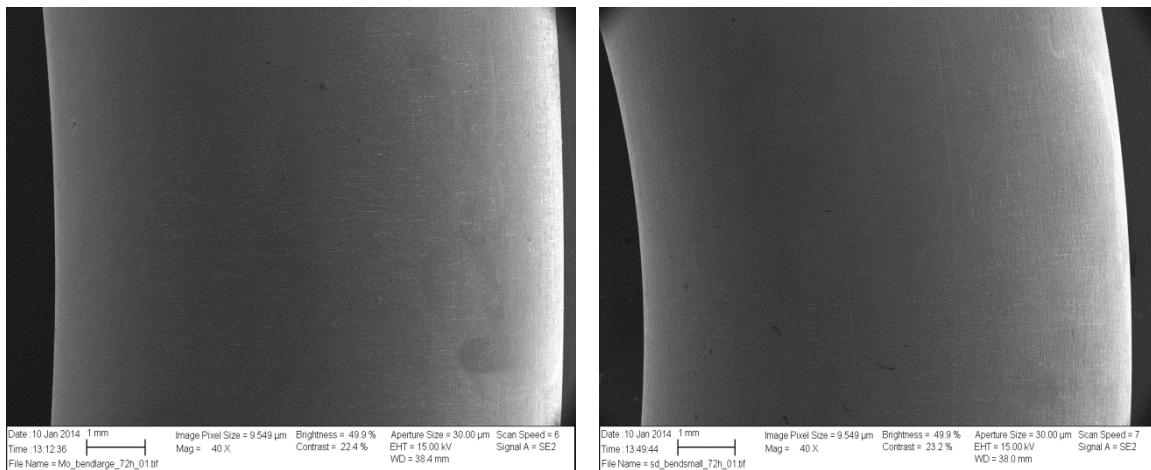


**Figure 34:** SEM Image of Super Duplex Bend Tubes after G48 Test at 40°C (Left: 5ND Bend Tubes, Right: 2.5ND Bend Tubes)

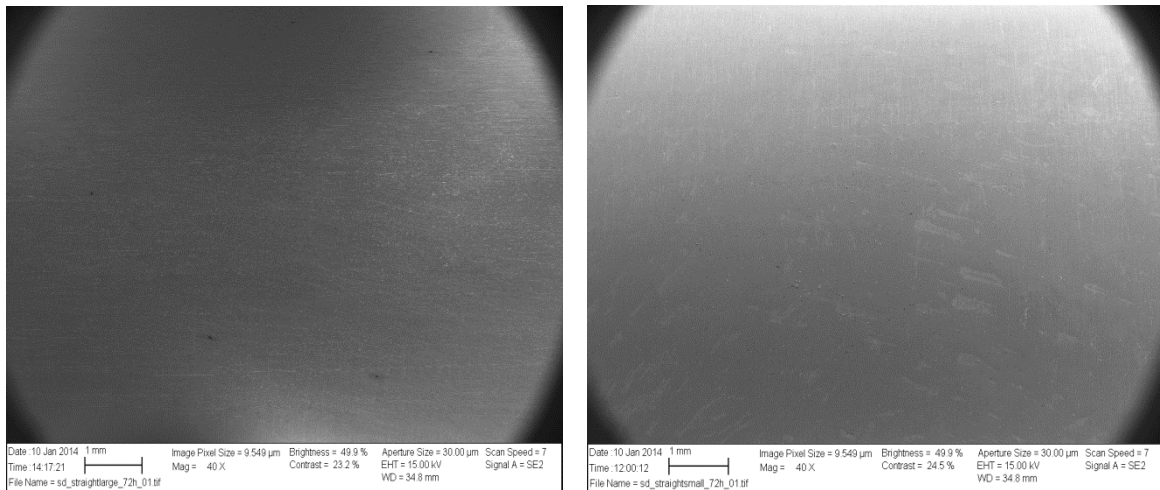


**Figure 35:** SEM Image of Super Duplex Straight Tubes after G48 Test at 40°C

As it can be seen in Figure 34 and Figure 35, there was no any pitting corrosion on the super duplex material. The critical pitting temperature was found to be more than 40 °C. The crevice corrosion was seen to be initiating at about 40 °C, making critical crevice temperature at a temperature range of about 40°C.

This series of experiments were ended after 96 hours of testing. The final exposure temperature was 50°C. In this temperature, the weight loss was found to be much more than 4 g/m<sup>2</sup>. The possible reasons for this observation have been discussed in Discussion section. The result obtained is shown in Table 19.

**Table 19:** Weight Loss per Unit Area for Super Duplex Specimens at 50°C

Super Duplex	Initial Weight (g)	Final Weight (g)	Weight loss per unit area (g/m <sup>2</sup> )
<b>UNS S32750</b>			
<b>Bigger Curve</b>	<b>55.5896</b>	<b>54.7501</b>	<b>124.0494343</b>
<b>Smaller Curve</b>	<b>52.8779</b>	<b>51.865</b>	<b>157.4769041</b>
<b>Straight large</b>	<b>17.8129</b>	<b>17.296</b>	<b>231.8432757</b>
<b>Straight small</b>	<b>12.6324</b>	<b>12.3426</b>	<b>179.4363227</b>

There was significant crevice corrosion on the material. Figure 36 compares the corrosion on straight and bended part at 50°C.

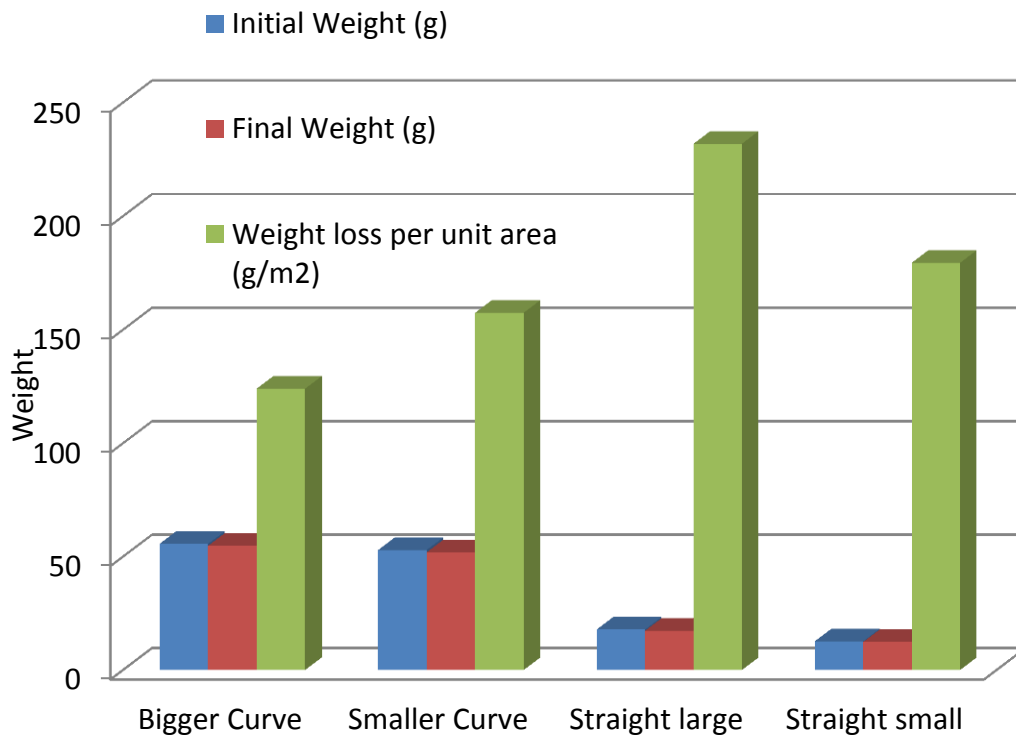


**Figure 36:** Comparison of weight loss on different specimens of Super Duplex at 40°C

The Figure 37, 38 and 39 illustrates the corrosion on super duplex at 50°C. These were the samples started to be treated from 22 °C.

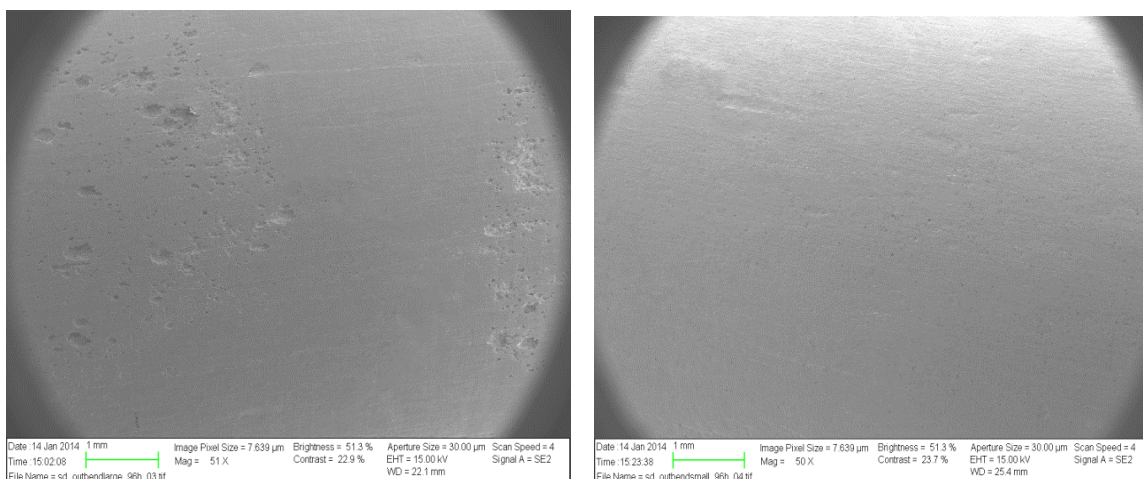


**Figure 37:** SEM Image of Super Duplex Bend Tubes after G48 Test at 50°C (Left: 5ND Bend Tubes, Right: 2.5ND Bend Tubes)



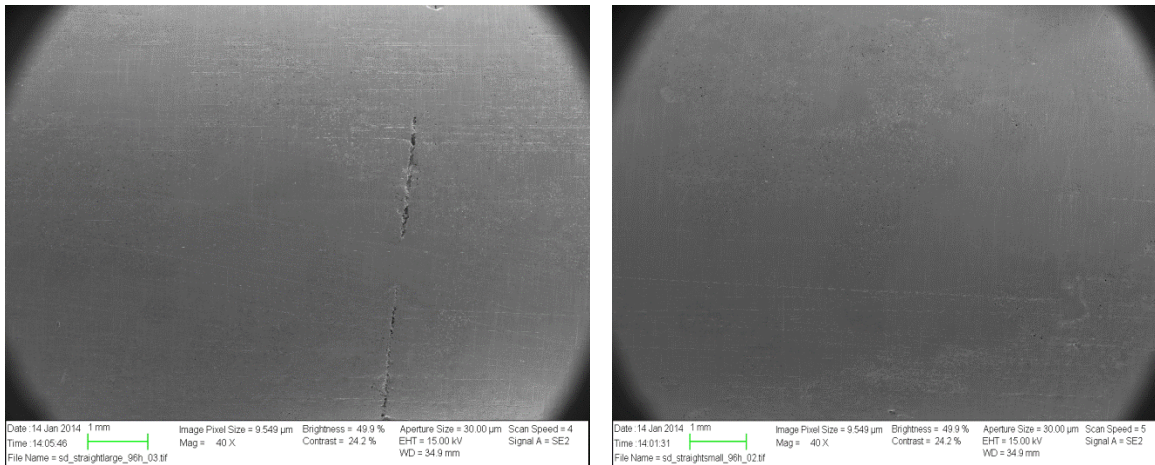


**Figure 38:** SEM Image of Super Duplex Straight Tubes after G48 Test at 50°C

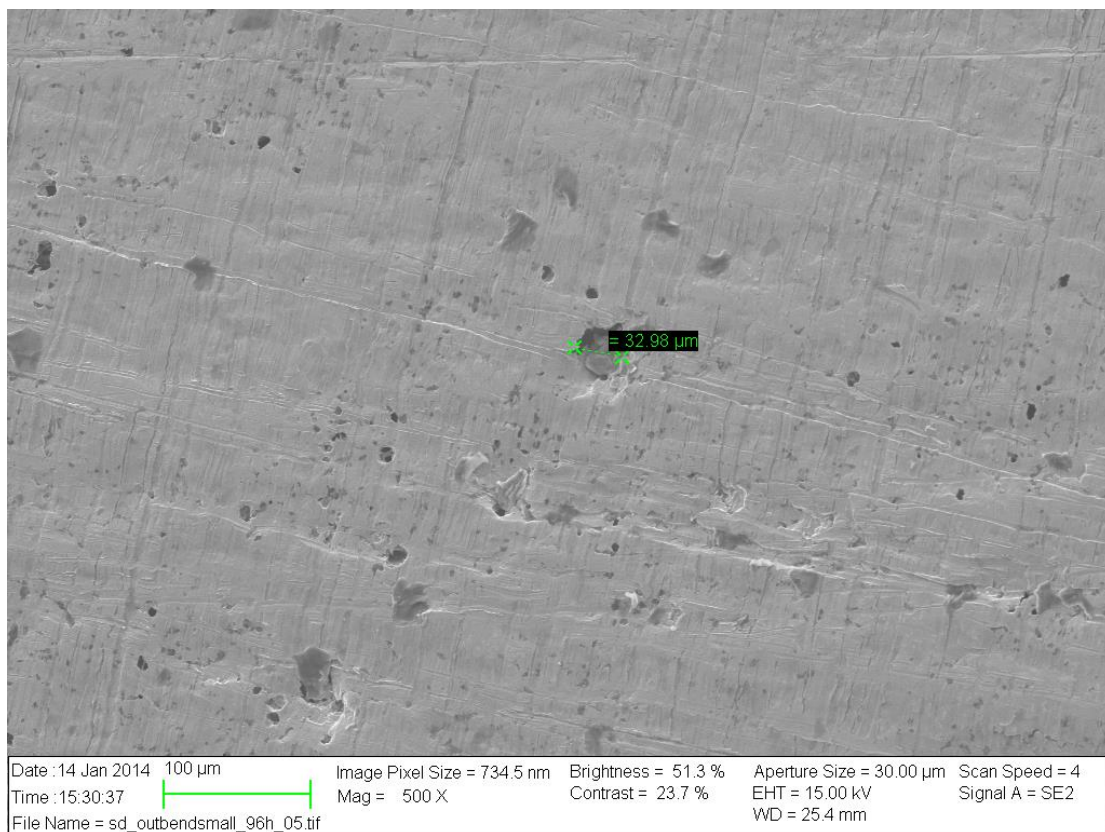


**Figure 39:** SEM image of Super Duplex 2.5ND Bend Tube at 500X Magnification

Figure 37 and Figure 38 show the presence of crevice corrosion on the surface of super duplex material. However, the pitting corrosion was not observed under 40X and 100X

magnifications. Super Duplex was observed to have very high resistance for pitting corrosion even at 50°C. Under 500X magnification, a pit of 32.98µm was noticed on a bend tube but it is of very small size to perceive any conclusion or make any decision out of it. There was not much variation in the structure of straight part and bend parts observed under 40X and 100X magnifications.

After these experiments and results, the final set up of G48 Test was performed considering all the experiences from past experiments. This final test was performed with more precision. The samples were prepared and directly exposed at 50 °C in ferric chloride solution for 24 hours. The area of the super duplex specimen calculated is shown in Table 20.

**Table 20:** Area Calculation for Super Duplex Specimen

Super Duplex	Inner diameter(cm)	Outer Diameter(cm)	Length(cm)	Area
Bigger Curve	0.5	0.935	12.5	57.33285
Smaller Curve	0.5	0.935	12.05	55.30417
Straight large	0.5	0.935	5	23.52146
Straight small	0.5	0.935	4.2	19.91491

The initial weight of the specimens was measured. After G48 Test was completed, final weight was measured and the weight loss per unit area was calculated. The results are shown in Table 21.

**Table 21:** Weight Loss per Unit Area for Super Duplex Specimens at 50°C

Super Duplex	Initial Weight(g)	Final Weight (g)	Weight Loss per unit area (g/m <sup>2</sup> )
Bigger Curve	42.7361	42.7275	1.500012518
Smaller Curve	40.7302	40.7294	0.14465455
Straight large	16.9456	16.9412	1.870632163
Straight small	14.2094	14.2088	0.301281781

No pitting corrosion was observed on the surface of the specimen. The weight loss per unit area was calculated and it was found to be in the range of acceptance. There was no any difference in the weight loss at straight and bend part of the tubes. The cold deformed parts (2.5 ND and 5 ND) were found to be resistant to pitting corrosion. In line with the result of the previous experiment, there was a presence of minor crevice corrosion at the connection point of nylon wire and metal. However, no any conclusion could be drawn on the issue that cold deformed tubes can cause high pitting corrosion. Figure 40 compares the weight loss for super duplex specimen after testing at 50°C.

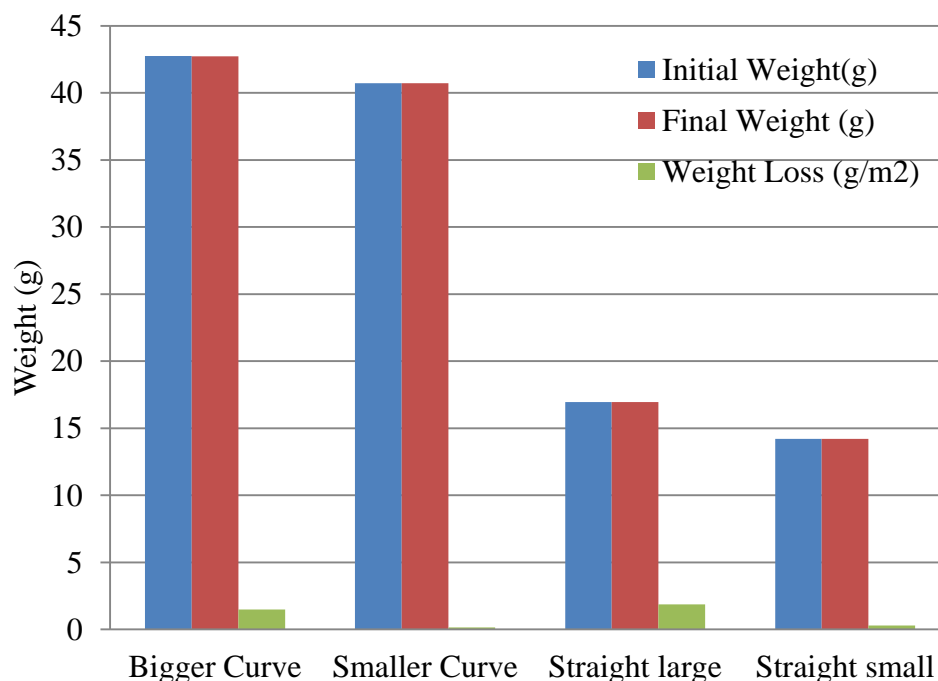


**Figure 40:** Comparison of weight loss on different specimens of Super Duplex at 50°C

As in the Figure 40, it can be seen that the bigger bend and large straight were found to be losing more weight; however, the loss was not significant compared to weight loss from other specimens.

These tested super duplex were again tested at 60 °C. At this temperature, some evidence of pitting corrosion on the metal was found. The materials were found to be weakened, especially at the site of connection of wire. Table 22 shows the weight loss per unit area for Super Duplex specimen at 60 °C.

**Table 22:** Weight loss per Unit area for Super Duplex at 60°C

Super Duplex	Initial Weight(g)	Final Weight (g)	Weight Loss per unit area (g/m <sup>2</sup> )
Bigger Curve	42.7361	41.896	146.5303
Smaller Curve	40.7302	39.86	157.348
Straight large	16.9456	16.3205	265.7573
Straight small	14.2094	13.869	170.9272

Figure 41 compared the weight loss per unit area between the straight and bended part of super duplex at 60 °C.

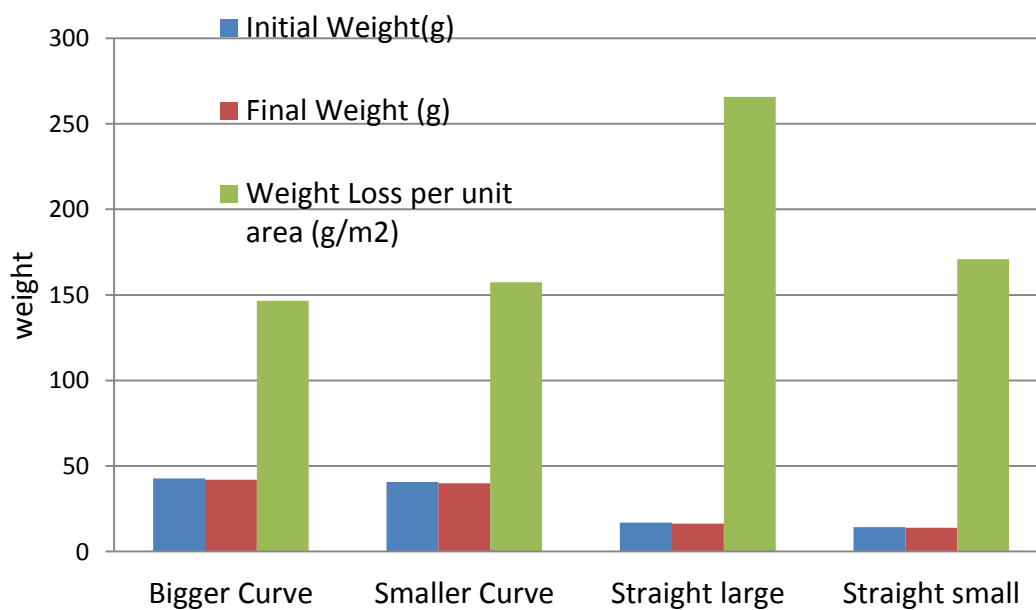


**Figure 41:** Comparison of weight loss on different specimens of Super Duplex at 60°C

Figure 42 illustrates the corrosion on the surface of super duplex after exposure at 60 °C.

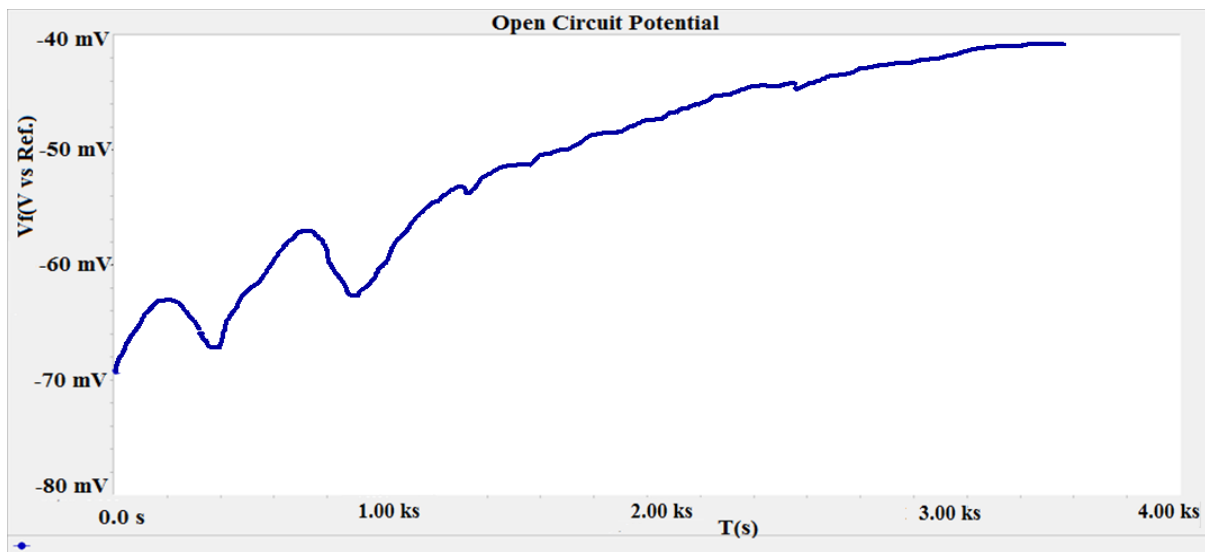


**Figure 42:** Super Duplex specimens after G48 Test at 60°C

At this temperature, it can be observed in Figure 42 that the bended parts suffered from high corrosion than the straight part. Though the weight loss was not observed higher for bend than straight, the bended parts were found to be quite fragile and the area of corrosion was seen more than straight part. This temperature limit was much higher than standard temperature for testing which makes it very corrosive. Thus, finally the bended part and straight part at very high temperature (60°C) showed its difference in corrosion property.

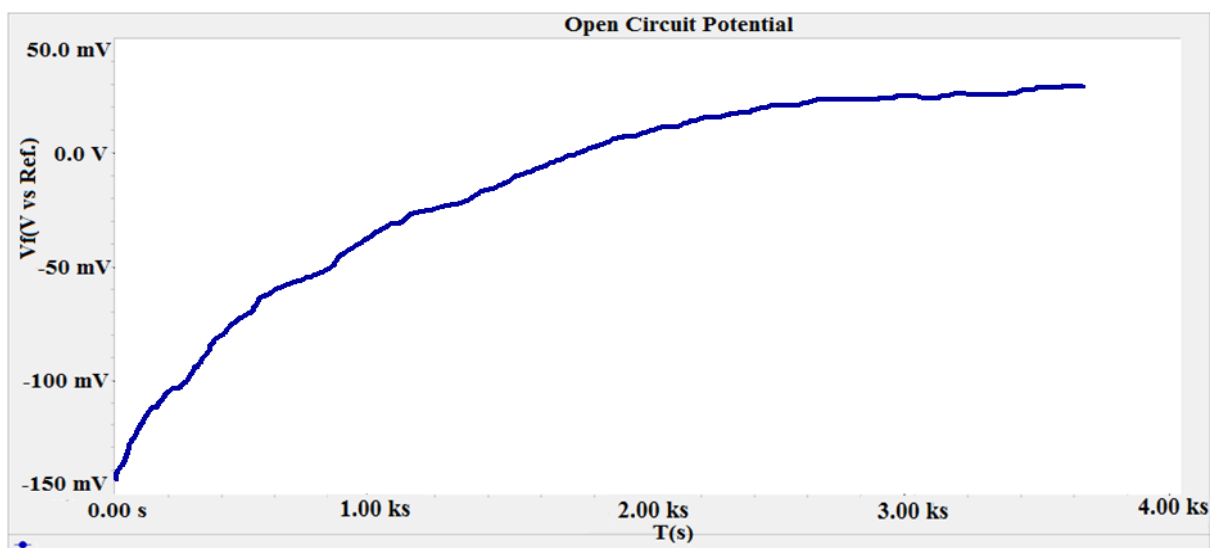
### 4.3 Analysis of ASTM G61 on Duplex

The ASTM G61 Test was performed to identify the pitting corrosion potential for straight and bend part of Duplex material. The objective was to see the difference and compare the pitting potential for straight and bend parts. Before the initiation of cyclic polarization, the open circuit potential (OCP) was run for one hour. The OCP obtained for straight, 5ND and 2.5ND Bend tubes are shown in Figures 43, 44 and 45.



Curve(DuplexOCP(30,01)DTA)

**Figure 43:** Open Circuit Potential of Straight Duplex Tube



Curve (Duplex.B.Bend.OCP(30,01).DTA)

**Figure 44:** Open Circuit Potential of 5ND Bend Duplex Tube



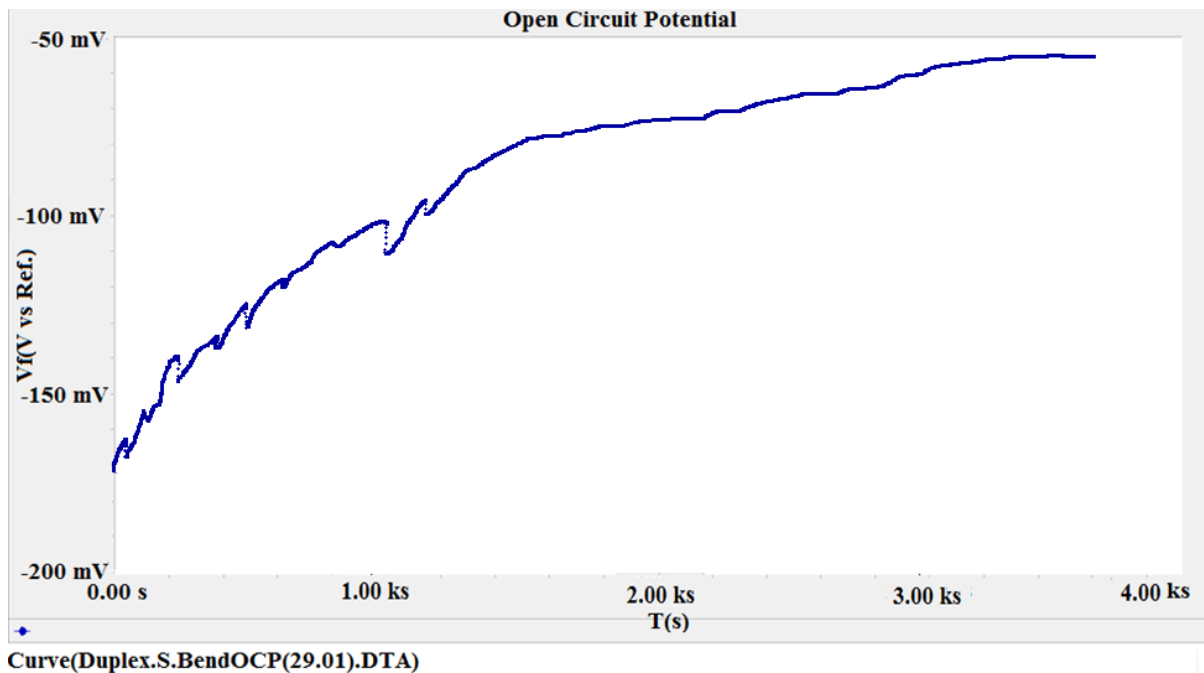


**Figure 45:** Open Circuit Potential of 2.5ND Bend Duplex Tube

The open circuit potential is the potential assumed by the metal in the absence of electrical connection to it. Sufficient time should be given to stabilize the potential for the specimen. For every specimen, the open circuit potential was run for an hour. The open circuit potential of Straight Duplex pipe shows that its corrosion potential is about -40 mV. There was variation of potential in the beginning up to 1500 s, and afterwards it increases steadily to -40mV. For Bigger Bend of Duplex, the corrosion potential was observed to be about 25 mV. Similarly, the smaller bend was found to have the potential nearing -50 mV. Among the three specimen of duplex, Bigger Bend Duplex material was found to have high corrosion potential. The fluctuation of the graph data at the beginning period was anticipated due to some noise in the experiment. However, it rose steadily after some period for all three specimens.

After obtaining open circuit potential curve and after knowing the corrosion potential of the materials, the potentiodynamic polarization scan was initiated. The Potential vs current was run and the results were interpreted to know the difference in critical pitting potential for straight, smaller bend and larger bend. Figures 46, 47 and 48 illustrate the Cyclic Polarization Curve for Straight, 5ND and 2.5ND Bend Duplex Tubes.

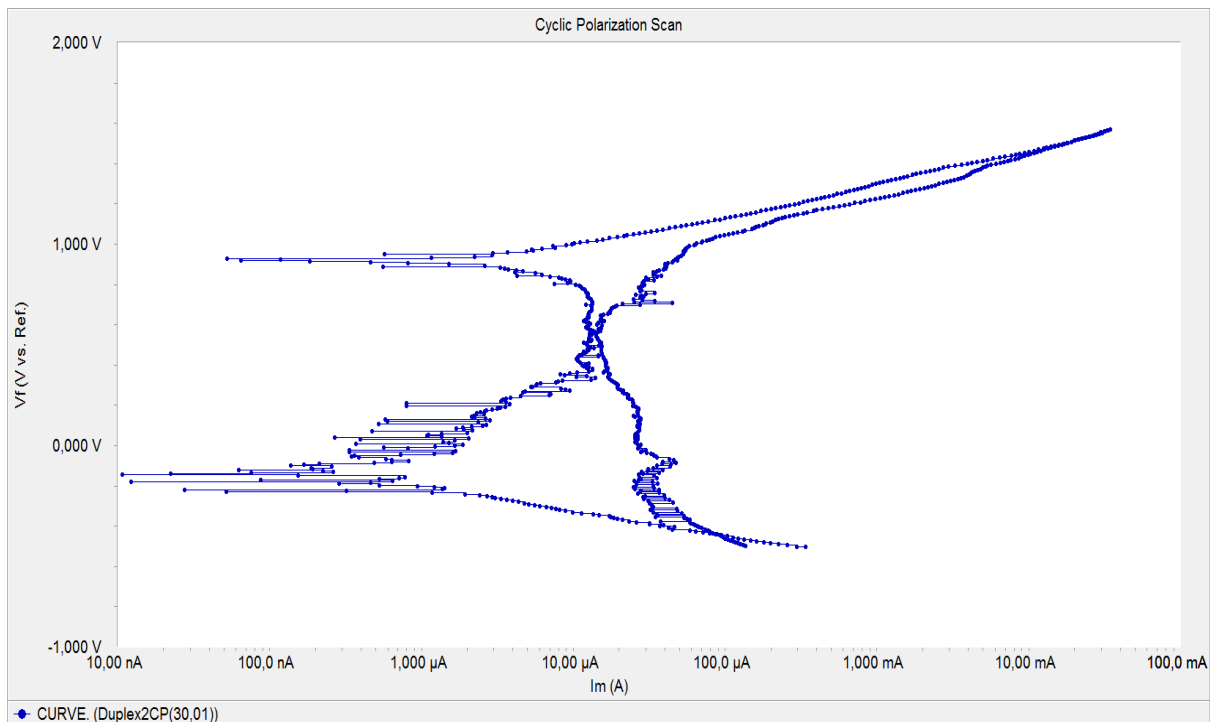


**Figure 46:** Cyclic Polarization Curve for Straight Duplex Tube

In Figure 43, it can be seen that the potential increment in polarization curve was not steady. There was much fluctuation in potential until it reached 0.4 V. Furthermore, the curve was observed to be quite stable than before. However, there was also evidence of transient burst of anodic current and metastable pit formations are supposed to be responsible for this action. The pitting potential was detected to be about 1 V. There was no observation of hysteresis in the curve.



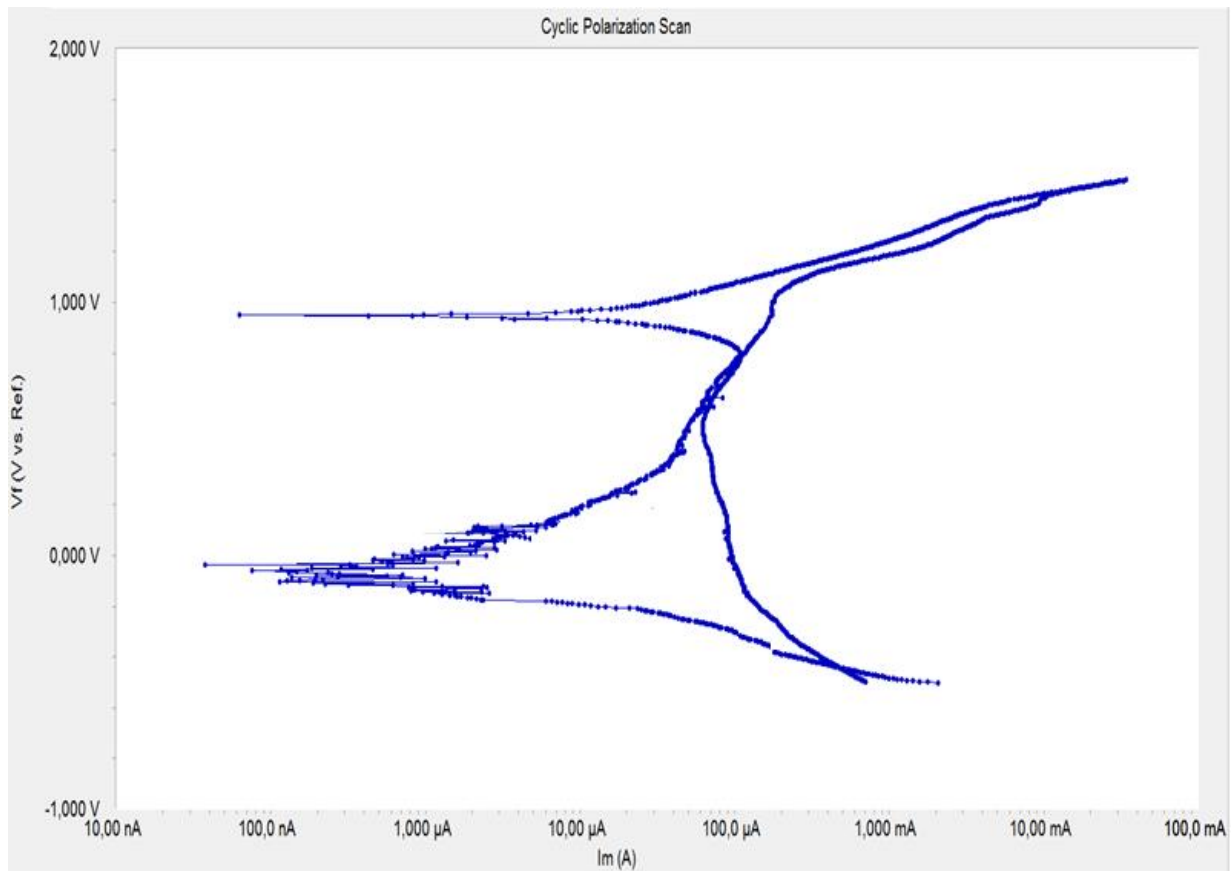


**Figure 47:** Cyclic Polarization Curve for Straight, 5ND Bend Duplex Tube

In Figure 44, for the cyclic polarization curve for Bigger (5ND) Bend Duplex material, there was absence of hysteresis curve. The graph was found to be steadier with minimal noise and minimal formation of metastable pits. The pitting potential was clearly observed at about 1 V.

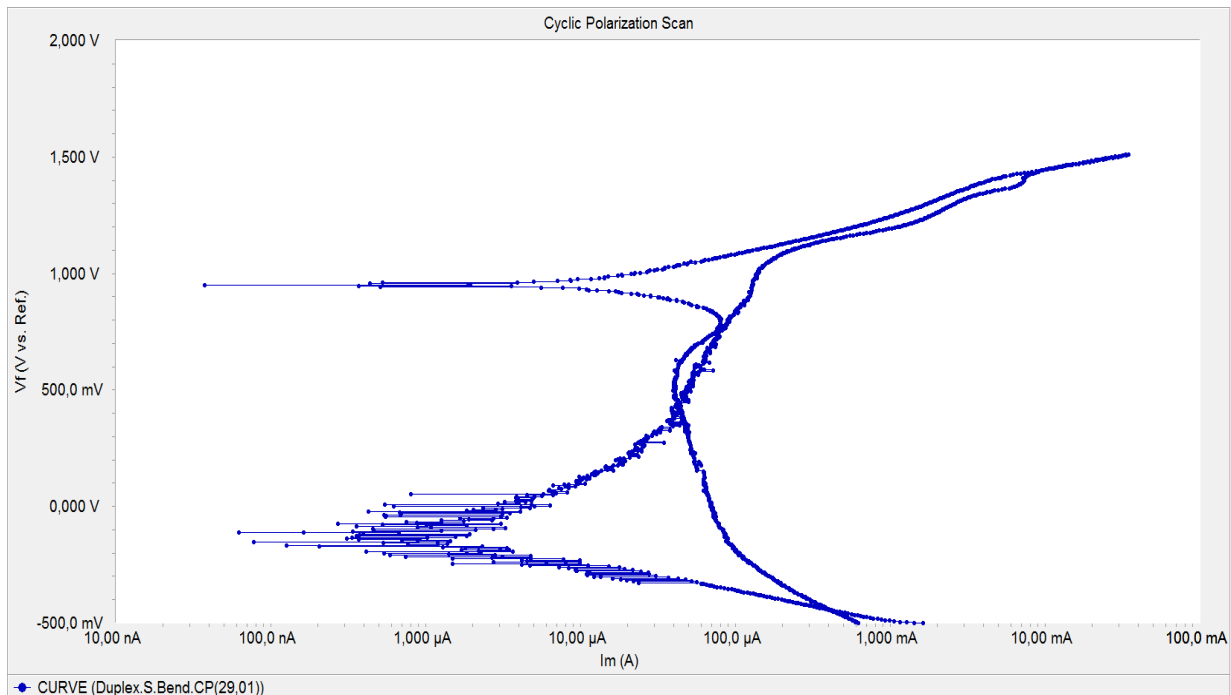
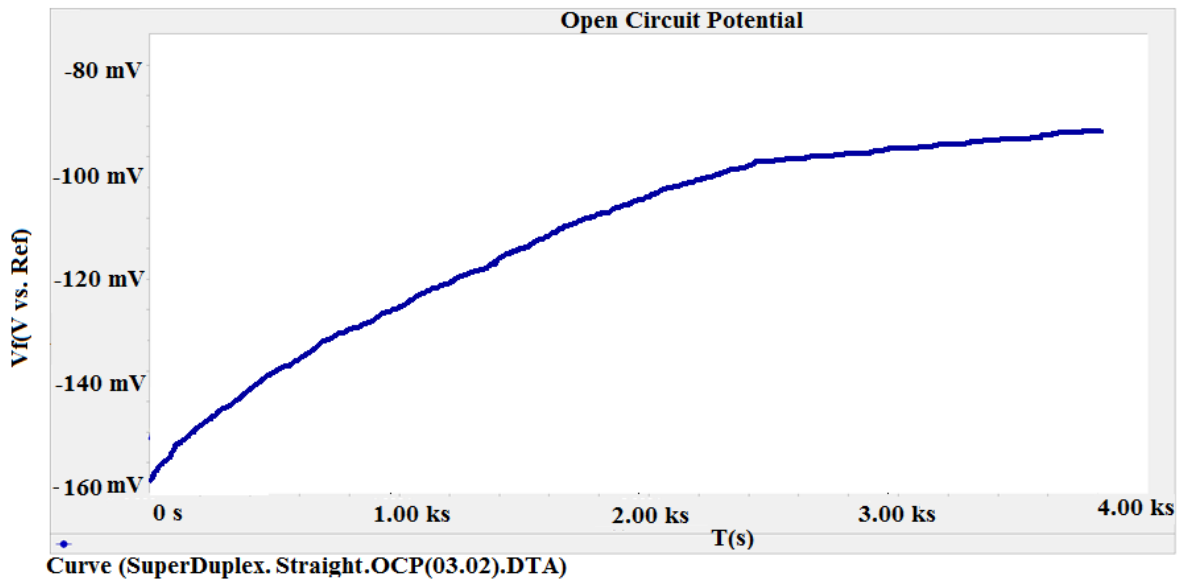


**Figure 48:** Cyclic Polarization Curve for 2.5ND Bend Duplex Tube

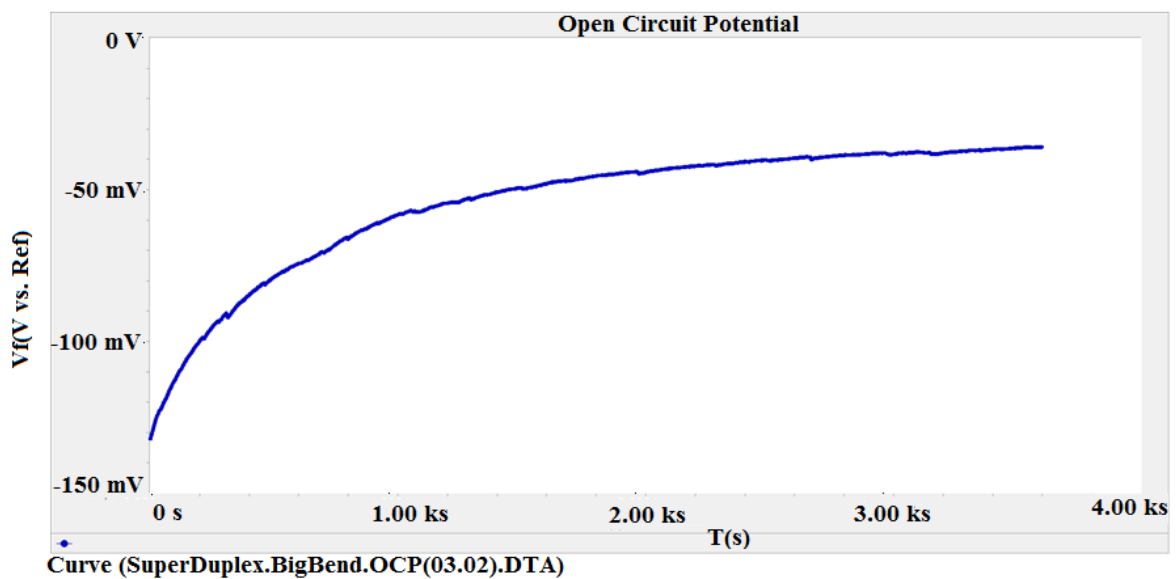
In Figure 45, the pitting potential was also observed to be at about 1 V. There was no hysteresis observed on the plot. The fluctuation in the potential was observed at the beginning which can be attributed either to the noise or to the metastable pits. No significant differences were found in the pitting potential obtained from three specimens of Duplex material. Also, the bend and straight parts behaved in a similar manner with some fluctuation in potential at the beginning and yielding no any hysteresis loop.

#### 4.4 Analysis of ASTM G61 on Super Duplex

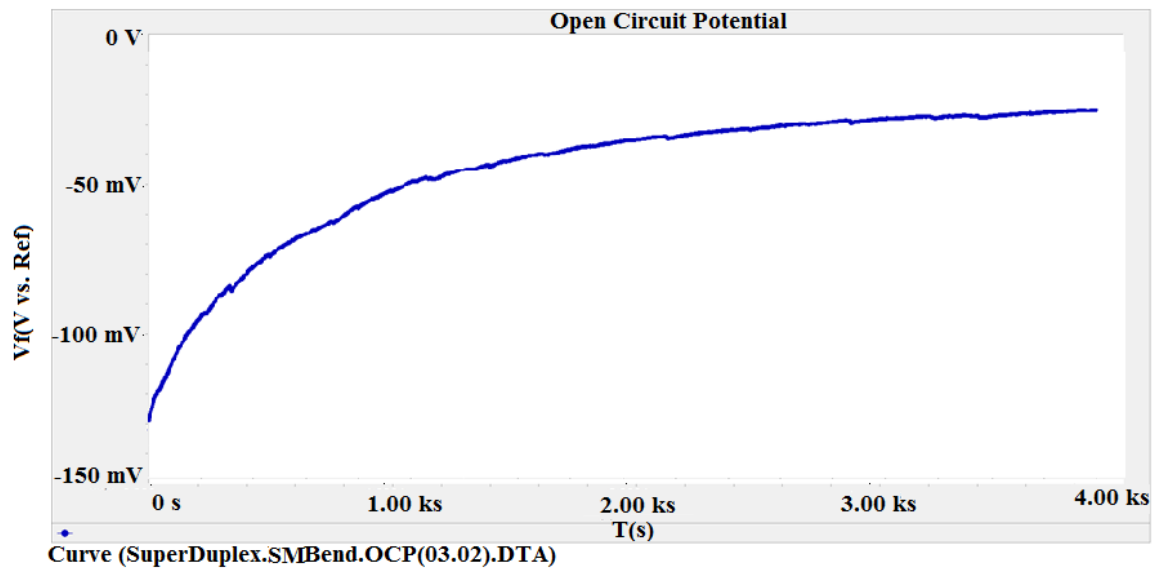
The open circuit potential curves for three types of super duplex specimen, Straight, Bigger Bend and Smaller Bend are shown in Figures 49, 50 and 51.



**Figure 49:** Open Circuit Potential of Straight Super Duplex Tube

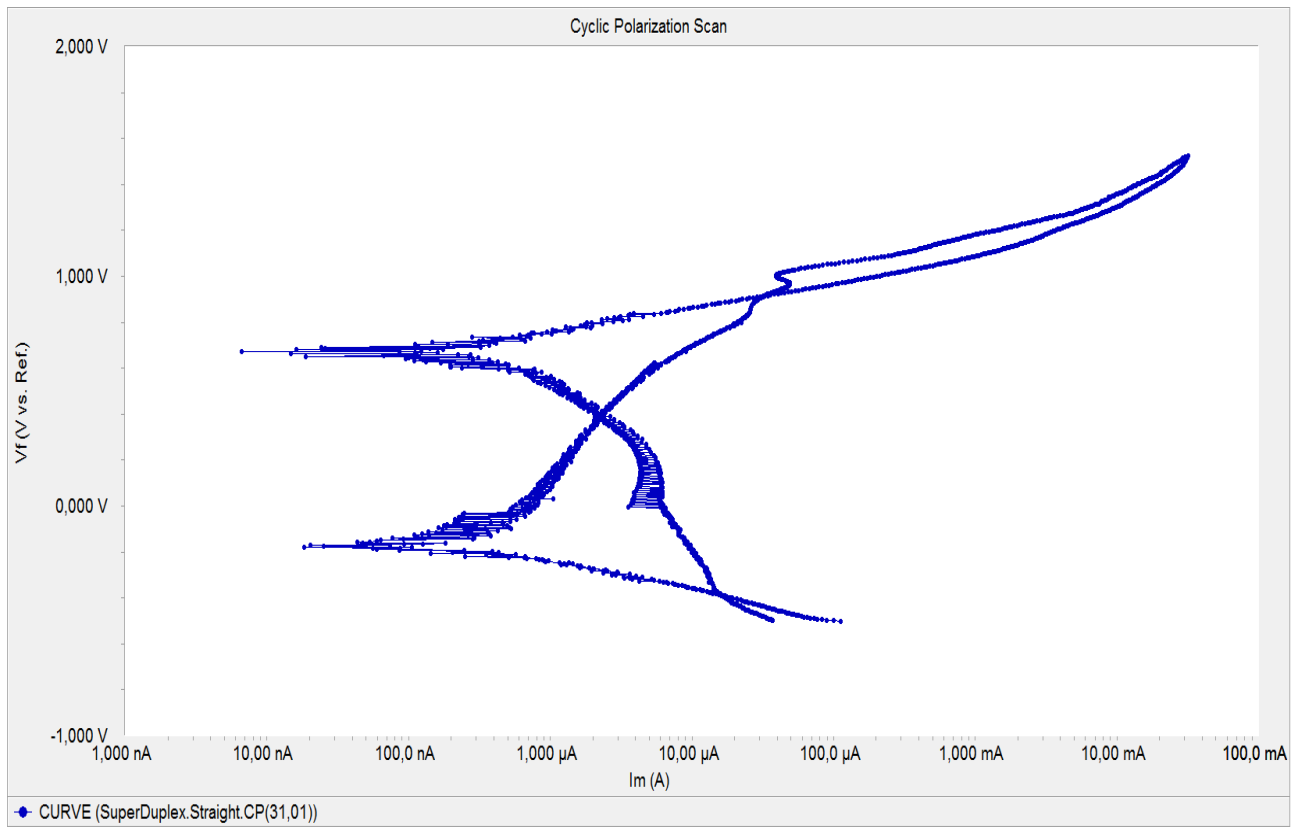


**Figure 50:** Open Circuit Potential of 5ND Bend Super Duplex Tube



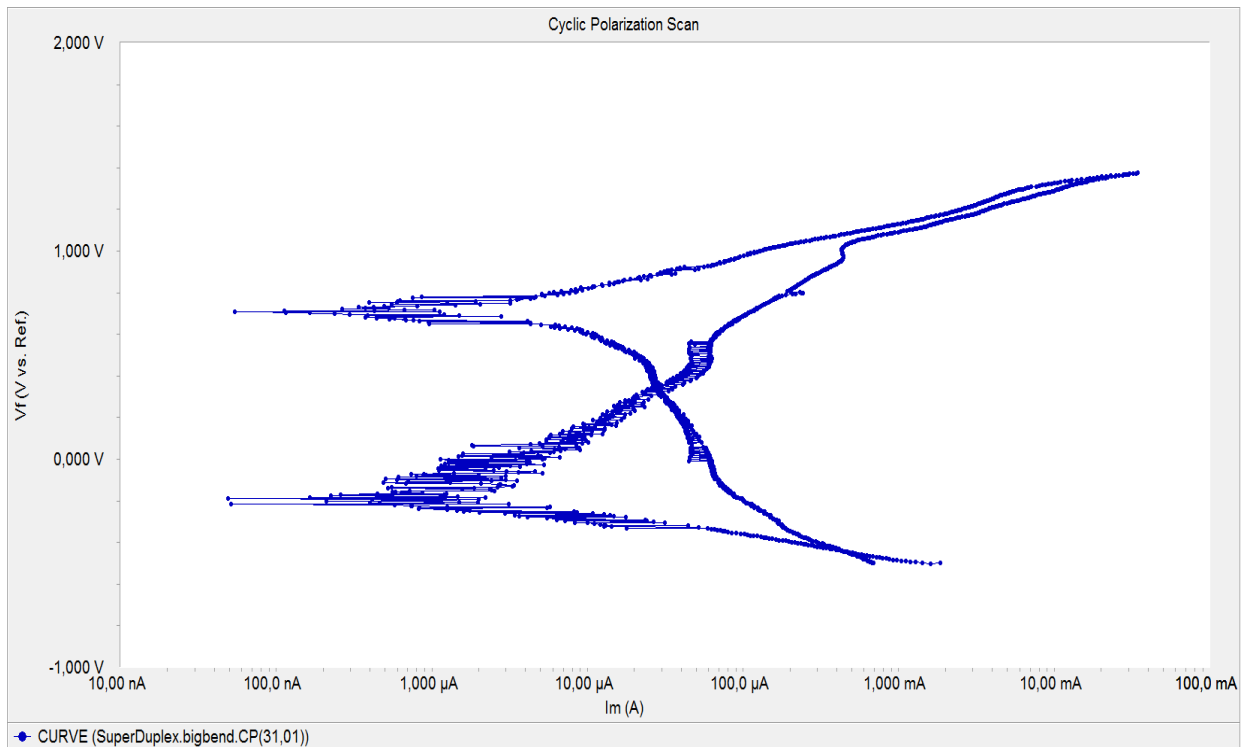
**Figure 51:** Open Circuit Potential of 2.5ND Bend Super Duplex Tube

It can be seen that the OCP for three specimens were steadily increased from the beginning. OCP curves for Super Duplex were very smooth and there was no any evidence of noise during the experiment. The corrosion potential for the straight super duplex was about -90 mV. Similarly, the corrosion potential for bigger bend and smaller bend was about -40 mV. The corrosion potential for the bended parts was found to be higher than the straight part. After one hour run of OCP, the potentiodynamic polarization scan was initiated. The graphs obtained for each specimen are presented in Figures 52, 53 and 54.



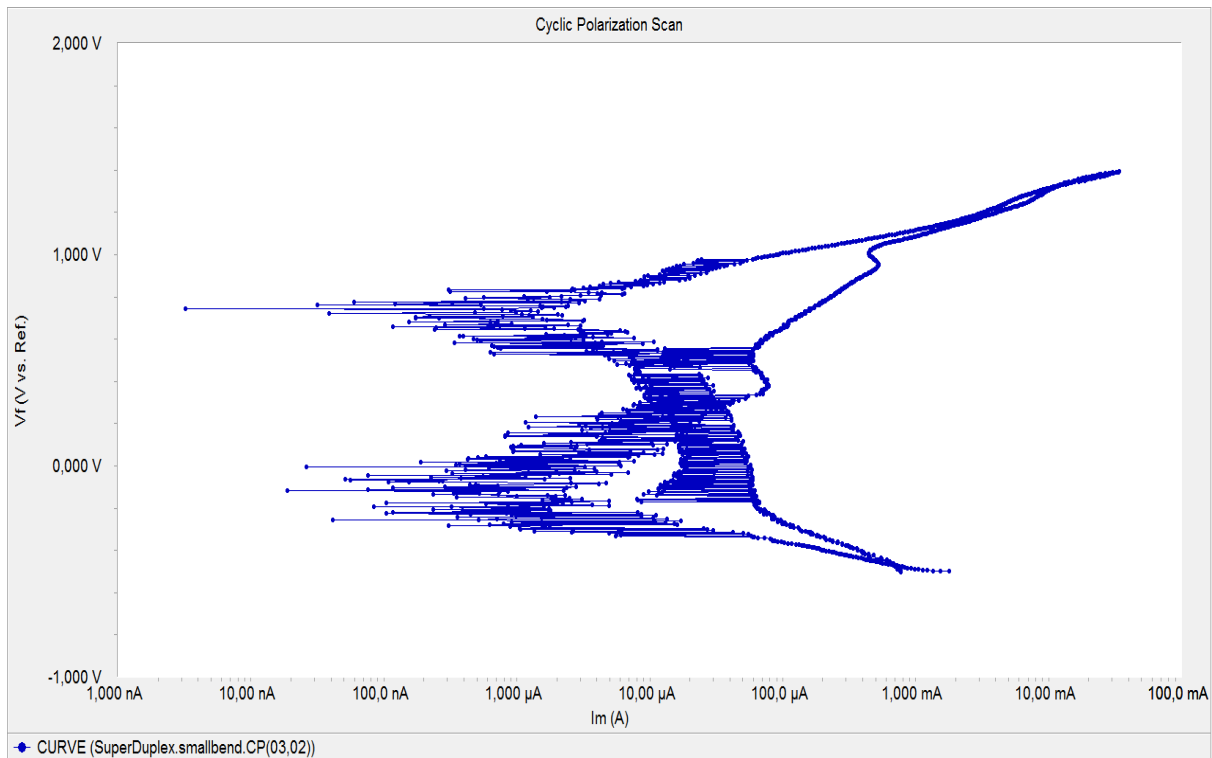
**Figure 52:** Cyclic Polarization Curve for Straight Super Duplex Tube

Figure 52 shows that there is a formation of hysteresis for straight part of super duplex. However, the area of hysteresis is very low which means the material is highly resistant to crevice corrosion. The pitting potential was found to be at about 1V. The repassivation potential was found to be at 0.9 V.



**Figure 53:** Cyclic Polarization Curve for 5ND Bend Super Duplex Tube

The plot for bend tube was not found to be as smooth as that for straight super duplex tubes. Some noise and/or some formation of metastable pits were observed during the experiment. The pitting potential was observed to be at about 1 V. The hysteresis loop was not present on the plot.



**Figure 54:** Cyclic Polarization Curve for 2.5ND Bend Super Duplex Tube

The plot for smaller curved super duplex bend was found to be more disturbed than previous two materials' plot. It was deduced that the noise during the experiment was responsible for the fluctuation of potential. Also the presence of metastable pits was anticipated for variation in potential. The pitting potential as well was observed in this case as well at about 1 V. There was no hysteresis formed.

The super duplex materials were found to be highly resistant to the crevice corrosion. The pitting potential for all three materials were found to be in the range of about 1 V.

The cyclic polarization curves with Potential vs. current density are shown in Appendix. The pitting potential at different current density observed from the cyclic polarization curves are presented in Table 23.



**Table 23:** Pitting Potential for different specimens

SN	Material	Pitting Potential (V)	Corresponding Current density (mA/cm <sup>2</sup> )
1	Duplex 2.5 ND	1	10 <sup>-5</sup>
2	Duplex 5ND	1.05	10 <sup>-5</sup>
3	Duplex Straight	1.05	10 <sup>-5</sup>
4	Super Duplex Straight	1	10 <sup>-5</sup>
5	Super Duplex Bend 2.5ND	1.13	10 <sup>-5</sup>
6	Super Duplex Bend 5 ND	1.13	10 <sup>-5</sup>

The corrosion rate was calculated for every specimen based on the  $I_{corr}$  value obtained from the polarization curve. Approximate Corrosion Rate calculated based on the aforementioned data are shown in Table 24.

**Table 24:** Corrosion Rate (milli inch per year) of Materials Based on Polarization Curve

Materials	$I_{corr}$	Corrosion Rate (milli inch per year)
Duplex Big curve	0.000005	0.05452819
Duplex Small Curve	0.000005	0.06053474
Duplex Straight	0.0000015	0.08606203
Super Duplex Big Curve	0.000002	0.02115348
Super Duplex Small Curve	0.0000025	0.02603332
Super Duplex Straight	0.0000005	0.05903673

#### 4.5 Hardness Test

The Hardness of Duplex and Super Duplex were examined. The hardness values obtained for the specimens are presented in Table 25. The results of hardness values have been discussed in discussion section of this report.

**Table 25:** Hardness Values of Specimens

SN	Materials	Before G48 Test		After G48 Test	
		HV10	HV5	HV10	HV5
1	Duplex Straight Part	300	-	292	-
2	Duplex Bend Tubes (5ND)	335	-	320	-
3	Super Duplex Straight Part	285	-	-	277
4	Super Duplex Bend Tubes (5ND)	305	-	-	288

## 5. DISCUSSION

The intention of this study was to envisage the difference between the pitting corrosion resistance property of Cold Deformed and Straight tubes of two materials namely Duplex UNS S32205 and Super Duplex UNS S32750. The attempt was to draw the attention of researchers and industries about the issue of cold bend and its behaviour on pitting corrosion. Duplex and Super Duplex are highly resistant to both pitting and crevice corrosion. But there has not been much paper published on the comparative study of pitting corrosion in straight and bended tubes of this material. ASTM G48 and ASTM G61 were the methods followed to carry out this study. As mentioned in the above section for ASTM G48, there were several tests done at different temperatures. Before starting the experiments on the real specimens, several trial of ASTM G48 were performed for 316SS tubes. After following due procedure for getting precise result and after the confirmation of getting reproducible result, the experiment was initiated.

The duplex and super duplex materials were observed to be highly resistant to corrosion at the temperature at 22 °C. There was no evidence of corrosion on any of the specimen. Some crevice corrosion was seen on duplex at 30°C accompanying some weight loss. Nonetheless, the weight loss per unit area was within the acceptance criteria according to NORSOK Standard MDS-630. The specimens of duplex after G48 at 30°C were checked with a SEM and there was no pitting corrosion seen. Also no any differences were noticed among the straight and 2.5ND and 5ND bended parts. A minor thin line like structure was seen which showed the initiation of the crevice. However, the formation of crevice on straight and cold deformed part was similar. Upon further increment of temperature to 40 °C, the duplex was found to be attacked by crevice corrosion significantly. The weight loss per unit exceeded the standard limiting value of limit 4 g/m<sup>2</sup>. The Duplex, when tested at 60 °C showed lots of corrosion over the surface. The objective of testing at high temperature was to expose the material at extreme corrosive environment and to observe the behaviour of material between straight and cold deformed (bend) part. The specimens were observed to have pits all over the body after the test was accomplished. It was not possible to measure the weight of the duplex as the particles from corrosion were stuck on the material. There was a lot of remaining corrosion product on the surface and cleaning of the tubes eroded and washed away the weakened outer surface layer, so it was irrelevant to measure the weight loss. Even, cleaning with soft brush removed some outer layer surface. Thus, only physical observation was done. The straight and bend parts were found to be affected severely at this temperature and no any difference could be documented. The cold deformation effect on the duplex material was not observed in terms of the pitting corrosion resistant property of the material. No observations were made on any relationship of weight loss per unit area between the straight and bended tubes (2.5ND and 5ND).

With the increase in temperature the weight loss per unit area increased, which supports the theory that the corrosion increases with increase in temperature. The critical pitting

temperature for Duplex UNS S32250 was anticipated to be more than 40 °C. Only crevice corrosion was observed until 40 °C. Similarly, the critical crevice temperature would be around/before 30 °C, as crevices were noticed at this temperature. The results obtained supported the information from the literature about Duplex UNS S32205. It was found that different company specification for this material have CPT of 50 °C and CCP at 25 °C. The results obtained were near to the specifications provided. And it was found similar for both straight and bended parts.

Similarly, in the case of super duplex, after observing no corrosion at 22 °C, materials were exposed at 30°C. Super Duplex, having high resistant to pitting and crevice, showed no corrosion on the surface. Minor weight loss per unit area was observed, but they were well within criteria. There was no any pattern of weight loss between straight and bend part. The SEM images of samples also proved that the materials were unaffected. The super duplex specimens were further exposed at 40°C. After 24 hours exposure, it was observed that there was decrement of ferric chloride solution volume. The water was evaporated since the beakers were not fully covered. It was an unexpected event. The calculation of weight loss per unit area showed that it had exceeded the acceptance criteria for the weight loss. One hypothesis about the high weight loss at this temperature would be the increment of concentration of ferric chloride in solution due to evaporation of water. This might have led to the specimens being exposed to a more acidic environment. There was observation of crevice corrosion on the surface of super duplex where it was supported by nylon wire. However, there was no pitting corrosion observed. The examination of tubes on SEM as well didn't show any significant pitting corrosion sign on the material. After exposure at 40°C, same specimens were exposed at 50°C and there was a huge corrosion seen on the material. Even pitting corrosion, initiated as a pit of size 32.98 µm, was observed. It was ascertained that these effects could have resulted due to the exposure of super duplex at very acidic environment at 40°C prior to 50 °C. The crevices formed on the 40°C were more developed more leading to the loss of excessive weight. However, super duplex material didn't show any variation in straight and cold deformed bend part on its exposure at 50 °C.

The final set of tests was done by taking the new specimens of Super Duplex and exposing it at 50 °C as initial temperature. It was in accordance with both ASTM G48 and Norsok Standard MDS-630. The problems and challenges faced during prior experiments were addressed properly while performing this test. The test results showed that the material was highly resistant to pitting corrosion. Unlike previous test at 40°C and 50°C, the weight loss was less than 4 g/m<sup>2</sup>. The beakers were covered properly confirming as minimum evaporation as possible. The images from SEM also did not show any pitting corrosion sign. The initiation of crevice corrosion was seen though at the site of nylon wire connection. However, the material showed its high corrosion resistant property at this test. Similarly, the straight and bend part showed they were affected in a similar ways with no sign of pitting corrosion but a sign of crevice at the site of support from nylon wire.

Also, the weight loss pattern did not show any relationship between the straight and bend part corrosion resistant property.

After ASTM G48 Test, the super duplex materials were found to have weaker outer surface. The hardness of the material was found to decrease. The reason for softening of the outer layer of super duplex material is not clear. It was not that significant in Duplex. It hence a matter for study as much literature regarding the softening of super duplex material after G48 Test was not found.

The ASTM G61 Test was performed after ASTM G48 to know about the pitting potential of straight and bend parts. Gamry Potentiostat was used and calibration was performed prior to the experiment. The open circuit potential was run for an hour before every cyclic polarization scan. The OCP curves obtained for all specimens were steady, though for straight duplex and small bend duplex, the beginning part of the curves was found to be fluctuating. The noise during the experiment was expected to disturb the steadiness of the potential increment. Also the reaction of surface outer layer with the electrolyte might have had some impact in the fluctuation of potential variation. The maximum corrosion potential was seen for bigger bend of duplex with 25 mV whereas the minimum was observed for smaller bend with -50 mV.

The cyclic polarization curve for duplex didn't show any hysteresis, showing its strong resistant property for crevice corrosion. Pitting potential and repassivation potential were the major matters of interest in this project. The pitting potential for all duplex specimens was about 1 V. A negative hysteresis loop was formed in polarization curves in duplex which indicates that the material is highly resistant to localized corrosion. There was observation of some metastable pits and some noise in the experiment which led to the unsteadiness of graphs in some points; however the values of pitting potential were clearly seen. The pitting corrosion potential for the straight and bend part was not found to be much different. Similarly for the super duplex materials, the pitting potential for all specimens was about 1 V, showing not much variation between straight and bend parts. There was a formation of small area of positive hysteresis loop on the cyclic polarization curve of straight super duplex tube. The small area indicates that it is highly resistant to the pitting and crevice corrosion. The pitting potential and the repassivation potential were very near values (pitting potential of 1 V and repassivation potential of about 0.95 V). However, hysteresis on bended parts was not observed. The potential during reverse scan was seen to be more than the potential during forward scan for the same current density for bended parts. From the curve, it can be said that the bended part of super duplex are more corrosion resistant to localized corrosion. However, the pitting potential values were found to be in the same range of about 1V.

The corrosion rates of the materials were calculated after obtaining the cyclic polarization curves. It shows that the corrosion rate of bended and straight part of duplex did not vary much. However, based on the graph and calculation, the corrosion rate of straight part was

found to be slightly more than the bended parts. Similar was with the case of super duplex. Though specific conclusion cannot be made based on these few data, it has been recommended to perform further tests to find the corrosion rate of materials based on the different degree of bending. Nevertheless, high corrosion rate due to cold deformation of tubes (2.5ND and 5ND) of Duplex and Super Duplex materials was not observed.

The hardness of the bended parts was measured to be higher than the straight part as expected. Similarly, the hardness of material was found to decrease due to the exposure at acidic solution. The Hardness of Super Duplex was seen to decrease after ASTM G48 Test. The cold bend part of Super Duplex had about 305 HV10 whereas the straight part was found to have about 285 HV10. After G48 test above 50 °C, the super duplex was found to be weakened and even a small force was able to leave a mark on the surface of the material. The hardness was found to be 277 HV10 and 288 HV10 for straight and bend part respectively. The hardness was supposed to decrease due to exposure at acidic environment. In the case of Duplex, the hardness of straight tube and bend was measured 292 HV10 and 320 HV10 respectively. After G48 test, the hardness decreased in Duplex as well. The hardness for straight and bend was measured to be at 292 and 320 HV10 respectively. The outer layer was found to have less hardness. However no significant visual impact was seen in duplex than that of super duplex. The limitation of specimen limited the study of hardness in this project. The quantification of hardness decrement is one of the subjects of study that could be done by testing many numbers of straight and bended parts of Duplex and Super Duplex specimens.

For highly resistant materials like duplex and super duplex, cold deformation to the certain level is an economical and efficient method to acquire the required shape of the tubes. The thinning and thickening of the outer and inner material respectively is the major structure change due to cold bending. Heat treatment normally is not necessary for these strong materials unless the degree of cold reduction exceed 25% [51]. The cold deformed material testing is essential prior to its application, especially in the harsh environmental conditions. Also, the deformation should be according to the given standard. There is the necessity of study of specific properties change due to cold deformation. Its detail study could generate the heavier implication of cold bend in different industries. It would also help in allotting the areas depending on the suitability of using the cold bend, due to change in some of the important properties of materials.

## **6. CONCLUSION AND RECOMMENDATIONS**

Based on results obtained, the following conclusions are drawn:

- Corrosion behaviour is directly proportional to temperature for even highly corrosion resistant materials like duplex and super duplex.
- The corrosion behaviour between straight and cold bended (2.5ND and 5ND) tubes are seen similar for duplex (UNS S32205) and super duplex (UNS S32750) based on accelerated coupon testing. The values observed for the weight loss per unit area ( $\text{g/m}^2$ ) between straight and bended parts render their consideration for practical applications to be irrelevant.
- The pitting potential values for straight and bended part are found to be in similar range. There has not been significant impact on pitting potential due to cold deformation of 2.5ND and 5ND for duplex and super duplex tubes.
- The hardness of the bended parts is high as expected, however the hardness of material was found to be affected after exposure at acidic environment at high temperature. The hardness values decrease slightly after accelerated coupon test.

Recommendations provided on the basis of study carried out for this study are mentioned below:

- The study of mechanical properties between straight and cold deformed parts should be carried out with consideration of change in micro structures and their effects on material properties.
- The outer surface of the Super Duplex was found to be weakened after ASTM G48 though no any pitting corrosion was seen. Hence, further studies should be carried out regarding this issue and comparison with other super duplex materials should be made.
- The study of hardness variation could be carried out in detail among the bended part so that the permissible bending criteria for these materials could be determined. Also the hardness variation after accelerated coupon testing should be further studied.
- It is recommended for the accelerated coupon test and electrochemical testing to be performed while analysing their corrosion properties so that the result obtained from one could complement another, thus helping in proper decision making.



## REFERENCES

1. A. M. Elhoud, N.C.R., W. F. Deans, *The effect of manufacturing variables on the corrosion resistance of a super duplex stainless steel*. The International Journal of Advanced Manufacturing Technology, 2011. **52**(5-8): p. 451-461.
2. Šárka HERMANOVÁ, L.D., Ladislav KANDER *EFFECT OF COLD DEFORMATION ON THE PROPERTIES OF NEW AUSTENITIC STAINLESS STEEL FOR BOILER SUPERHEATER TUBES*. in *International Conference on Metallurgy and Materials METAL 2014*. 2014. Brno, Czech Republic, EU: TANGER Ltd.
3. Trethewey, K.R. and J. Chamberlain, *Corrosion for Science and Engineering*. 1995: Addison Wesley Longman. 30.
4. Petersen, M.B. and E. Mahn. *Atmospheric Corrosion of Metallic coatings measured by EIS*. in *Corrosion Congress*. 1989. Stavanger: Centrum Trykkeri AS.
5. Marcus, P., *Preface*, in *Corrosion Mechanisms in Theory and Practice*, P. Marcus, Editor. 2002, Marcel Dekker, Inc.
6. Devis, J.R., *Corrosion: Understanding the Basics*. 2000: ASM International.
7. Revie, R.W. and H.H. Uhlig, *Corrosion and Corrosion Control*. Fourth ed. 2008: John Wiley and Sons, Inc.
8. *Corrosion Cost and Preventive Strategies in the United States*. NACE International: 1440 South Creek Drive Houston, TX, US.
9. Cicek, V. and B. Al-Numan, *Corrosion Chemistry*. 2012, Hoboken, NJ, USA: Wiley.
10. Bell, G.E.C. *Basic Mechanism of Corrosion and Corrosion control for Water and Waste water system.*; Available from: [http://www.ohiowea.org/docs/Wed0800Coll\\_Basic\\_Mech\\_Corrosion.pdf](http://www.ohiowea.org/docs/Wed0800Coll_Basic_Mech_Corrosion.pdf).
11. *Corrosion engineering handbook*, P.A. Schweitzer, Editor. 1996, Marcel Dekker: New York. p. X, 736 s. : ill.
12. *General Attack Corrosion*. 10.30.2013]; Available from: <http://www.nace.org/Pitting-Corrosion/>.
13. Pohlman, S.L., "*General Corrosion*" in *Corrosion*. Ninth ed. Vol. 13. 1987: ASM International.
14. Dexter, S.C., "*Localized Corrosion*", in *Corrosion*. Vol. 13. 1987: ASM International.
15. McCafferty, E., *Introduction to Corrosion Science*. 2010: Springer New York.
16. Stanbury, E.E. and R.A. Buchanan, *Fundamentals of Electrochemical Corrosion*. 2000, Materials Park, OH, USA: ASM International.
17. *Different Types of Corrosion*. [cited 2014 February 16]; Available from: [http://www.corrosionclinic.com/types\\_of\\_corrosion/pitting\\_corrosion.htm](http://www.corrosionclinic.com/types_of_corrosion/pitting_corrosion.htm).
18. *Pitting Corrosion*. 2010 [cited 2014 January 20]; Available from: <http://www.misumi-techcentral.com/tt/en/surface/2010/09/056-pitting-corrosion.html>.
19. Schweitzer, P.A., *Encyclopedia of Corrosion Technology*. 1998, New York: Marcel Dekker, INC.
20. Cobb, H.M., *History of Stainless Steel*. 2010, Materials Park, OH, USA: ASM International.
21. *Stainless Steel and Corrosion*. 2010 2013.10.30]; Available from: [http://www.aperam.com/uploads/stainlesseurope/Brochures/Leaflet%20corrosion\\_Eng\\_374Ko.pdf](http://www.aperam.com/uploads/stainlesseurope/Brochures/Leaflet%20corrosion_Eng_374Ko.pdf).
22. Dereu, B., *Raw and Finished Materials : A Concise Guide to Properties and Applications*. 2011, New York, NY, USA: Momentum Press.
23. Verhoeven, J.D., *Steel Metallurgy for the Non-Metallurgist*. 2007, Materials Park, OH, USA: ASM International.
24. Schweitzer, P.A., *Fundamental of Metallic Corrosion*. Second ed. Atmospheric and Media Corrosion of Metals. 2007: CRC Press, Taylor and Francis Group , London , New York.

25. McGuire, M.F., *Stainless Steels for Design Engineers*. 2008, Materials Park, OH, USA: ASM International.
26. Society, A.W. *Classification of stainless steel*. 1998 [2013.11.01]; Available from: <http://www.aws.org/w/a/wj/1998/11/kotecki>.
27. Lai, J.K.L.S., Chan Hung Lo, Kin Ho, *Stainless Steels : An Introduction and Their Recent Developments*. 2012, SAIF Zone, Sharjah, UAE: Bentham Science Publishers.
28. *Stainless Steels : An Introduction and Their Recent Developments*. 2012, SAIF Zone, Sharjah, UAE: Bentham Science Publishers.
29. Penn Stainless Products, I. *Duplex 2205 Stainless Steel*. 2014 [cited 2014 May 21]; Available from: <http://www.pennstainless.com/stainless-grades/duplex-grades/duplex2205-stainless-steel/>.
30. Ltd, L.A. *Duplex 2205*. 2011 [cited 2014 21 May]; Available from: <http://www.langleyalloys.com/ALLOY2205.php>.
31. J.R.Davis, D.a.A., *Corrosion of Weldments*. 2006, Materials Park, OH, USA: ASM International.
32. *Duplex Stainless Still '91*. Vol. 1. les editions de physique.
33. ; Available from: <http://www.nyk.co.jp/en/products/alloys/corrosion/74n.html>.
34. Bardal, E., *Corrosion and protection*. 2004, London: Springer. XI, 315 s. : ill.
35. Perez, N., *Electrochemistry and Corrosion Science*. 2004, Hingham, MA, USA: Kluwer Academic Publishers.
36. Wessel, J.K., *Handbook of Advanced Materials : Enabling New Designs*. 2004, Hoboken, NJ, USA: Wiley.
37. Tan, Y., *Heterogenous Electrode Processes and Localized Corrosion*. 2013, John Wiley and Sons, Inc.
38. Chamberlain, K.R.T.a.J., *Corrosion for Science and Engineering* 1995: Addison Wesley Longman.
39. *Martensitic Stainless Steel*. 2007 [2013.11.05]; Available from: <http://www.keytometals.com/page.aspx?ID=CheckArticle&site=kts&NM=199>.
40. *Bending Stainless Steel Tubes-Design Benefits in Engineering and Architecture*. Material and Applications Series. 15.
41. *Tube Bending*. 2013, Woolf Aircraft products, INC.
42. *Bending Guide*, I. Hines Bending System, Editor., Hines Bending System, INC: 2710 Swamp Cabbage Court, Fort Myers, Florida, US.
43. *Welding Training: Ferrous Metals for Welding 200*. [cited 2014 May 23]; Available from: <http://www.toolingu.com/definition-650200-77305-yield-strength.html>.
44. Robert G. Kelly, J.R.S., David W. Shoesmith, Rudolph G. Bucheit, *Electrochemical Techniques in Corrosion Science and Engineering*. 2003, 270 Madison Avenue, New York, US: Marcel Dekker, Inc.
45. Herrmann, K., *Hardness testing: principles and applications*. 2011, Materials Park, Ohio: ASM International. 1 online resource (vi, 255 s.) : ill.
46. Materials, A.S.f.T.a., *Standard ASTM/G48-11 : Standard Test Methods for Pitting and Crevice Corrosion Resistance of Stainless Steels and Related Alloys by Use of Ferric Chloride Solution*. ASTM International: West Conshohocken, PA, United States.
47. Norway, S., *Material Data Sheets and Element Data Sheets for Piping, Norsok Standard, M-630*. 2010: Strandveien 18, P.O. Box 242, N-1326 Lysaker, NORWAY.
48. Materials, A.S.f.T.a., *Standard ASTM/G61-86 : Standard Test Method for Conducting Cyclic Potentiodynamic Polarization Measurements for Localized Corrosion Susceptibility of Iron-, Nickel-, or Cobalt Based Alloys*. 2003, ASTM International: West Conshohocken, PA, United States.

49. *DC 105TM- CorrosionTechniques Software*. 2010, Gamry Instruments: 734 Louis Drive, Warminster, PA 18974, US.
50. *MERLIN Compact and SIGMA HD*. 2014, Carl Zeiss: Germany.
51. *STAINLESS STEEL PLATE, SHEET & COIL*. 2014 [cited 2014 6 April]; Available from: [http://www.macsteel.co.za/files/macsteel\\_vrn - stainless steel plate sheet coil - saf 2205.pdf](http://www.macsteel.co.za/files/macsteel_vrn_-_stainless_steel_plate_sheet_coil_-_saf_2205.pdf).

## APPENDICES

### Appendix 1: Images from SEM of Super Duplex

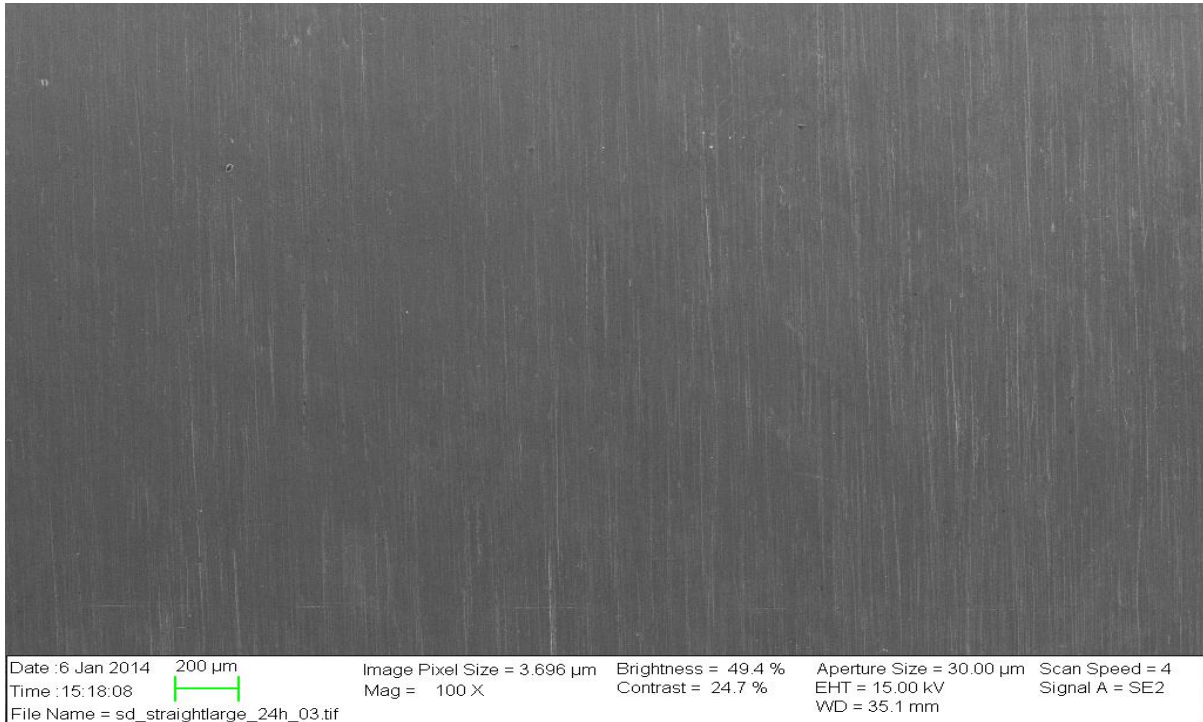


Image: Super Duplex large straight part after G48 test at 22°C

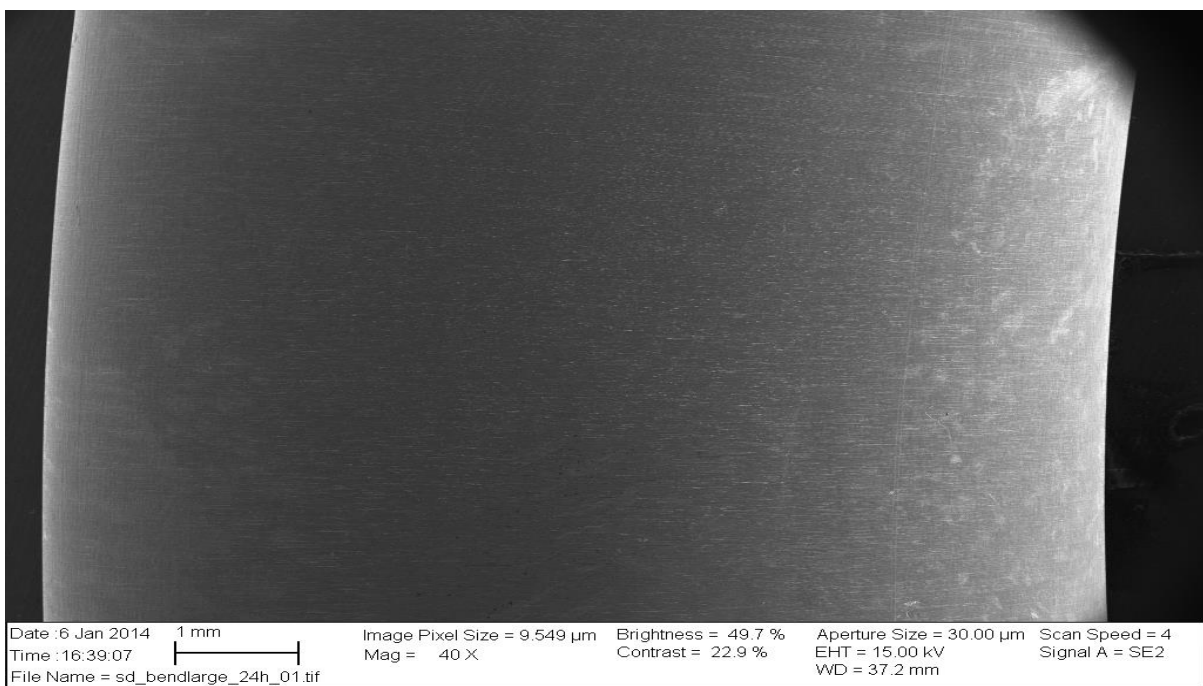


Image: Super Duplex Bigger Bend part after G48 test at 22°C



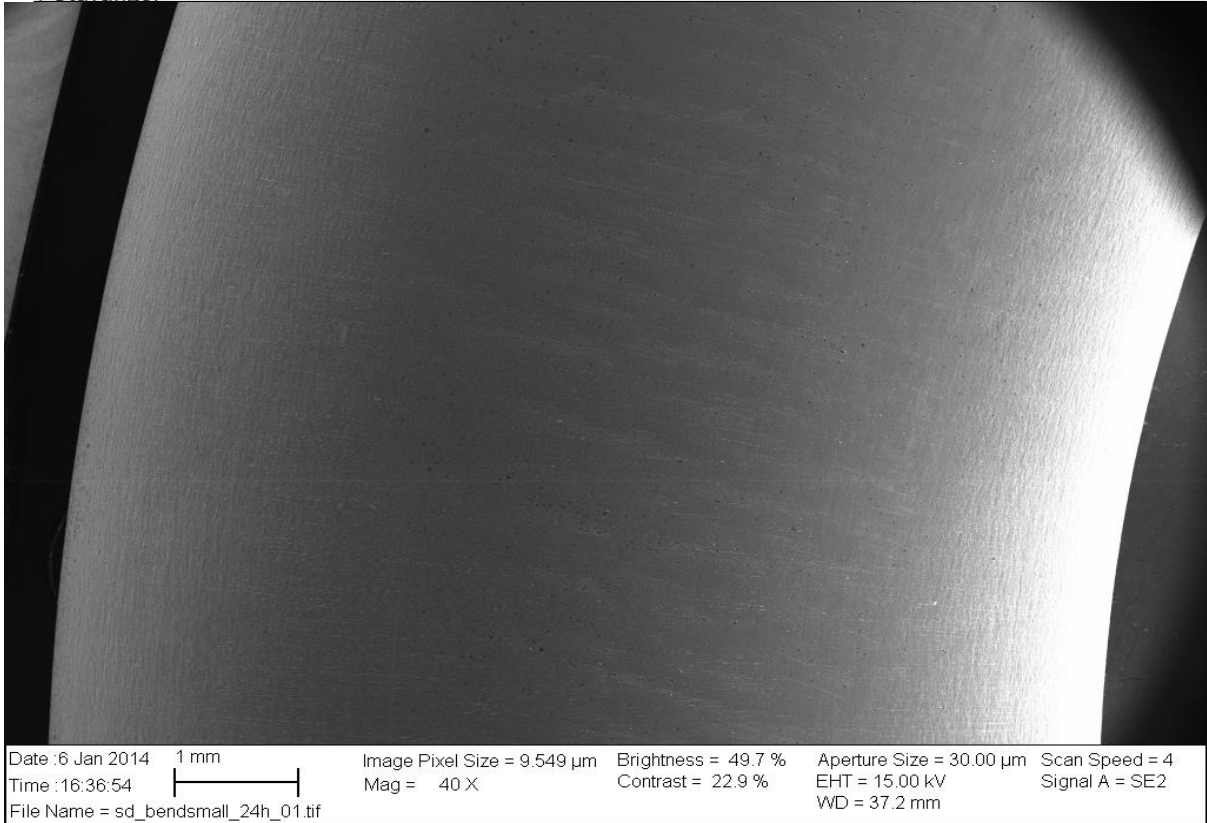


Image: Super Duplex smaller Bend part after G48 test at 22°C

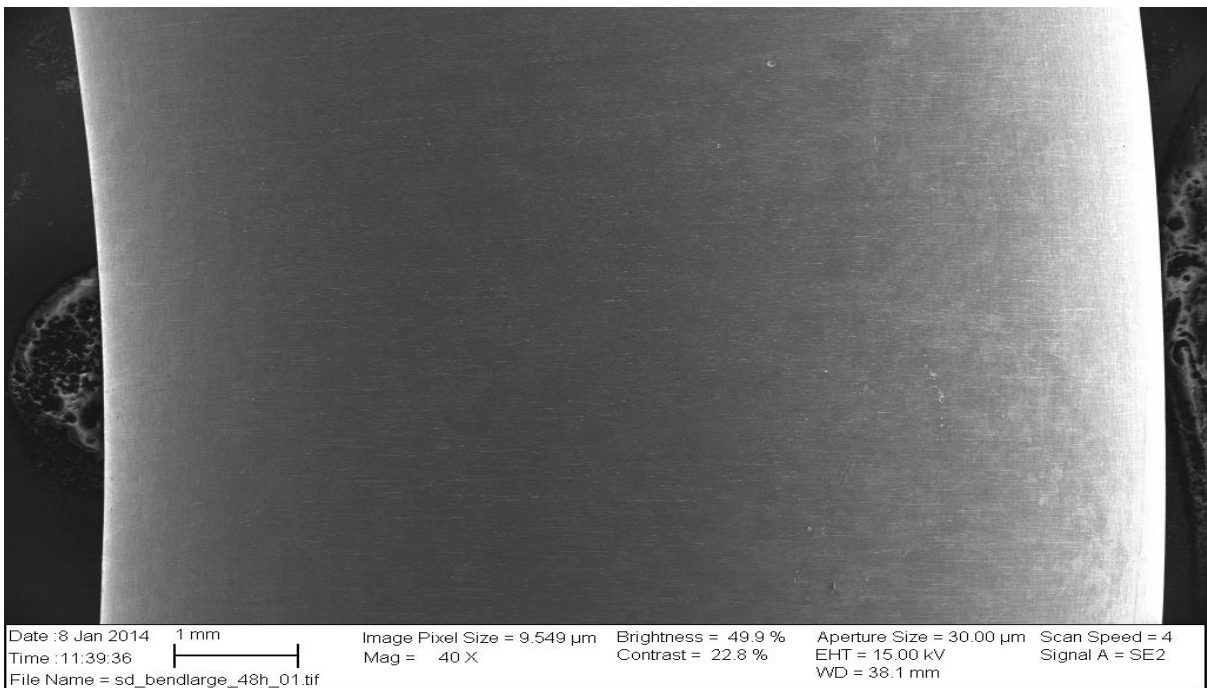


Image: Super Duplex Bigger Bend part after G48 test at 30°C



Universitet  
i Stavanger

# Investigation of Corrosion Resistance Property of Cold Deformed (Bended) Duplex and Super Duplex Stainless Steel Tubes

## Master Thesis

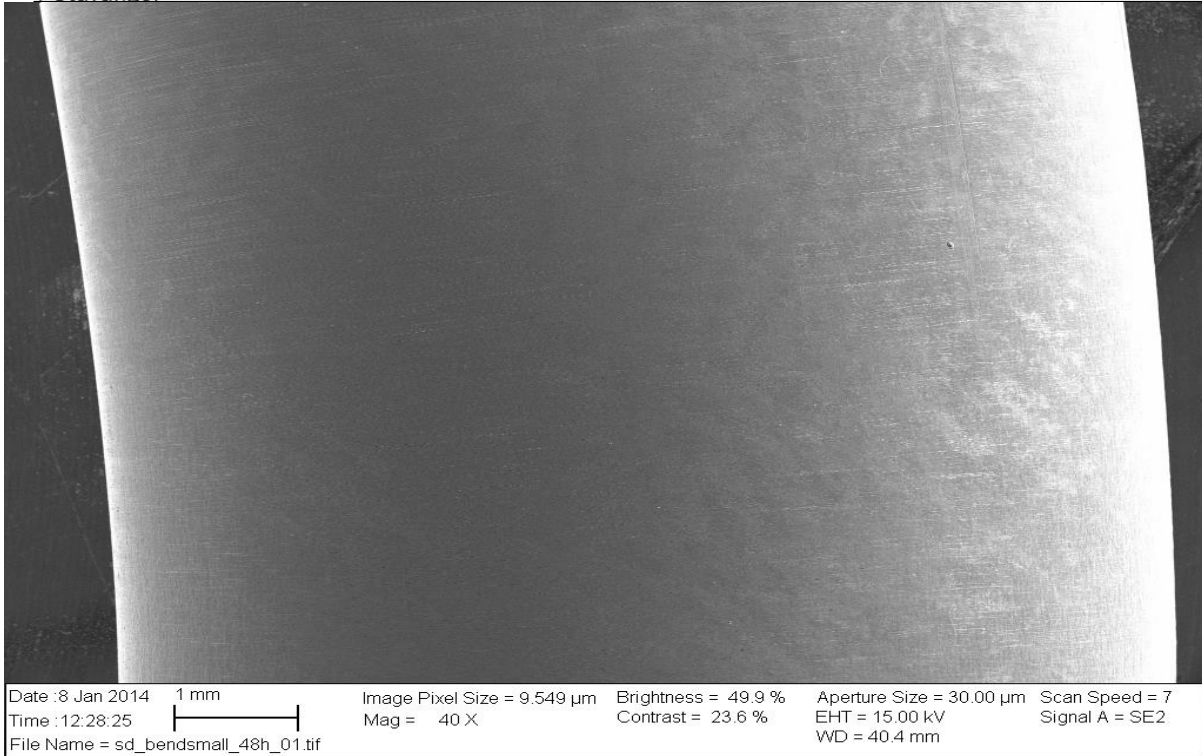


Image: Super Duplex smaller Bend part after G48 test at 30°C

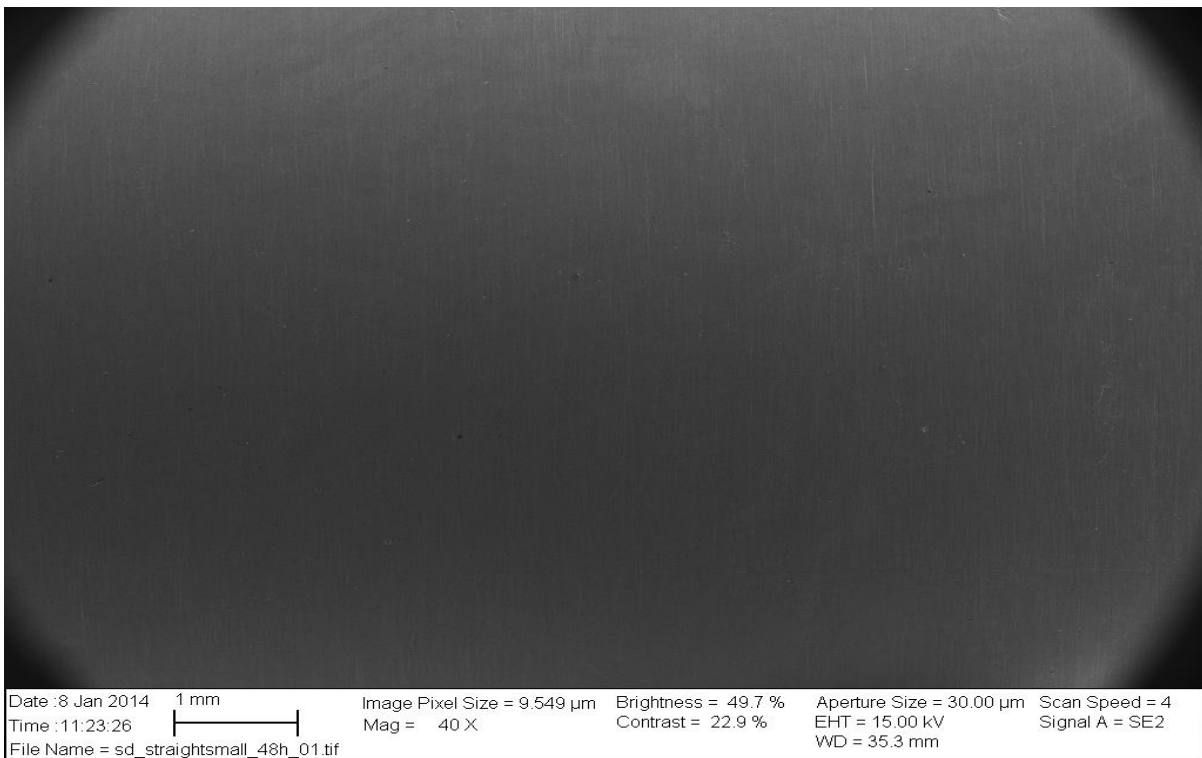


Image: Super Duplex smaller straight part after G48 test at 30°C



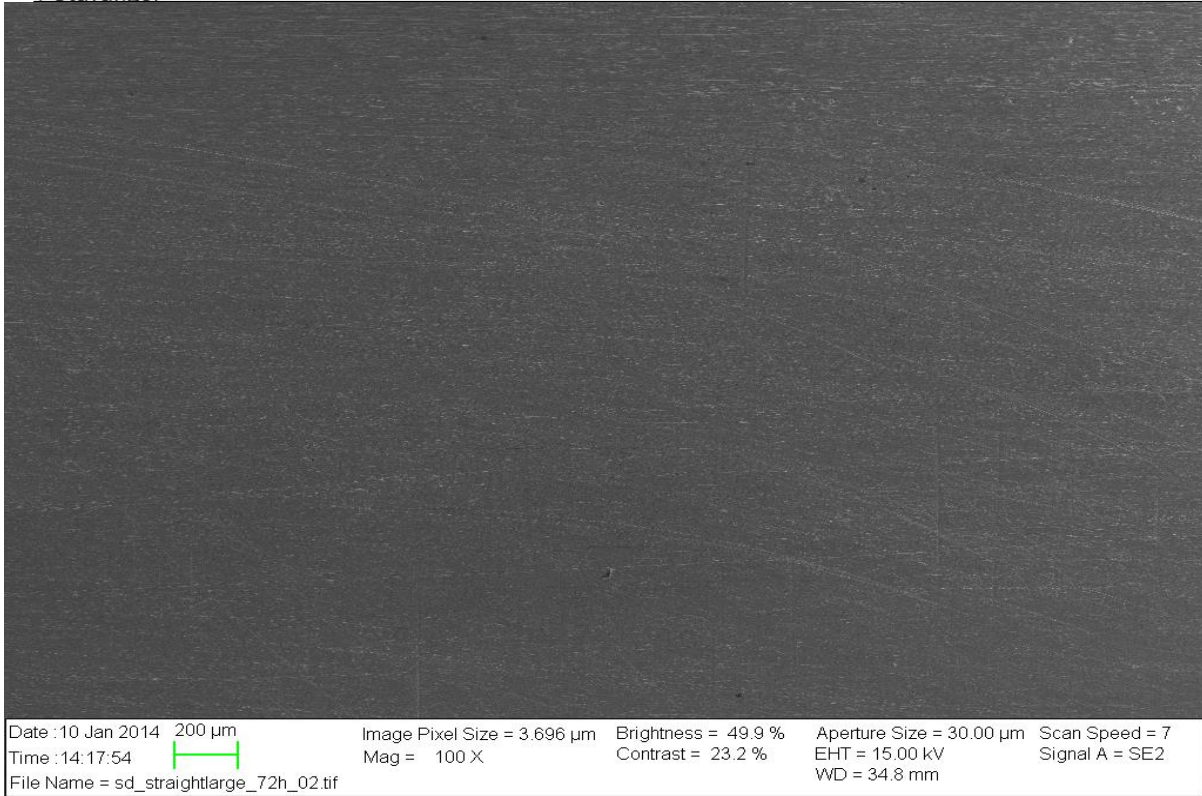


Image: Super Duplex large straight part after G48 test at 40°C

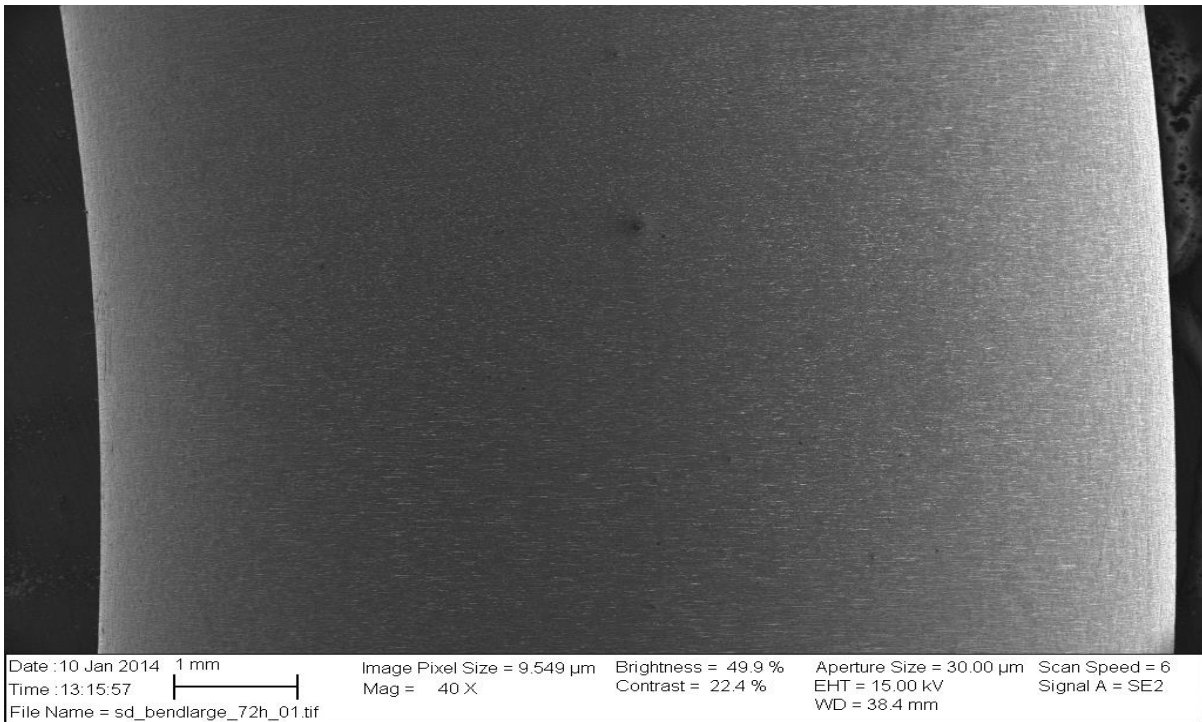


Image: Super Duplex Bigger Bend part after G48 test at 40°C



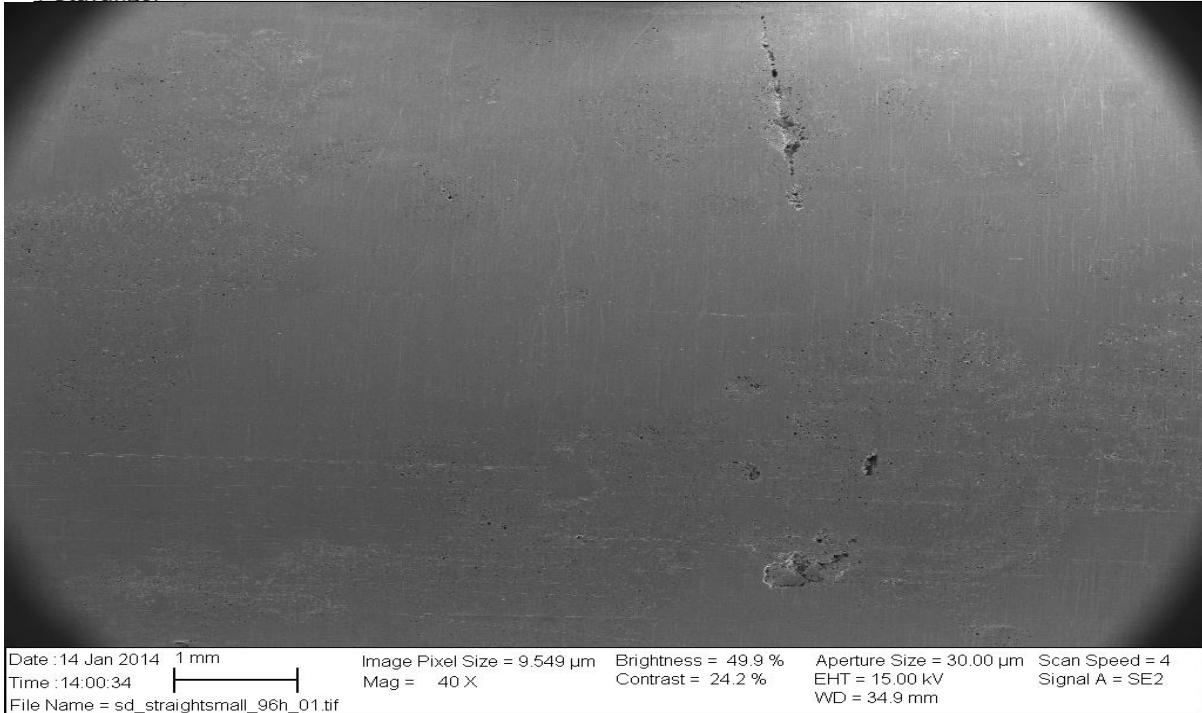


Image: Crevice corrosion seen on straight part of super duplex at 50°C

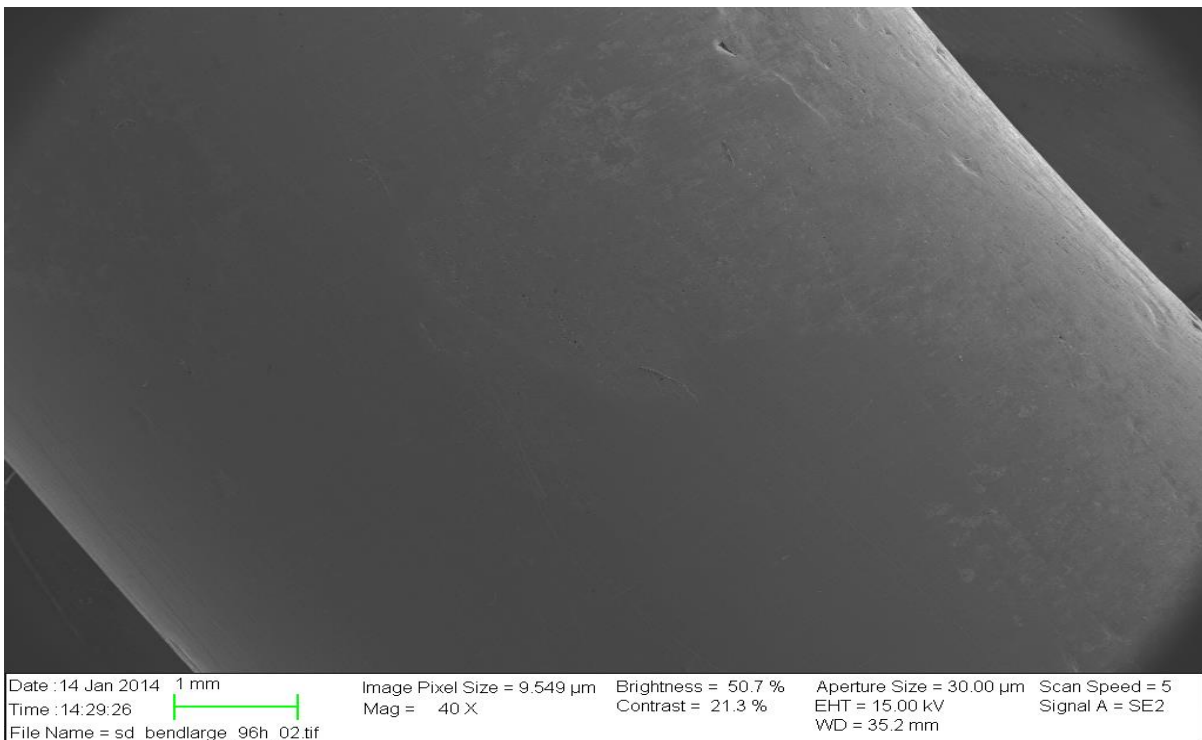


Image: Super Duplex Bigger Bend part after G48 test at 50°C



Universitetet  
i Stavanger

# Investigation of Corrosion Resistance Property of Cold Deformed (Bended) Duplex and Super Duplex Stainless Steel Tubes Master Thesis

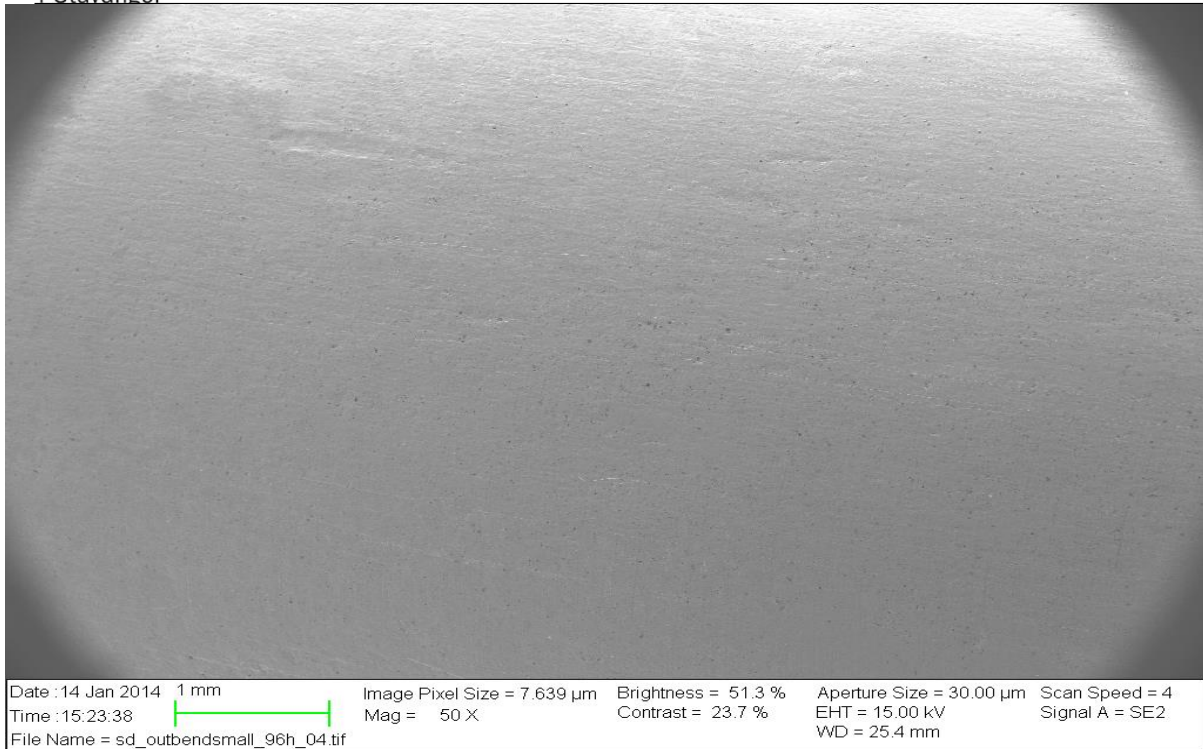


Image: Super Duplex Smaller Bend after G48 Test at 50°C

**Appendix 2: Images from SEM of Duplex**



Image: Duplex Smaller Bend after G48 Test at 22°C

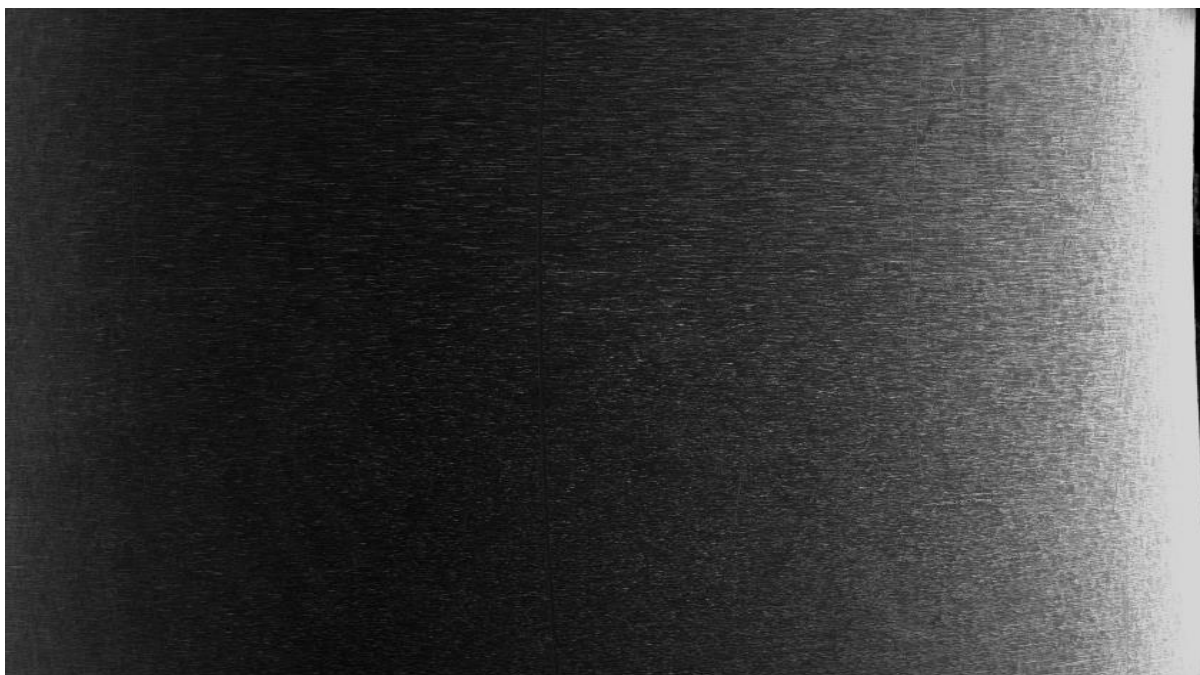


Image: Duplex Bigger Bend after G48 Test at 22°C





Image: Duplex Large Straight after G48 Test at 22°C

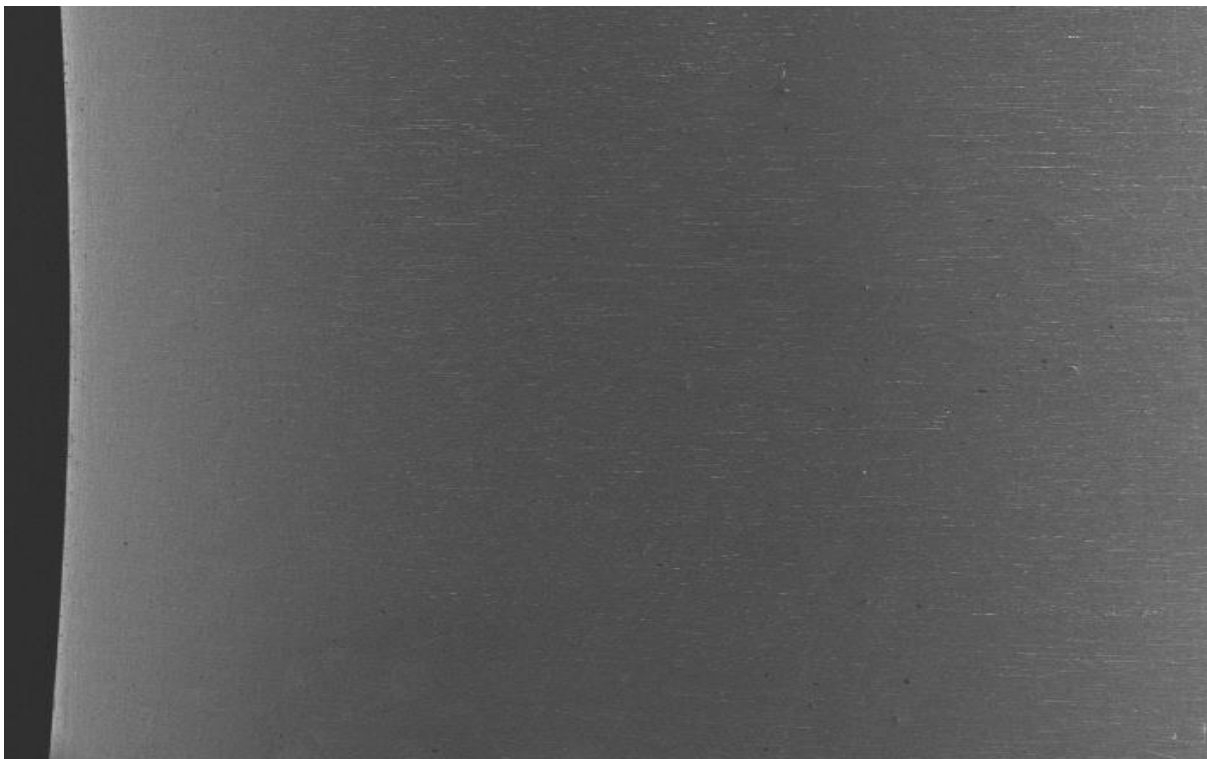


Image: Duplex Bigger Bend at after G48 Test at 30°C



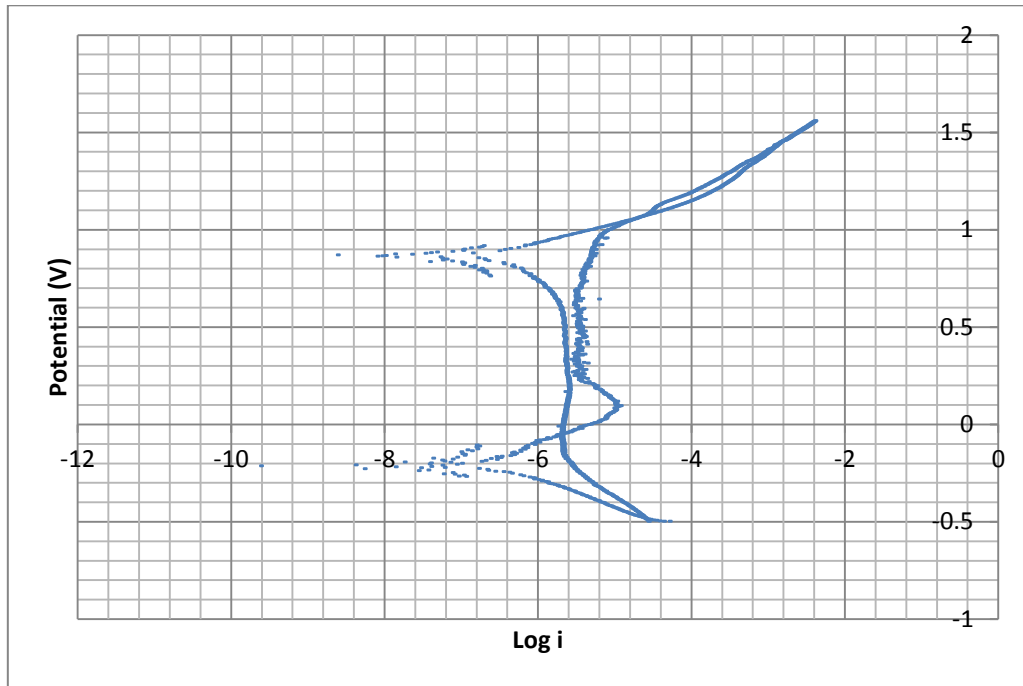
Image: Duplex Smaller Bend at after G48 Test at 30°C



Image: Duplex Large Straight at after G48 Test at 30°C

### Appendix 3: Cyclic Polarization Curve (Potential vs current density) for Super Duplex

The graphs are plotted for Potential (V) vs. Log i ( $A/cm^2$ ).



**Figure: Cyclic Polarization Curve for Straight part of Duplex**

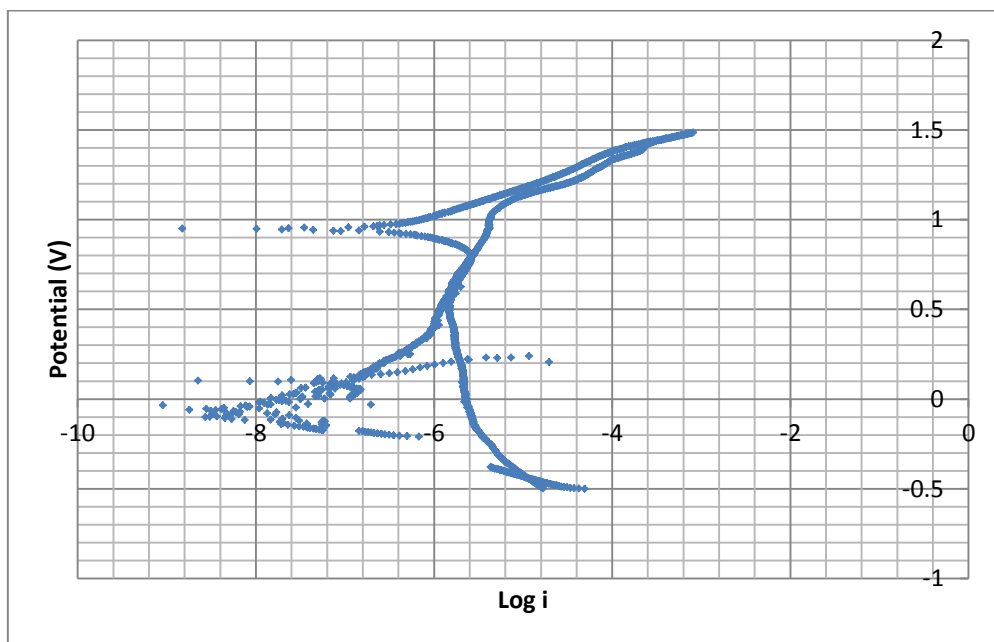


**Figure: Cyclic Polarization Curve for Bigger Bend Duplex**

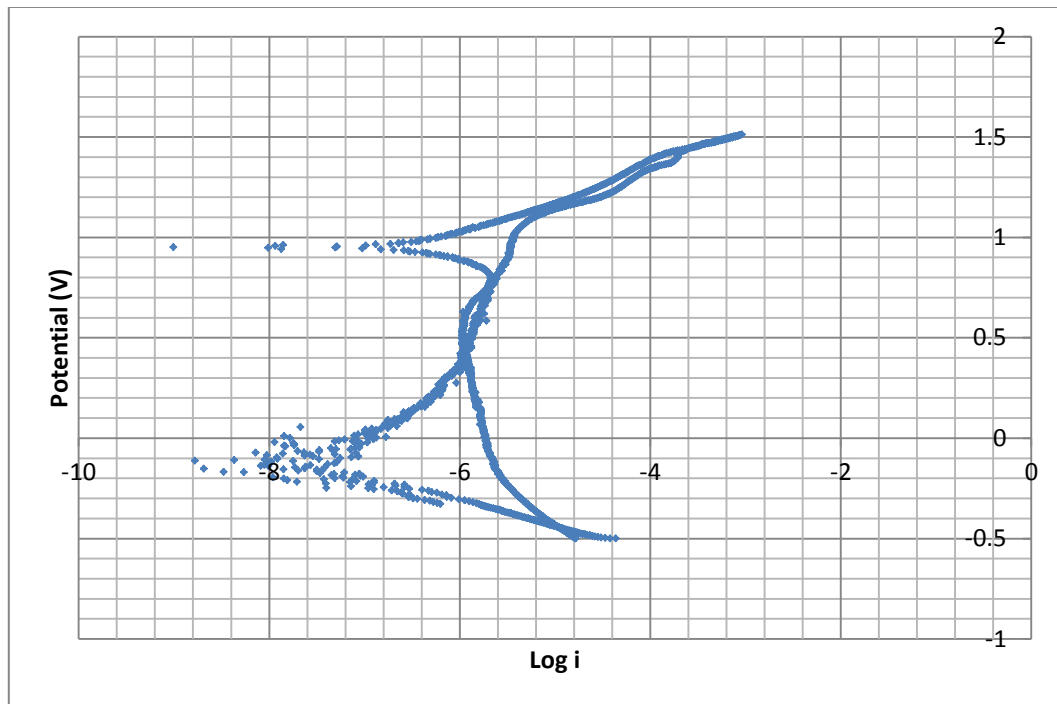


**Figure: Cyclic Polarization Curve for Smaller Bend Duplex**



**Appendix 4: Cyclic Polarization Curve (Potential vs current density) for Duplex**

The graphs are plotted for Potential (V) vs. Log i ( $A/cm^2$ ).

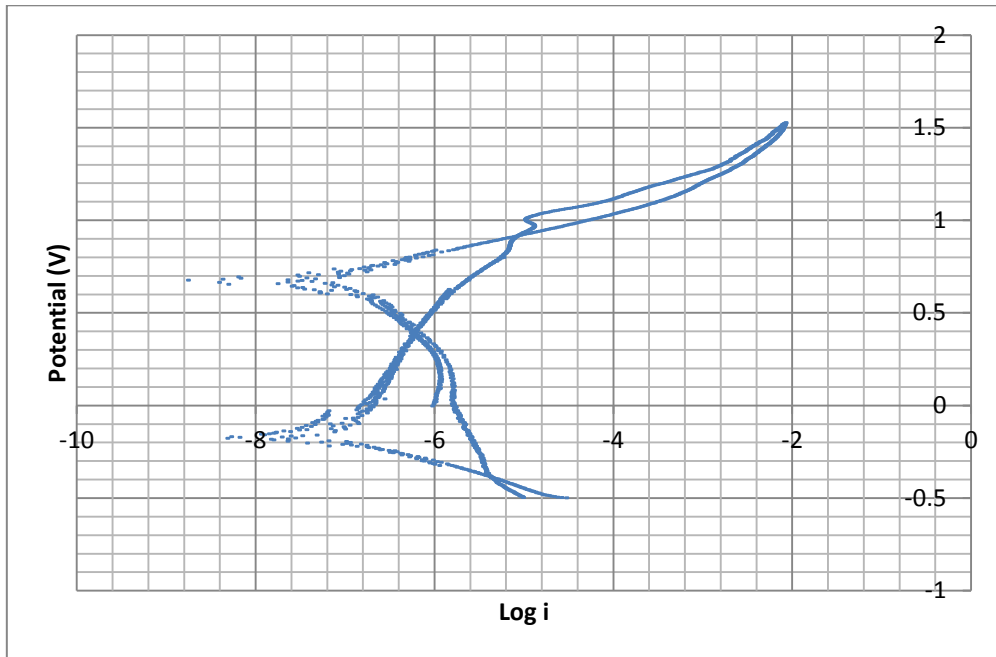


**Figure: Cyclic Polarization Curve for Straight part of Super Duplex**

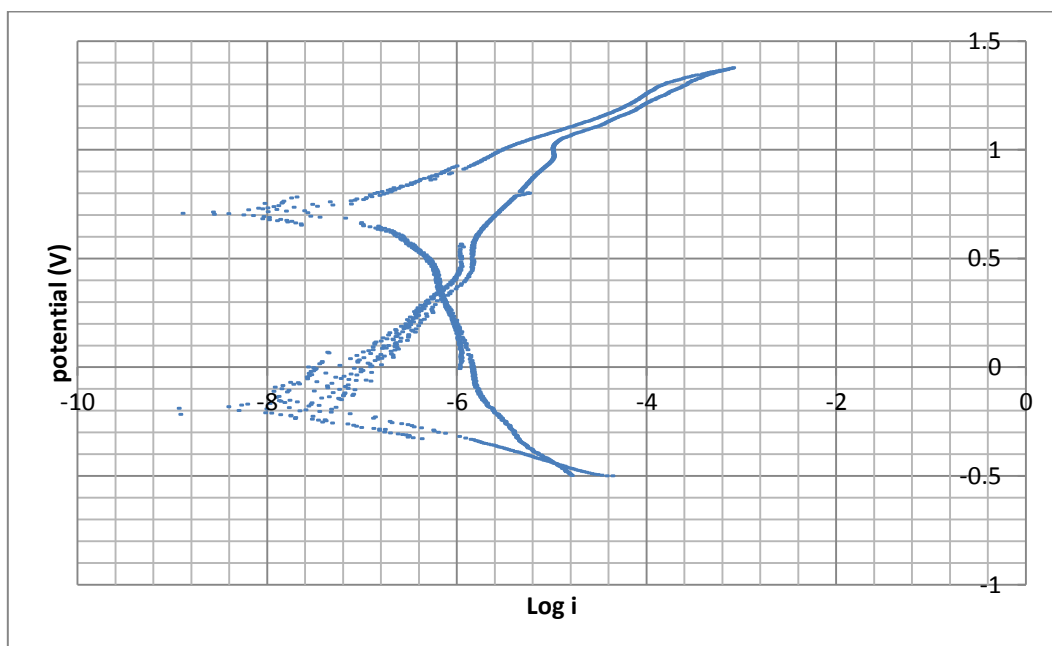


**Figure: Cyclic Polarization Curve for Bigger Bend Super Duplex**

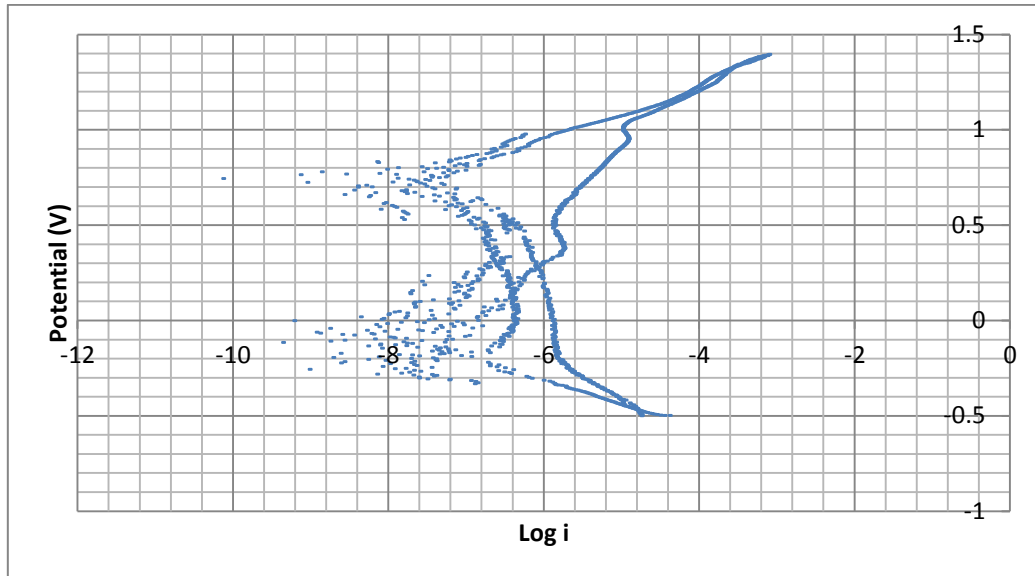
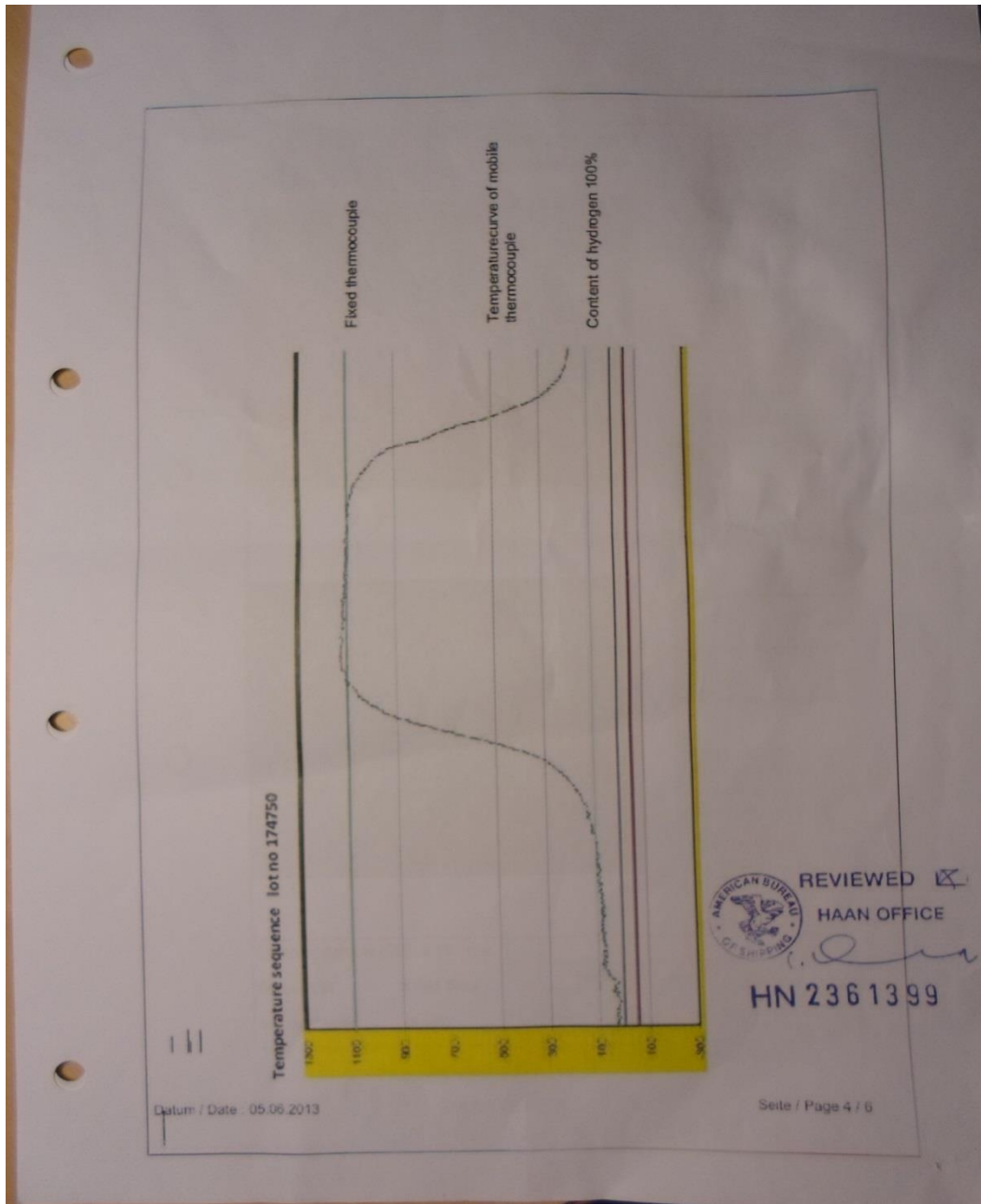


**Figure: Cyclic Polarization Curve for Small Bend of Super Duplex**

**Appendix 5: Specimen for Testing and reviewing the material (SAF 2507)**

Parker		Autoclave Engineers		<b>MS15-504</b>								
LOT #	O.D.	I.D.	Grade	Heat No.	SMLS	Spec #						
174750	0.365"	0.198"	SAF 2507	528525	Yes	AES 625 Rev 9						
<b>CHEMICAL COMPOSITION</b>												
Element:	C	Mn	P	S	Si	Cr	Ni	Mo	N	Cu	PREw	Temper
Ladle :	0.014	0.39	0.022	0.001	0.32	25.43	6.40	3.84	0.28	0.10	42.58	Heat treated (controlled atmosphere)
<b>MECHANICAL PROPERTIES</b>												
Offset Yield		Ultimate Tensile Strength				% Elongation		Hardness				
MPa (0.2%) (N/mm <sup>2</sup> )	MPa (1%)	Mpa (N/mm <sup>2</sup> )				in 2 inches		(HRC)				
722	N/a	888				31.8		32-32				
706		889				32.0		32-33		27-31		
<b>ADDITIONAL TESTING</b>												
Surface Roughness	Hydrostatic	Corrosion Test ASTM G48 A	Visual & Dimensions; Wall Control	Eddy Current	Alloy Verification (PMI tested)	Flare	Flattening					
0.23-0.36 µm	OK 2070 bar	OK	OK	OK	OK	Ok	Ok					
Grain Size & Structure	Depth of ID Defects	Ferrite Content	Sigma Phase	Cooling Rate	Melt Process	Testing Witnessed By						
<8/fine grain	<10µm	43.94%	<0.01%	118.8°C/min	Electromelt	American Bureau of Shipping						
						Hamburg						
<small>Ref 41130 Raw Material Source: Sweden No weld repair was performed on this product. Visual and dimensional inspection acceptable.            During the manufacturing, test, and inspections this material did not come in direct contact with mercury, or its compounds, nor with any single boundary containment.            Recording of false or fraudulent data on this report may be punishable under Federal Statutes.            Material is in full compliance with specifications listed, unless noted otherwise. This report is designed to meet the requirements of 3.1 certification per EN10204.            Certified by: Liam O'Connor, Technical Manager (Authorized Signatory) Note: Electronically-created document, therefore unsigned.            Date: 1 July 2013</small>												
										1204		



## Investigation of Corrosion Resistance Property of Cold Deformed (Bended) Duplex and Super Duplex Stainless Steel Tubes

### Master Thesis

<b>SANDVIK</b>	<b>Metallographic examination</b>	Sandvik P&P ZN der Sandvik GmbH Dammsstrasse 27-29 D-33824 Werther																
 165 : 1	 165 : 1	Certificate - No.: 41130 Lot - No.: 174750/11 Dimension: 9,27x2,12 Material: SAF 2507 Specification: ASTM E582																
		Depth of defects (ID)  <table style="width: 100%; border-collapse: collapse;"> <tr> <td style="width: 80%; text-align: center;"><math>\mu\text{m}</math></td> <td style="width: 20%;"></td> </tr> <tr> <td style="text-align: center;">5,93</td> <td></td> </tr> <tr> <td style="text-align: center;">6,26</td> <td></td> </tr> <tr> <td style="text-align: center;">4,25</td> <td></td> </tr> <tr> <td style="text-align: center;">3,44</td> <td></td> </tr> <tr> <td style="text-align: center;">7,13</td> <td></td> </tr> <tr> <td style="text-align: center;"><math>\mu\text{m}</math></td> <td></td> </tr> </table>	$\mu\text{m}$		5,93		6,26		4,25		3,44		7,13		$\mu\text{m}$			
$\mu\text{m}$																		
5,93																		
6,26																		
4,25																		
3,44																		
7,13																		
$\mu\text{m}$																		
Depth of defects (OD): < 10 $\mu\text{m}$ Grain size: 8 und finer Sigma-Phase: < 0,01%		<table border="1" style="width: 100%; border-collapse: collapse;"> <tr> <td style="width: 25%;"></td> <td style="width: 25%;"></td> <td style="width: 25%;"></td> <td style="width: 25%;"></td> </tr> <tr> <td style="text-align: center;">Austenit</td> <td style="text-align: center;">Area</td> <td style="text-align: center;">Fenit</td> <td style="text-align: center;">Area</td> </tr> <tr> <td style="text-align: center;"><math>\mu\text{m}^2</math></td> <td style="text-align: center;">%</td> <td style="text-align: center;"><math>\mu\text{m}^2</math></td> <td style="text-align: center;">%</td> </tr> <tr> <td style="text-align: center;">186078,93</td> <td style="text-align: center;">59,08</td> <td style="text-align: center;">145858,01</td> <td style="text-align: center;">43,94</td> </tr> </table>					Austenit	Area	Fenit	Area	$\mu\text{m}^2$	%	$\mu\text{m}^2$	%	186078,93	59,08	145858,01	43,94
Austenit	Area	Fenit	Area															
$\mu\text{m}^2$	%	$\mu\text{m}^2$	%															
186078,93	59,08	145858,01	43,94															
Date: 28.05.2013 Inspection: K. Yörük																		
Datum / Date : 05.06.2013																		
REVIEWED <input checked="" type="checkbox"/> HAAN OFFICE 		Seite / Page 5 / 6 <b>HN 236 13 99</b>																



## Investigation of Corrosion Resistance Property of Cold Deformed (Bended) Duplex and Super Duplex Stainless Steel Tubes

### Master Thesis

<b>SANDVIK</b>	<b>PMI test</b>	05.05.2013
	Sandvik P&P Branch of Sandvik Materials Technology Deutschland GmbH	

Material	SAF 2507
Method	X-ray (RFA)
Equipment	Spectro x Sort
Result	Material is acc. SAF 2507

Lot No.	174750
Certificate No.	41130
Heat No.	528525
<b>Chemical Element</b>	
Mn	0,40
Cr	25,1
Mo	4,13
Ni	8,54
Co	0,33
Cu	0,23
Nb	< 0,012
Ti	< 0,041
V	0,11
Fe	60,9

**REVIEWED**   
**HAAN OFFICE**  
*[Signature]*  
**HN 236 13 99**

C. Treichel / QA  
Sandvik P & P

ZN der Sandvik Materials Technology  
Deutschland GmbH  
Dammstraße 27-29

D-33624 Werther  
Tel. +49 (0)5203 9109-0  
Fax: +49 (0)5203 9109-22

Handelsregister-Nr.:  
HRB 6210, Amtsgericht Düsseldorf

USt-Id-Nr. DE119266885  
Steuer-Nr. 103/5757/0208  
FA Düsseldorf-Alstadt

Bankverbindung:  
Deutsche Bank AG, Düsseldorf

BLZ: 300 700 10  
Konto-Nr.: 349100300  
IBAN: DE34300700130349100300

Datum / Date: 05.05.2013

Geschäftsführer: Manfred Herder, Matthias Kleihans, Stefan Schatz  
SWIFT-BIC: DEUTDE33